



National Library
of Canada

Bibliothèque nationale
du Canada

Canadian Theses Service

Service des thèses canadiennes

Ottawa, Canada
K1A 0N4

NOTICE

The quality of this microform is heavily dependent upon the quality of the original thesis submitted for microfilming. Every effort has been made to ensure the highest quality of reproduction possible.

If pages are missing, contact the university which granted the degree.

Some pages may have indistinct print especially if the original pages were typed with a poor typewriter ribbon or if the university sent us an inferior photocopy.

Reproduction in full or in part of this microform is governed by the Canadian Copyright Act, R.S.C. 1970, c. C-30, and subsequent amendments.

AVIS

La qualité de cette microforme dépend grandement de la qualité de la thèse soumise au microfilmage. Nous avons tout fait pour assurer une qualité supérieure de reproduction.

S'il manque des pages, veuillez communiquer avec l'université qui a conféré le grade.

La qualité d'impression de certaines pages peut laisser à désirer, surtout si les pages originales ont été dactylographiées à l'aide d'un ruban usé ou si l'université nous a fait parvenir une photocopie de qualité inférieure.

La reproduction, même partielle, de cette microforme est soumise à la Loi canadienne sur le droit d'auteur, SRC 1970, c. C-30, et ses amendements subséquents.

CHEMICAL SHIFT ANISOTROPY IN ^{119}Sn , ^{77}Se , AND ^{125}Te

by

YINGTIAN HE

B.Sc. Nankai University (China), 1984

A THESIS SUBMITTED IN PARTIAL FULFILLMENT OF
THE REQUIREMENTS FOR THE DEGREE OF
MASTER OF SCIENCE
in the Department
of
CHEMISTRY

© YINGTIAN HE 1988

SIMON FRASER UNIVERSITY

December, 1988

All rights reserved. This work may not be reproduced in whole or in part, by photocopy or other means, without permission of the author.



National Library
of Canada

Bibliothèque nationale
du Canada

Canadian Theses Service Service des thèses canadiennes

Ottawa, Canada
K1A 0N4

The author has granted an irrevocable non-exclusive licence allowing the National Library of Canada to reproduce, loan, distribute or sell copies of his/her thesis by any means and in any form or format, making this thesis available to interested persons.

The author retains ownership of the copyright in his/her thesis. Neither the thesis nor substantial extracts from it may be printed or otherwise reproduced without his/her permission.

L'auteur a accordé une licence irrévocable et non exclusive permettant à la Bibliothèque nationale du Canada de reproduire, prêter, distribuer ou vendre des copies de sa thèse de quelque manière et sous quelque forme que ce soit pour mettre des exemplaires de cette thèse à la disposition des personnes intéressées.

L'auteur conserve la propriété du droit d'auteur qui protège sa thèse. Ni la thèse ni des extraits substantiels de celle-ci ne doivent être imprimés ou autrement reproduits sans son autorisation.

ISBN 0-315-59336-9

APPROVAL

Name: Yingtian He

Degree: Master of Science

Title of Thesis: Chemical Shift Anisotropy in ^{119}Sn , ^{77}Se ,
and ^{125}Te

Examining Committee:

Chairman: Dr. P.W. Percival

Dr. I.D. Gay (Senior Supervisor)

Dr. F.W.B. Einstein

Dr. C.H.W. Jones

Dr. E.J. Wells (Internal Examiner)

Date Approved:

Feb 27 / 1989

PARTIAL COPYRIGHT LICENSE

I hereby grant to Simon Fraser University the right to lend my thesis, project or extended essay (the title of which is shown below) to users of the Simon Fraser University Library, and to make partial or single copies only for such users or in response to a request from the library of any other university, or other educational institution, on its own behalf or for one of its users. I further agree that permission for multiple copying of this work for scholarly purposes may be granted by me or the Dean of Graduate Studies. It is understood that copying or publication of this work for financial gain shall not be allowed without my written permission.

Title of Thesis/Project/Extended Essay

CHEMICAL SHIFT ANISOTROPY IN ^{119}Sn , ^{77}Se , AND ^{125}Te

Author:

(signature)

Yingtian He

(name)

Feb. 28, 1989

(date)

ABSTRACT

The chemical shielding tensors of the ^{119}Sn , ^{77}Se , and ^{125}Te nuclei in single crystals of $[\text{tBu}_2\text{SnS}]_2$, $[\text{tBu}_2\text{SnSe}]_2$, and $[\text{tBu}_2\text{SnTe}]_2$ were determined by employing high-resolution solid state NMR techniques. From our NMR data, the orientations of the two-fold screw rotational axis of these compounds in the holder axis system are determined. A two-circle optical goniometer was also used to perform crystallographic investigation of these single crystals which gave us the orientations of these single crystals in the holder system. The results from these two sources are compared and found in good agreement. A mathematical method employing symmetry arguments has been developed to assign the corresponding principal axes to the crystal frame. This mathematical method can be used to find the three Eulerian angles in the transformation of the holder system to the crystallographic axis system, if the crystal we investigate has enough non-redundant symmetry elements. Some speculations have been made about the orientations and the principal values of the chemical shielding tensors in relation to the molecular structures of the compounds. J-coupling tensors ($J_{\text{Sn-Se}}$ and $J_{\text{Sn-Te}}$) for these compounds are also investigated.

The results of our coupling tensor indicate that the Fermi contact terms in ^{119}Sn , ^{77}Se , and ^{125}Te are not the dominant contribution in the J-coupling tensor. The isotropic values of chemical shift tensor and J-coupling tensor from our experiment are nearly the same as those from solution NMR, so the crystal packing effects in these compounds are small (~ 10 ppm).

DEDICATION

to my mother and carol

ACKNOWLEDGEMENT

I would like to thank Dr. I.D. Gay for his helpful and patient supervision as well as for his continuous and informative advice. I am very grateful to Dr. R.D. Sharma for helping me to prepare the crystal samples.

I also express my gratitude to Dr. F.W.B. Einstein, Dr. E.J. Wells, and Dr. C.H.W. Jones for their criticisms, discussions, and comments.

TABLE OF CONTENTS

APPROVAL.....	ii
ABSTRACT.....	iii
DEDICATION.....	v
ACKNOWLEDGMENT.....	vi
TABLE OF CONTENTS.....	vii
LIST OF TABLES.....	ix
LIST OF FIGURES.....	x
INTRODUCTION.....	1
PREVIOUS MEASUREMENTS.....	4
THE OBJECTIVE OF THIS RESEARCH WORK.....	10
EXPERIMENTAL SECTION.....	13
THEORY.....	16
Chemical shielding tensor.....	16
J-Coupling tensor.....	25
METHOD.....	33
RESULTS AND DISCUSSION.....	45
Determination of the chemical shielding tensors.....	45
Determination of the Eulerian angles.....	46
Determination of the principal values of chemical shielding in crystallographic axes.....	55
Conclusion.....	63

Future work.....64
TITLES OF FIGURES 8-18.....66
Figures 8-18.....68
APPENDIX I.....97
APPENDIX II.....118
REFERENCES.....122

LIST OF TABLES

<u>Table</u>		<u>Page</u>
1	Lattice constants of the crystals	14
2	Bond lengths and angles of the crystals	14
3	The results of angle θ	50
4	The final results of angles α and θ	51
5	Principal values and direction cosines of the chemical shielding tensors relative to the crystallographic axes	56
6	Principal values and direction cosines of the D tensor relative to the crystallographic axes	58
7	The isotropic values of the chemical shift and J-coupling	59

LIST OF FIGURES

<u>Figure</u>		<u>Page</u>
1	B_0 in (x,y,z) system	22
2	(x,y,z) fixed to the holder	33
3	Instrument system	34
4	Orientation 1 (O1)	35
5	Orientation 2 (O2)	36
6	Orientation 3 (O3)	37
7	Orientation of the cube axes with respect to the crystallographic axes	41
8-18		66
19	Miller indices and morphology of a single crystal $[tBu_2SnSe]_2$	52
20	Relationship between (a,b,c*) and (x,y,z) of single crystal $[tBu_2SnSe]_2$	53
21	Miller indices and morphology of a single crystal of $[tBu_2SnTe]_2$	54

INTRODUCTION

The chemical shift arises from the electronic screening of the nucleus by the surrounding electrons. Since this screening is a three-dimensional quantity, the chemical shift will be anisotropic. As the anisotropy in shifts results from the distribution of electrons surrounding the nucleus, chemical shift tensors give new information about electronic structure and present a detailed three-dimensional view of important features of chemical bonding.

The complete chemical shielding interaction is given by a tensor which depends upon the electronic structure of the molecule and can be used to describe how the NMR resonance frequency changes with the molecular orientation in the external magnetic field. In nonviscous liquids, however, only the average of the principal values of the tensors, i.e. the isotropic liquid shift, is observed due to the averaging from the rapid rotational motion, and empirical chemical shift/structure relationships have made solution NMR the most widely used technique for the elucidation of unknown structures.

The determination of these tensors is important for several reasons: firstly, these tensorial shifts with three principal values have the potential to reveal up to 3 times the information of isotropic shifts available from conventional liquid experiments. Therefore the comparison with theoretical calculations is much more sensitive and meaningful. Secondly, these tensors reflect the local structure and symmetry around the nucleus. The orientation of the principal axes of the shielding tensors follows the local symmetry and therefore can be used as a probe to obtain a "three-dimensional" view of important features of chemical bonding. Finally, the orientations of the principal axes of the chemical shielding tensors and their magnitudes are also sensitive to the molecular conformation, molecular motion and the strength of any intermolecular hydrogen bonding involved.

Studies of electron-coupled spin-spin interactions which are observed in nuclear magnetic resonance spectra of liquids are of considerable interest because of the strong dependence of these interactions on the electronic environments of the coupled nuclei. In attempting to correlate this wealth of information with other physical properties of molecules, many theoretical studies have been made. In spite of the theoretical and computational difficulties of such calculations, a surprising degree of success has been achieved

in the correlation of measured spin-spin coupling constants with molecular orientation, substituent effects, and other properties. [1]

The indirect electron-coupled spin-spin interaction between two nuclei (J coupling) is also anisotropic, [2] described by a second rank tensor J:

$$H_1 = I_1 \cdot J \cdot I_2 \quad (1)$$

This coupling is usually observed as its isotropic average J observed in liquids.

$$J_{iso} = 1/3 \cdot \text{Tr } J \quad (2)$$

Why one should wish to study the anisotropy of J coupling? The reason is that the J coupling is a probe of molecular electronic structure. The eigenvalues and eigenvectors of the coupling tensor potentially provide much more stringent tests than the angular average coupling J of molecular wave functions. On a more empirical level, experimental knowledge of J-coupling tensors may lead to better correlations between NMR and structure than J itself has done.

PREVIOUS MEASUREMENTS

So far, most of shielding tensor works have studied ^1H , and ^{13}C . Some dealt with ^{19}F ; ^{31}P , and ^{29}Si . Papers on the heavy metal elements are very few and mainly on simple inorganic solids[3,4].

Proton shielding tensors In this most difficult domain of high resolution NMR in solids, a breakthrough has been brought about by the multiple-pulse methods. Haeberlen and co-workers [5-7] have pushed this field and determined a large number of shielding tensors from powder and single crystal samples. They investigated the prototype compounds containing 'typical' aliphatic-, aromatic-, olefinic-, and carboxylic- bonding situations to look for a relation between bonds and the tensor properties of shifts.[5]

Carbon-13 shielding tensors The biggest supply of ^{13}C shielding tensors has been furnished by Pines, Waugh and co-workers[8,9] applying cross-polarization techniques. Shielding tensors of ^{13}C in various kind of functional groups can be found in ref.[10]. A detailed discussion of ^{13}C shielding tensors may be found in the reviews of Spiess [11] and Veeman [12].

Recently, the papers on the chemical shielding tensor are mainly in the following aspects.

1. Determination of the chemical shielding tensor of a specific compound.

Looser and Brinkmann investigated ^{109}Ag chemical shift in RbAg_4I_5 , KAg_4I_5 , $\text{Ag}_{26}\text{I}_{16}\text{W}_4\text{O}_{16}$ and Ag_3BrS . [13]

Brownlee and co-workers investigated ^{95}Mo in $[\text{Mo}(\text{CO})_{6-n}(\text{pyridine})_n]$ complexes. [14]

Van Calstern and co-workers determined ^{31}P chemical shielding tensor in 2-aminothylphosphonic acid. [15]

2. Use chemical shielding tensor as a probe to investigate molecular structures, intermolecular or intramolecular interactions, and molecular motions.

Haeberlen and co-workers investigated and determined principal components and direction cosines of the proton shielding tensors of waters of hydration in single crystals of $\text{Na}_2\text{Fe}(\text{CN})_5\text{NO}\cdot 2\text{H}_2\text{O}$ [16, 17] and $\text{K}_2(\text{C}_2\text{O}_4)\cdot \text{H}_2\text{O}$ [18].

Variable temperature studies of these crystals revealed motions of the H_2O molecules in addition to the well-established flips. The temperature dependence of the rate constant of the flip motions corresponds to an activation energy of 64.4 kJ/mol in the oxalate

monohydrate.

^{13}C shielding tensors in single crystals of dimedone (5,5-dimethyl-1,3-cyclohexanedione) [19] and tetraacetylene[20] are determined in a study of the effects of the intermolecular hydrogen bonding on the carbonyl carbon in dimedone and the effects of intramolecular hydrogen bonding on the carbonyl and adjacent carbons in the acetylacetonate residues in the second compound. The two important effects are that (a) the shielding tensor component along the $\text{C}=\text{O}$ bond direction shows a strong deshielding (~ 50 ppm) and (b) this becomes the least shielded component so the shielding tensor ellipsoid has a different long axis compared to acetophenone, for example.

The chemical shielding tensors of the ^{13}C nuclei in Meldrum's acid (2,2-dimethyl-1,3-dioxane-4,6-dione) were also determined.[21] The tensors of two ester carbon nuclei in Meldrum's acid were compared with each other and also with those of the carboxyl carbon nuclei in Malonic acid. Takegoshi and McDowell assumed that differences in the tensors of the two ester carbon nuclei are attributed to the different intermolecular $\text{C}=\text{O} \cdots \text{H}-\text{C}$ interactions reported in an X-ray crystallographic study.[22] They

applied a one-dimensional exchange NMR technique[23] at various temperatures to determine the rate of the interchange of the location of the two ester carbon nuclei in the crystal lattice. The dynamic process is postulated to be ring inversion plus a rotation of the molecule by 180° , and the associated activation energy was determined to be 91.4 kJ/mol.

Floch and Pannetier used ^1H NMR to investigate the defect pyrochlores $\text{H}_2\text{Ta}_2\text{O}_6$, HTaWO_6 and their hydrates.[24]

Hinton and Metz showed $^{205}\text{Tl}^+$ NMR spectroscopy is a good technique for studying the interaction between antibiotic ionophores and metal cations.[25]

3. Combination with theoretical calculations.

Facelli and co-workers showed that the combination of low-temperature ^{13}C NMR with quantum mechanical calculation of the chemical shielding tensors is very valuable to validate the ab initio wave functions which provide information on the electronic structure of small organic molecules.[26]

Studies on carbon atoms in a wide range of bonding situations have been completed, including methyl groups [27], methine carbons[28], methylene carbons[29] and olefinic carbons [30]. Other studies have looked at

carbons in linear molecules [31] and in the series cyclopropane, bicyclo [1.1.0] butane, and [1.1.1] propellane [32]. In their recent work, Facelli and co-workers reexamined the relationship of ^{13}C shielding tensors with an anisotropic π -electron charge distribution on aromatic compounds by using available ^{13}C tensorial information [33] on C_7H_7^+ , C_6H_6 , and C_5H_5^- . They also found that the experimental ^{13}C shielding tensors also can be used as a powerful tool in the analysis of the degree of delocalization of π -electrons in aromatic compounds.[26]

Amm and Hunter have made an investigation on ^1H NMR line shape of the anhydrous alkali metal hydroxides. They discussed a planar zigzag array of four-spins. Second moment calculations show that the observed line shapes are consistent with known crystal structure.[34]

Wasylishen and co-workers determined isotope shift and spin-spin coupling constants in the ^{13}C and ^{17}O NMR spectra of carbon monoxide and carbon dioxide and compared experimental results with theoretical calculation.[35]

The pioneering work on J-coupling anisotropy was done by Tutunjian and Waugh.[36] They determined the ^{31}P - ^{31}P spin-spin coupling tensor from a single crystal NMR study of tetraethyldiphosphine disulfide. Jokisaari *et al.* determined anisotropy of the indirect ^{13}C - ^{19}F spin-spin coupling of methyl fluoride- ^{13}C in nematic liquid crystal.[37] The topic of J coupling anisotropy from NMR spectroscopy of molecules oriented by liquid crystal solvents has also been reviewed by these workers [38]. Emsley *et al.* reviewed the coupling constants in fluorine compounds [39] and Hansen extensively reviewed the carbon-hydrogen spin-spin coupling constants [40]. Kowalewski has a good review of theoretical calculation of J coupling [41].

THE OBJECTIVE OF THIS RESEARCH WORK

Multiple pulse NMR and Cross-polarization of dilute spins are the most prominent techniques for evaluating the chemical shielding tensor σ of nuclei in solids. Other methods for partial determination of the chemical shielding tensor, like the "second moment" analysis, the NMR of partially oriented molecules dissolved in clathrates or liquid crystals are mostly unreliable. Reviews of these methods have been given by Bastiaan *et al.* [42], Emsley and Lidon [43], and Appleman and Dailey [44].

The measurement of chemical shielding tensors involves the analysis of single-crystal rotation data or line shape analysis of powder samples where small crystallites orient in all possible directions. The cross-polarization method is used to enhance the sensitivity with high-power ^1H decoupling to eliminate the ^1H -metal dipolar interactions.[45,46]

The principal tensorial shielding values can be obtained from spectral patterns obtained on powdered solids. However, no information is obtained about the orientation of the principal axes of the tensor.

When the molecule contains several chemically different atoms, the powder spectrum is a superposition of powder line shapes of the individual atoms. Usually this makes it very difficult to determine the principal elements of the shift tensor for each chemically distinct atom, and in these cases magic angle spinning (MAS) can be very helpful. In an MAS experiment, the powder pattern breaks up into a relatively narrow line at the isotropic chemical shift (the centerband) and sidebands at distances nw_R ($n = 1, 2, \dots$; w_R is the spinning frequency) from the centerband. The intensities of the sidebands are related in a complicated way to the spinning frequency w_R and the chemical shift tensor parameters [47]. Therefore, the principal values of the shift tensor can be determined from the sideband intensities.[48]

Use of single-crystal spectroscopic techniques provides a superior method for obtaining both principal tensorial values as well as the orientation of the corresponding principal axes, but unfortunately, single-crystal methods suffer from the difficulties associated with growing crystals, which must be larger than those typically used for X-ray structural analysis, and from the need for extensive methods of data reduction.

In the present research, the single-crystal method is used to measure the chemical shielding tensor of $[(t\text{-Bu})_2^{119}\text{SnS}]_2$, $[(t\text{-Bu})_2^{119}\text{Sn}^{77}\text{Se}]_2$, and $[(t\text{-Bu})_2^{119}\text{Sn}^{125}\text{Te}]_2$.

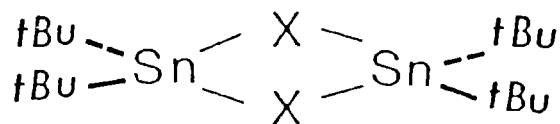
The reason we choose these compounds is two-fold. (1). These compounds can be easily grown as big crystals. (2). The proton relaxation time of these compounds is relatively short due to the motion of the methyl group in these compounds.

The crystal structures of these three compounds are not completely known, (there are only partial data available) [50]. A mathematical method employing symmetry arguments has been developed to assign the corresponding principal axes to the crystal frame.

J-coupling ($J_{\text{Sn-Se}}$ and $J_{\text{Sn-Te}}$) tensors for these compounds are also investigated. The three principal values in the crystal frame have been obtained.

EXPERIMENTAL SECTION

We have synthesized di-tert-butyltin chalcogenides

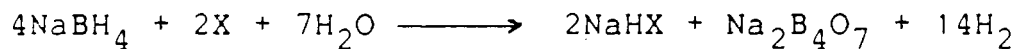


(a), X=S

(b), X=Se

(c), X=Te

by the following routes according to references [49,50].



X = Se, Te

and



Single crystals of $[\text{tBu}_2\text{SnX}]_2$ were grown by slow evaporation from a saturated hexane solution at ambient temperature.

The crystals are monoclinic having two molecules in the unit cell [50]. The crystal data from reference [50] have been listed in Table 1 and Table 2.

Table. 1. Lattice Constants

	a [Å]	b [Å]	c [Å]	β [°]	cell vol. [Å ³]	space group
a[51]	11.05	16.50	6.31	96.2	1144.7	$P2_1-C_2$
b[52]	8.77	12.25	12.01	114.8	1172.5	$P2_1/c-C_2h$
c[53]	8.74	12.50	12.14	114.0	1213.1	$P2_1/c-C_2h$

Errors in these values are not available.

Table. 2. Bond Lengths [Å] and Angles [°]

	Sn-X	Sn-C	XSnX	SnXSn	CSnC
a	2.49 2.38	2.21 2.17	94.3	84.0	114.4
	2.47 2.42	2.23 2.26	94.0	87.6	117.3
b	2.55	2.16 2.20	97.5	82.5	115.1

Errors in these values are not available.

NMR spectra were obtained at ambient temperature by proton-enhanced nuclear induction spectroscopy using a FT spectrometer constructed in this laboratory. The crystal was attached to a single-circle goniometer. The goniometer could be read with an accuracy of $\pm 2^\circ$.

Spectra were recorded at 22.38MHz, 11.4405MHz and 18.914MHz, respectively, for Sn^{119} , Se^{77} and Te^{125} . The cross-polarization technique was used, and 5000 to 20000 transients were collected with use of a contact time of 1 to 2 ms and recycle times of 0.5 sec. Experimental shieldings were referenced to external samples of Me_4Sn , H_2SeO_3 and ph_2Te_2 for Sn^{119} , Se^{77} and Te^{125} , respectively. Calculations were performed to change references from H_2SeO_3 and ph_2Te_2 to Me_2Se and Me_2Te , respectively, in the case of Se^{77} and Te^{125} spectra, using data from ref. [54]

Spectra were collected at 10° intervals in the range of 0° - 180° without interruption. The experimental data were analyzed by using the MINUIT fitting program[75,76].

THEORY

1. Chemical Shielding Tensor

In a nuclear magnetic resonance experiment, the resonance frequency of a nuclear spin I is determined not only by the gyromagnetic ratio but also by the interaction of the nuclear spin with the surrounding electrons. When a magnetic field is applied to a sample, a precession is superimposed on the motion of all electrons in the sample. This rotation of the electron cloud will give rise to a secondary magnetic field at the nuclei which for spherically symmetric molecules, opposes the external magnetic field, and this causes a shielding of the nuclear spins from the external magnetic field.

In molecules where the electron distribution is not at least tetrahedrally symmetric, the electron cloud in general is not free to precess around the direction of the external magnetic field. Then the induced local field at a certain nuclear spin in general is not parallel to the applied field B_0 .

The quantum mechanical expressions for shielding can be derived from second-order perturbation theory. The classical energy of interaction between a magnetic moment μ_α and a magnetic field B_β is given by

$$E = \sum \mu_\alpha (1 - \sigma_{\alpha\beta}) B_\beta \quad (\alpha, \beta = x, y, z) \quad (3)$$

It can be shown that the shielding tensor can be expressed in the following differential forms:

$$\sigma_{\alpha\beta} = \frac{\delta^2 E}{\delta B_\beta \delta \mu_\alpha} = \frac{\delta^2 E}{\delta \mu_\alpha \delta B_\beta} \quad (4)$$

$$\sigma_{\beta\alpha} = \frac{\delta^2 E}{\delta B_\alpha \delta \mu_\beta} = \frac{\delta^2 E}{\delta \mu_\beta \delta B_\alpha} \quad (5)$$

It is clear that these two expressions are not necessarily equivalent — an asymmetry may exist. So σ must be represented by a 3x3 matrix. In a coordinate system x, y, z tied to the frame of the molecule under consideration, the chemical shift tensor is represented by nine components:

$$\sigma = \begin{bmatrix} \sigma_{xx} & \sigma_{xy} & \sigma_{xz} \\ \sigma_{yx} & \sigma_{yy} & \sigma_{yz} \\ \sigma_{zx} & \sigma_{zy} & \sigma_{zz} \end{bmatrix} \quad (6)$$

It is convenient to express the shift tensor as sum of a "diamagnetic part" σ^d and a "paramagnetic part" σ^p . [55,56]

$$\sigma = \sigma^d + \sigma^p \quad (7)$$

The diamagnetic part σ^d of the chemical shift has the following explicit form: [57]

$$\sigma_{\alpha\beta}^d = -\frac{\mu_0}{4\pi} \frac{e^2}{2m_e} \sum_i \left\langle \frac{r_i^2 \delta_{\alpha\beta} - r_{i\alpha} r_{i\beta}}{r_i^3} \right\rangle = \sigma_{\beta\alpha}^d \quad (8)$$

where μ_0 is the permeability of free space and $r_{i\alpha}$ is the position vector of the i th electron relative to some origin (usually chosen at the nucleus of interest); $\delta_{\alpha\beta}$ is the Kronecker delta and $\langle \rangle$ implies an average over the appropriate stationary state (normally the ground state). It is obvious from inspection that the diamagnetic term can be represented by a symmetric second rank tensor with maximum of six components. However, the paramagnetic part σ^p is not necessarily symmetric.

$$\begin{aligned} \sigma_{\alpha\beta}^p = & -\frac{\mu_0}{4\pi} \frac{e^2}{2m_e} \sum_i \{ (E_0 - E_k)^{-1} \langle 0 | \sum_i L_{\alpha i} | k \rangle \langle k | \sum_i L_{\beta i} / r_i^3 | 0 \rangle \\ & + \langle 0 | \sum_i L_{\beta i} / r_i^3 | k \rangle \langle k | L_{\beta i} | 0 \rangle \} \end{aligned} \quad (9)$$

where $L_{\alpha i}$ is the α component of the angular momentum operator of electron i about the nucleus under consideration. E_k is the energy of the state $|k\rangle$.

The "diamagnetic" term $\sigma_{\alpha\beta}^d$ contains only matrix elements involving the ground state wavefunctions, whereas, the "paramagnetic" term, resulting from second order perturbation theory displays the "mixing in" of excited states into the ground state due to the vector potential of the magnetic field. Although this term is of second order, it is by no means small compared with the diamagnetic term.

Any second rank tensor can be written as the sum of an isotropic part, a traceless symmetric part and an antisymmetric part,

$$\sigma_{\alpha\beta} = \sigma\delta_{\alpha\beta} + \sigma_{\alpha\beta}^s + \sigma_{\alpha\beta}^a \quad (10)$$

Where

$$\sigma = 1/3 \sum \sigma_{\gamma\gamma} \quad (11)$$

$$\begin{aligned}\sigma_{\alpha\beta}^s &= \sigma_{\beta\alpha}^s \\ &= 1/2 (\sigma_{\alpha\beta} + \sigma_{\beta\alpha}) - \sigma_{\alpha\beta}^a\end{aligned}\quad (12)$$

$$\sigma_{\alpha\beta}^a = 1/2 (\sigma_{\alpha\beta} - \sigma_{\beta\alpha}) = -\sigma_{\beta\alpha}^a\quad (13)$$

The physical property described by this tensor is observed through the energy E in equation (3). However, only the symmetric parts of σ occur to the first order in the energy; for the anti-symmetric parts $\sigma_{\alpha\beta}^a$, it has been shown [58-60] that it affects the NMR line positions only in the second order and therefore we shall neglect it. A discussion of the antisymmetric chemical shift and how its effect might be observed has been presented by Haeberlen [3]. When only the symmetric part of σ is considered, six unknowns have to be determined before the complete tensor is known.

By a suitable choice of coordinate system, the principal axis system x', y', z' , σ may be converted to a diagonal form with three principal elements $\sigma_{x'x'}$, $\sigma_{y'y'}$, $\sigma_{z'z'}$. These serve to characterize the three-dimensional nature of the shielding. The principal axis systems, one for each nuclear spin, are

fixed to the molecular or crystal frame, at least as long as the molecule is rigid. The chemical shift tensor is completely characterized when the three principal elements and the directions of the three principal axes are known. When the atom observed in the solid lies on a symmetry plane or axis, the directions of these principal axes are, at least partly, determined by these symmetry elements of the point group.

When anisotropic interactions are present, the position of a spin resonance line depends on the orientation of the external magnetic field B_0 relative to the molecular or crystal axes. We can derive an equation for the resonance frequency of a certain spin as a function of the angles the external field B_0 makes with the axes of some coordinate system.

The shift of the eigenstate $|m\rangle$ of the Zeeman Hamiltonian in the presence of chemical shielding is:

$$\langle m | \gamma B_0 \cdot \sigma \cdot I | m \rangle \quad (14)$$

The chemical shift tensor σ is defined in some axis system x, y, z , according to (6). The field B_0 in this system is defined by polar angles θ and ϕ (Fig.1)

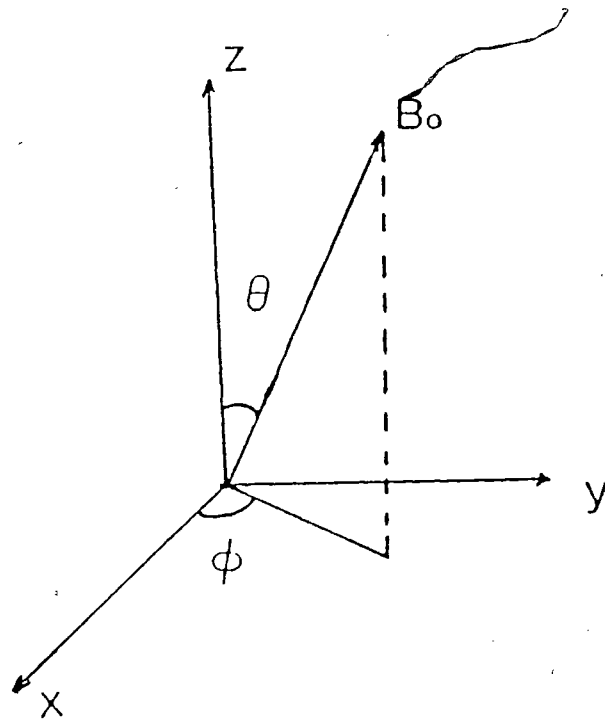


Fig. 1 B_0 in (x,y,z) system

The matrix element in (14) can be easily evaluated when the shift tensor is transformed to an axis system where the z-axis is along B_0 . In this coordinate system only the I_z operator gives a contribution to the matrix element. The transformation of the shift tensor is performed by two consecutive rotations. First around the z-axis of Fig.1 over an angle ϕ and then around the y-axis over the angle θ . The transformed shift tensor σ_L is obtained by:

$$\sigma_L = R_Y(\theta)R_Z(\phi)\sigma R_Z^{-1}(\phi)R_Y^{-1}(\theta) \quad (15)$$

Where $R_Y(\theta)$ and $R_Z(\phi)$ are the rotation matrices and σ_L is the chemical shift tensor in the axis system where B_0 is along the z-axis.

$$R_Z(\phi) = \begin{bmatrix} \cos\phi & \sin\phi & 0 \\ -\sin\phi & \cos\phi & 0 \\ 0 & 0 & 1 \end{bmatrix} \quad (16)$$

$$R_Y(\theta) = \begin{bmatrix} \cos\theta & 0 & -\sin\theta \\ 0 & 1 & 0 \\ \sin\theta & 0 & \cos\theta \end{bmatrix}$$

The matrix element (14) then becomes:

$$\langle m | \gamma B_0 \cdot \sigma' \cdot I | m \rangle = m \gamma B_0 \sigma_L \quad (17)$$

Where

$$\begin{aligned} \sigma_L = & \sigma_{xx} \sin^2\theta \cos^2\phi + \sigma_{yy} \sin^2\theta \sin^2\phi + \sigma_{zz} \cos^2\theta \\ & + \sigma_{yx} \sin^2\theta \sin 2\phi + \sigma_{zx} \sin 2\theta \cos\phi + \sigma_{zy} \sin 2\theta \sin\phi \end{aligned} \quad (18)$$

For spin $I=1/2$ the shift in resonance is given by $\gamma B_0 \sigma_L$ and eq(18) expresses the orientation dependence of the frequency shift. A common procedure consists of the following steps:

1. Mount the crystal in a reorientable holder with assigned axes (x,y,z) .
2. Orient the crystal employing X-ray techniques or symmetry arguments. This gives the crystallographic axes (a,b,c) relative to the holder axes (x,y,z) .
3. Obtain NMR spectra for rotations of the crystal about (x,y,z) perpendicular to B_0 .
4. Analyze the rotation plots to obtain the shielding tensors σ in the holder axes.
5. Transform σ from holder axis system to crystallographic axis system, and diagonalize it. This gives the eigenvalues σ_{ii} and the orientation of the principal axis system $(1,2,3)$ relative to (a,b,c) .

2. J-Coupling tensor

The interaction of nuclear spins is important in high resolution nuclear magnetic resonance spectroscopy; it is composed of a direct dipolar coupling T and an indirect interaction via electrons, J . Our NMR spectroscopic experiment by itself provides the sum of direct dipolar interaction and spin-spin interactions

$$D^{\text{exp}} = T + J \quad (19)$$

The appropriate Hamiltonian for the interaction of nuclei A and B is:[61]

$$H_{AB} = \hbar I_A \cdot (T+J) \cdot I_B = \sum \hbar I_{\alpha}^A \cdot (T_{\alpha\beta} + J_{\alpha\beta}) \cdot I_{\beta}^B \quad (20)$$

where $\hbar I_A$ and $\hbar I_B$ are the angular momenta of the two nuclei. If R is the vector joining them

$$T_{\alpha\beta} = \frac{\hbar}{2\pi} \gamma_A \gamma_B (R^2 \delta_{\alpha\beta} - 3R_{\alpha} R_{\beta}) R^{-5} \quad (21)$$

where γ_N is the gyromagnetic ratio of nucleus N . T is symmetric and traceless, i.e., $T_{\alpha\beta} = T_{\beta\alpha}$ and $\sum T_{\alpha\alpha} = 0$. The

components of T vary as R^{-3} and may have magnitudes of the order of 10^4 or 10^5 Hz. The components of J normally have magnitudes under 10^3 Hz (rarely over 50 Hz for nuclei which are not directly bonded), and may be of either sign [61].

The discovery of J-coupling splittings in the NMR lines of liquids, made independently by Gutowsky *et al* [62,63] and Hahn and Maxwell [64,65] dates back to the initial days of nuclear magnetic resonance. The interaction energy could be expressed by:

$$E_{NN'} = \sum h J_{NN'} \cdot I_N \cdot I_{N'} \quad (22)$$

where h is Planck's constant and $J_{NN'}$ is a coupling constant between nuclei N and N', having nuclear spin I_N and $I_{N'}$, respectively. The interaction between nuclear moments given in Eq.(22) is independent of the applied field and, in contrast to the direct dipolar interaction between nuclear spins, it is independent of the orientation of the coupled spins, and will not vanish when averaged over all orientations by the rapid tumbling motions common in liquids.

It was originally suggested by Hahn and Maxwell [64,65] that the anisotropy of this interaction might give rise to the observed couplings. Quantitative estimates were, however, at

least an order of magnitude smaller than the observed effect.

The mechanism for coupling proposed by Ramsey and Purcell [66] assumes that nuclear spins interact through magnetic polarization by the spin of nearby molecular electrons, and theoretical estimates of this interaction are sufficiently large to account for the observed spectral features. The theoretical developments of Ramsey and Purcell [2,66] form the basis of almost all subsequent work. Ramsey suggested three mechanisms by which the nuclear coupling could be transmitted, and the contribution of each mechanism to the hamiltonian was stated. Thus the total hamiltonian H is written as:

$$H = H_1 + H_2 + H_3 \quad (23)$$

The first part is

$$H_1 = \sum_k (1/2m) [(\hbar/i) \nabla_k + (e/c) \sum_N \hbar \gamma_N I_N \times (r_{kN}/r_{kN}^{-3})]^2 + V + H_{LL} + H_{LS} + H_{SS} \quad (24)$$

where m is the electron mass, r_{kN} is $r_k - r_N$, and r_k is the coordinate of the k 'th electron. The first term in the parentheses allows for the kinetic energy of the electrons and

their interaction as moving charged particles in the magnetic field of the nuclei. The remaining terms, V , H_{LL} , H_{LS} , H_{SS} , are respectively the electrostatic potential energy and the electron orbital-orbital, spin-orbital, and spin-spin interactions, none of which involve the nuclear spin I_N .

The second term is

$$H_2 = 2\beta\hbar \sum_k \sum_N \gamma_N \{ 3(I_N \cdot r_{Nk})(s_k \cdot r_{kN})r_{kN}^{-5} - (I_N \cdot s_k)r_{kN}^{-3} \} \quad (25)$$

and represents the dipole-dipole interactions between the nuclear magnetic moments and the electronic magnetic moments. s_k is the electron spin vector and β is the Bohr magneton $eh/2mc$.

The third part

$$H_3 = \frac{16\pi}{3} \beta\hbar \sum_{k,N} \gamma_N \delta(r_{kN}) s_k \cdot I_N \quad (26)$$

is less easy to interpret in classical terms. $\delta(r_{kN})$ is a Dirac δ function which picks up the value at $r_{kN}=0$ in any intergration over the coordinates of electron k . A term of this sort was introduced by Fermi[67] to explain hyperfine

structure in atomic spectra. Since the δ function depends on the properties of electrons at the nucleus, it is sometimes referred to as the contact term.

To find the nuclear-coupling energies by interaction via the electronic system, it is necessary to treat those parts of the hamiltonian which depend on I_N as a perturbation on the remainder and carry the perturbation calculation to second order. The perturbation hamiltonian can be divided into the part involving the interaction of the electron orbital motion with the nuclear magnetic moments (appropriate terms in H_1) and the part involving the corresponding interaction of the electron spins (H_2 and H_3). Therefore, the total spin coupling constant $J_{NN'}$ in Eq.(22) is, in general given by:

$$J_{NN'} = J_1 + J_2 + J_3 + J_4 \quad (27)$$

Expressions for calculating these terms have been given by Buckingham *et al.* for the SOS (sum over states) method,[68] and the LCAO (linear combination of atomic orbitals) method,[61] and by Ditchfield and Ellis for the FP (finite perturbation) method.[69]

J_1 is the spin-orbital term. It arises from the interaction of the orbital electronic currents with the nuclear magnetic moments. The calculation of J_1 , which arises from H_1 , depends only on a knowledge of the unperturbed wavefunction. It is in general nonsymmetric, the magnitude of this term is always small [39]

$$J_1 = \frac{e^2 \hbar}{3\pi m c^2} \gamma_N \gamma_{N'} \langle 0 | \sum_k \mathbf{r}_{kN} \cdot \mathbf{r}_{kN'} r_{kN}^{-3} r_{kN'}^{-3} | 0 \rangle$$

$$- \frac{4}{3\pi} \beta^2 \hbar \gamma_N \gamma_{N'} (E_n - E_0)^{-1} X \quad (28)$$

$$\langle 0 | \sum_{kj} \sum \mathbf{r}_{kN}^{-3} \mathbf{r}_{jN'}^{-3} (\mathbf{r}_{kN} \times \nabla_k) \cdot (\mathbf{r}_{jN'} \times \nabla_j) | 0 \rangle$$

J_2 , the spin-dipolar term, arising from the direct magnetic dipole interaction between electronic and nuclear spins (hamiltonian H_2), is a second-order term, nonsymmetric and has non-zero diagonal and off-diagonal terms.

$$J_2 = \frac{\hbar}{3\pi} (2\beta)^2 \gamma_N \gamma_{N'} (E_n - E_0) X$$

$$\{ 0 | [3(\mathbf{s}_k \cdot \mathbf{r}_{kN}) \mathbf{r}_{kN} r_{kN}^{-5} - \mathbf{s}_k r_{kN}^{-3}] \cdot$$

$$[3(\mathbf{s}_j \cdot \mathbf{r}_{jN'}) \mathbf{r}_{jN'} r_{jN'}^{-5} - \mathbf{s}_j r_{jN'}^{-3}] | 0 \}$$
(29)

J_3 , the Fermi-contact term, arises from H_3 . In contrast with the other contributions to coupling, the tensor J_3 is symmetric and isotropic. The magnitude of $J_{3\alpha\alpha}$ are such that they are often the dominant contribution to the magnitude of total coupling tensor [61, 77-78].

$$J_3 = -\frac{\hbar}{3\pi} \left(\frac{16\pi\beta}{3}\right)^2 \gamma_N \gamma_{N'} \sum_{nkj} \sum_{\Sigma\Sigma\Sigma} (E_n - E_0)^{-1} \times \quad (30)$$

$$[0 | \delta(\mathbf{r}_{kN}) s_k | n] \cdot [n | \delta(\mathbf{r}_{jN'}) s_j | 0]$$

J_4 , the spin-dipolar, Fermi-contact cross term, is symmetric and has zero sum for the diagonal elements. Ramsey [2] showed that it would average to zero under the condition of frequent collisions.

The coupling tensor J is therefore not necessarily symmetric and in general has nine components. However, symmetry may reduce this number. The isotropic part of J does not vanish.

In the principal axis system which is defined by z-axis along the internuclear vector, the dipolar interactions are directly related to internuclear vectors.

$$T = \frac{\mu_0}{4\pi r^3} (\gamma_1 \gamma_2) h \begin{bmatrix} 1 & 0 & 0 \\ 0 & 1 & 0 \\ 0 & 0 & -2 \end{bmatrix} \quad (31)$$

where r is the distance between two spins 1 and 2. If we know r from the crystal structure we can calculate T , then using equation (19) we can evaluate J .

METHOD

The crystal to be investigated is mounted in a nylon right angle, all sides of which are of equal length. The holder can be connected to a simple goniometer in three orthogonal ways. The rotation axis of the goniometer is perpendicular to the external magnetic field B_0 . We define an axis system x, y, z fixed to the holder — the holder system, where x, y, z are perpendicular to three faces of the holder.

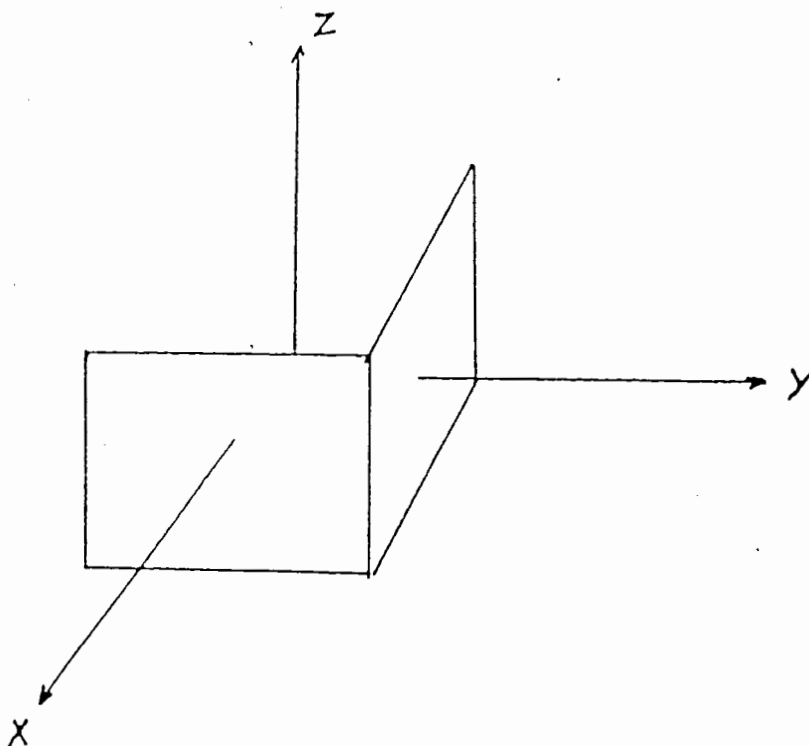


Fig.2 (x, y, z) fixed to the holder

B_0 in this system can be determined by polar angle θ and ϕ . (see fig.1) The general equation of chemical shielding tensor σ in this cube system can be expressed by equation (18). In our NMR instrument, we can define another axis system P, B_0 and R fixed to the instrument — instrument system, where P is the pointer of the goniometer; B_0 is the external magnetic field and R is the rotational axis.

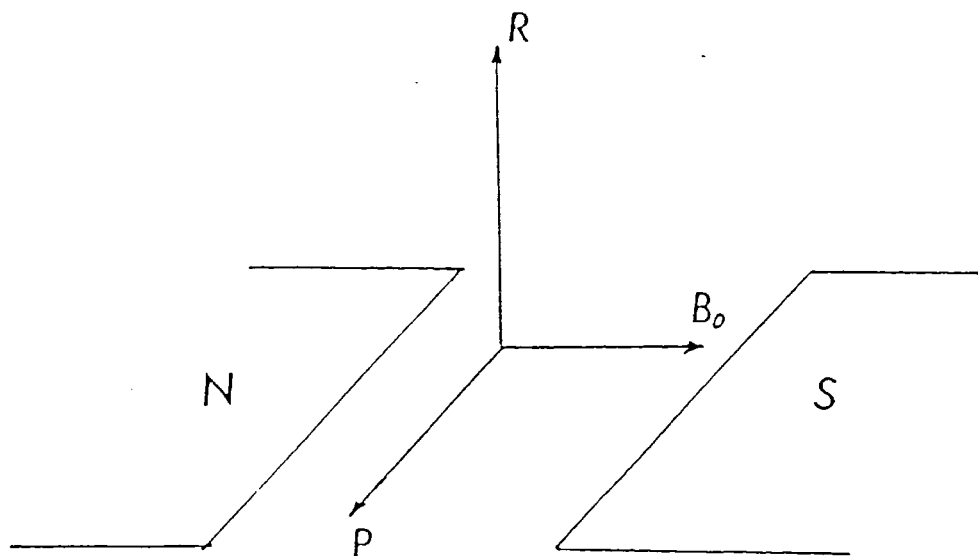


Fig.3 Instrument system

To determine chemical shielding tensor σ in the holder system (x,y,z) , we will mount holder to the instrument in the following way:

For the first rotational plot (O1), z is parallel to the rotational axis R . The magnetic field B_0 , is rotated in the xy plane. The starting position of B_0 is parallel to y , so P is parallel to x automatically.

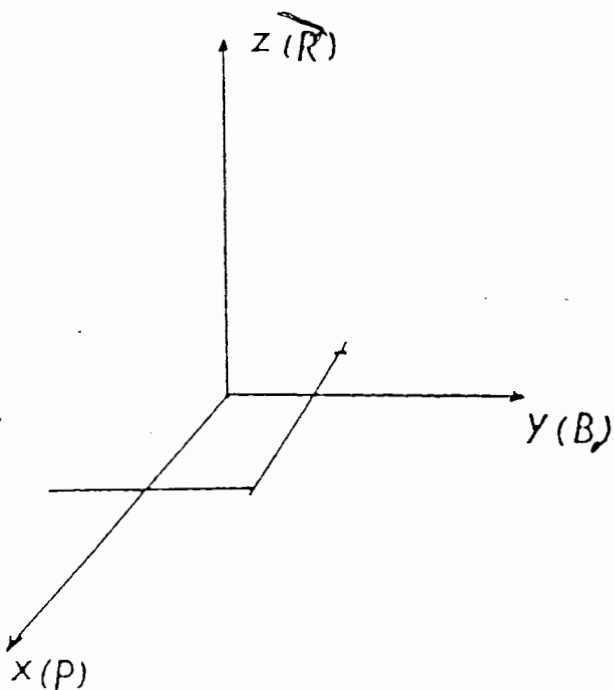


Fig. 4 Orientation 1 (O1)

In this case, the polar angle $\theta=90^\circ$. $\phi=90^\circ+\delta$; δ is the reading on the goniometer, i.e. in O1 δ is the angle between x and P. The observed chemical shielding will be

$$\sigma = \sigma_{xx} \sin^2 \delta + \sigma_{yy} \cos^2 \delta - \sigma_{xy} \sin 2\delta \quad (32)$$

For the second rotational plot (O2), y is the rotational axis and B_0 is rotated in the xz plane. The starting position is that B_0 is parallel to x and P is parallel to z; then the polar angle $\theta' = 90^\circ + \delta$, $\phi = 0^\circ$; the chemical shielding is

$$\sigma = \sigma_{xx} \cos^2 \delta + \sigma_{zz} \sin^2 \delta - \sigma_{xz} \sin 2\delta \quad (33)$$

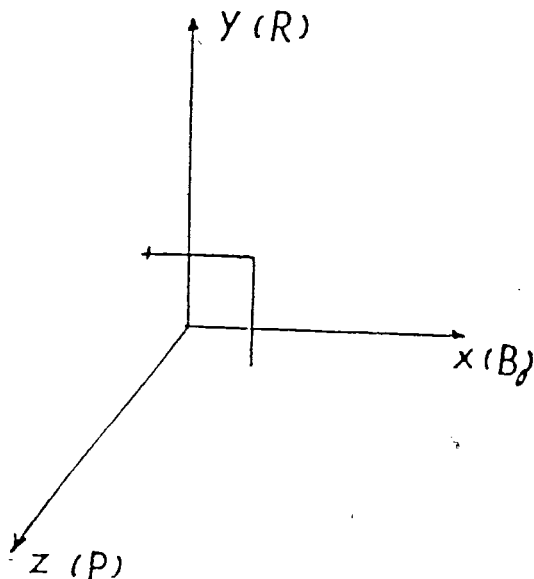


Fig. 5 Orientation 2 (O2)

For the third rotational plot (O3), x is the rotational axis and B_0 is rotated in the yz plane. The starting position is that B_0 is parallel to z and P is parallel to y .

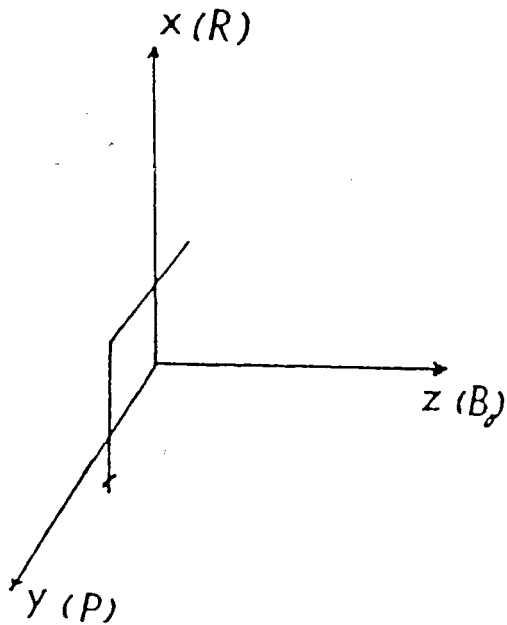


Fig. 6 Orientation 3 (O3)

The polar angle $\theta = -\delta$, $\phi = 90^\circ$; the chemical shielding tensor σ is

$$\sigma = \sigma_{yy}\sin^2\delta + \sigma_{zz}\cos^2\delta - \sigma_{yz}\sin 2\delta \quad (34)$$

Thus from each rotational plot, three components can be determined by measuring the experimental shift as a function of δ and using the MINUIT fitting program. After measuring and fitting the three rotational plots, we can determine the chemical shielding tensor σ in the cube system *i.e.* the holder system (x,y,z) .

We are interested in the orientation of the chemical shift principal axes relative to the molecular axes and therefore have to know the tensor components in the molecular system. It is, however, convenient to transform first from the holder axis system (x,y,z) to the crystal axis system. In the crystal axis system the relation between tensors belonging to symmetry related molecules takes a particularly simple form. Two tensors belonging to chemically equivalent functional groups in two molecules related by certain symmetry operation, should be transformable into each other by applying that symmetry operation. If not, the difference gives an indication of the accuracy of the measured tensor elements.

An orthogonal crystal axis system a, b, c is defined. For an orthorhombic crystal, for instance, the choice of the axes is evident. For monoclinic crystal, if we assign the b -axis as the unique axis, the c -axis of the above defined axis system corresponds to the monoclinic c^* -axis.

The transformation from the holder axis system (x, y, z) to the crystal axis system (a, b, c^*) is performed in two steps. For the first step, use has to be made of one symmetry element of the crystal under study. For instance, in the monoclinic system, the ac^* -plane is a plane of reflection, i.e. when B_0 lies in the ac^* -plane, all symmetry-related molecules in the unit cell become magnetically equivalent. Each rotational plot contains such an angle (since all planes cross the ac^* -plane unless a rotation axis is fortuitously along the b -axis.) and this, in principle, can be used to find the orientation of the ac^* -plane relative to the holder axes [70]. Figure 7 shows the orientation of the holder axis system (x, y, z) in the crystal axis system (a, b, c^*) .

Step 1: with a rotation around the z -axis we transform to the primed sample axis system (x', y', z') for which $z'=z$ and the y' -axis is parallel to the line of intersection between the xy -plane and ac^* -plane. Then, automatically, the x' -axis is located in the plane formed by the z' -axis and the

crystallographic b-axis. This transformation is described by the rotation matrix R_1 :

$$R_1 = \begin{bmatrix} \cos\alpha & \sin\alpha & 0 \\ -\sin\alpha & \cos\alpha & 0 \\ 0 & 0 & 1 \end{bmatrix} \quad (35)$$

where α is the angle between x and x' ; α can be determined from the first orientation plot, using the fact that the ac^* -plane is a plane of reflection in the monoclinic system.

Step 2: the primed sample axis system (x',y',z') is rotated to the crystal axis system (a,b,c^*) by first a rotation over θ around the y' -axis and then a rotation over $-\phi$ around the b -axis. The transformation matrices are R_2 and R_3 . A positive rotation is defined here as one that advances a right-hand screw along the axis of rotation.

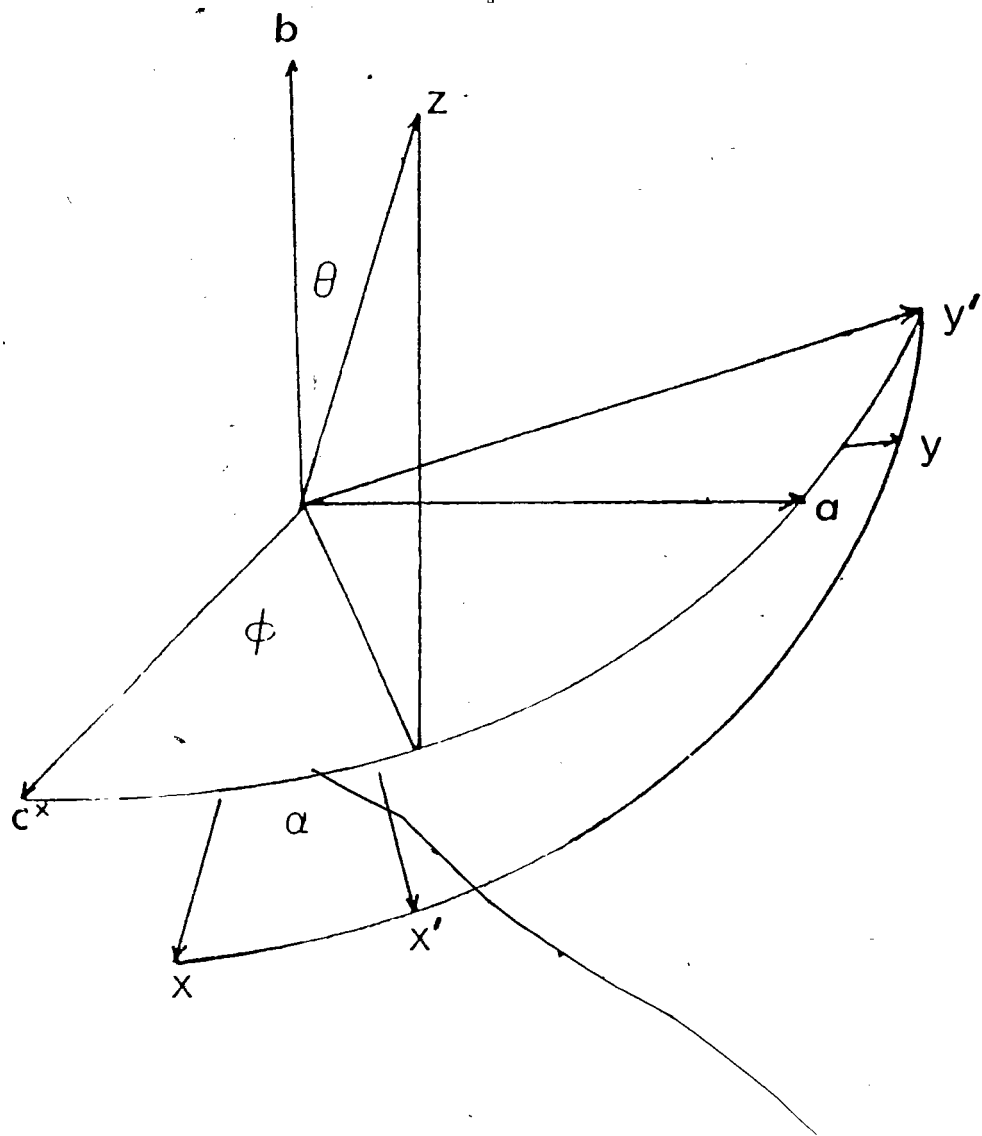


Fig. 7 Orientation of the Cube Axes with Respect to the Crystallographic Axes

The total rotation operator is now a product of three operators:

$$R_T = R_3 R_2 R_1 \quad (36)$$

Equation (36) expresses the fact that the rotation R_T is carried out by the three successive Euler rotations. The axes of rotations are coordinate axes of different coordinate systems. Namely, the coordinate system obtained by the previous rotation. We know that [71,72] a linear homogeneous transformation which preserves lengths and angles (unitary transformation V) transforms an operator σ into $V\sigma V^{-1}$. Thus the expressions of the transform matrices can be derived according to fig.7.

$$R_2 = \begin{bmatrix} \cos\theta & 0 & \sin\theta \\ 0 & 1 & 0 \\ -\sin\theta & 0 & \cos\theta \end{bmatrix}$$

$$R_3 = \begin{bmatrix} \cos\phi & -\sin\phi & 0 \\ \sin\phi & \cos\phi & 0 \\ 0 & 0 & 1 \end{bmatrix} \quad (37)$$

Where θ and ϕ are the polar angles of the holder axis z in the crystal axis system (a, b, c^*) . (see fig.7)

In principle the orientation of this holder axis z (the first rotation axis) with respect to the crystal axis system can be determined by X-ray diffraction. In that case, the problem is solved. Using the transformation matrices (35) and (37) we obtain the chemical shift tensor $\sigma(k)$ for peak k in the crystal axis system:

$$\sigma(k) = R_T \sigma_C(k) R_T^{-1} \quad (38)$$

$\sigma_C(k)$ is the chemical shift tensor for peak k in the cube system. If the crystal structure is known, the tensors $\sigma(k)$ can then be transformed to the molecular axes. Diagonalization in the molecular axis system, finally, yields the principal elements and the orientation of the principal axes relative to the molecular axes.

If the orientation of the first rotation axis z can't be determined by X-ray techniques, then in many cases symmetry arguments can be used to determine θ and ϕ . We know that any physical property of a crystal must be invariant under the symmetry operations of the point group of the crystal. Otherwise, observation of the property could distinguish among what are supposed to be indistinguishable directions. This is known as Neumann's principle. For example, suppose that in the crystal two molecules 1 and 2 are related by a symmetry

operation S, the molecules are chemically equivalent but magnetically inequivalent. The two chemical shift tensors in the crystal axis system, $\sigma(1)$ and $\sigma(2)$, are related according to the transformation:

$$\sigma(2) = S\sigma(1)S^{-1} \quad (39)$$

From the relations

$$\begin{aligned} \sigma(1) &= R_T \sigma_C(1) R_T \\ S\sigma(1)S^{-1} &= R_T \sigma_C(2) R_T \end{aligned} \quad (40)$$

where $\sigma_C(i)$ is the chemical shielding tensor in the holder system, expressions can be found for θ and ϕ . Once θ and ϕ are known, we can proceed by transforming to the crystal axis system and by using crystal structure data, to the molecular axis system.

Results and Discussion

1. Determination of the chemical shielding tensors

The NMR spectra for single crystals of compounds **a**, **b**, and **c** were obtained as a function of the angle of rotation about the three orthogonal axes x , y , and z . Representative single crystal NMR spectra of compounds **a**, **b**, and **c** are presented in Figures 8-10, and Figures 11-18 show the orientation dependence of the ^{119}Sn , ^{77}Se , and ^{125}Te NMR line positions when the static magnetic field is in the xy , xz , and yz planes respectively. The experimental values of the orientational dependence of chemical shift, $\sigma(\delta)$, were MINUIT fitted to the equations 33-35, according to the orientation. The detailed results are collected in Appendix I.

The di-tert-butyltin chalcogenides have two molecules in the unit cell and hence four Sn or chalcogen atoms in the unit cell, the space group of these compounds is $P2_1/c$ [50]. Since atoms related by a centre of inversion always have the same resonance frequency, this means that there is only one line when the static magnetic field is in the crystallographic ac^* plane, and in any other situation, there should be two lines.

One thing we should mention at this point, in the reference 50, H. Puff *et al.* determined the space group of compound a as $P2_1$. If this is correct, there will be no center of symmetry, therefore, we should see four lines instead of two lines when the static magnetic field is not in ac^* -plane, and two lines instead of one line when the static magnetic field is in ac^* -plane. From Figure 8, we can see that this is definitely not our case, so we believe that there is a center symmetry in compound a. The alternative would be space group $P2_1$ with only one molecule in the unit cell, but from Table 2 we can see that cell volumes of these three compounds are almost the same, so we can eliminate this possibility.

2. Determination of the Eulerian Angles

The orientation of a crystal in space may be specified in terms of three Eulerian angles α , θ , and ϕ , which show the relationships between a set of cartesian axes e_i that are fixed in space and another set of cartesian axes e'_i that are attached to the crystal. In our case, e_i is the holder axis system (x,y,z) and e'_i is the crystal axis system (a,b,c^*) , the relationship between these two axis systems is shown in Fig.7.

(1) Determination of Angles α and θ

The angle α in R_1 is the angle between x and x' . From O_1 we can see that after R_1 , B_0 will be along the y' -axis (the intersection of the ac^* plane and the xy plane), that means at the angle α only one line appears in the NMR spectrum. Thus α can be read from O_1 . This analysis produced two results of the angle α for each determination.

The angle θ can be determined by using the relationship between a plane in space and a line in space. From O_2 and O_3 , we know intersections of the ac^* plane with the xz plane and the ac^* plane with the yz plane (see Fig.5 and Fig.6), from these two lines and a point $(0,0,0)$, we know the expression of the ac^* plane, say it is,

$$Ax + By + Cz + D = 0 \quad (41)$$

the b -axis is perpendicular to the ac^* plane. Suppose it has the expression

$$\frac{x - x_1}{p_1} = \frac{y - y_1}{q_1} = \frac{z - z_1}{r_1} \quad (42)$$

then p_1, q_1, r_1 and A, B, C have the relation

$$p_1/A = q_1/B = r_1/C \quad (43)$$

Angle θ is the angle between the b -axis and the z -axis, the expression for z -axis is:

$$x = y = 0 \quad (44)$$

so we have:

$$p_2 = 0, \quad q_2 = 0, \quad r_2 = 1. \quad (45)$$

$$\cos\theta = \frac{p_1 p_2 + q_1 q_2 + r_1 r_2}{[(p_1^2 + q_1^2 + r_1^2)(p_2^2 + q_2^2 + r_2^2)]^{1/2}} \quad (46)$$

$$= \frac{C}{(A^2 + B^2 + C^2)^{1/2}}$$

This method produced two results of the angle θ for each angle α . The results are collected in Table 3.

Now let us consider the equation 39, after we applied the symmetry consideration on them, the two symmetry-related tensors σ_{ij} and σ'_{ij} are related by a two-fold rotational axis,

hence will have the following equations

$$\begin{aligned}\sigma_{13} &= -\sigma'_{13} \\ \sigma_{23} &= -\sigma'_{23} \\ \sigma_{33} &= \sigma'_{33}\end{aligned}\tag{47}$$

From these equations, we will have another set of θ for each α . Comparing the results from these two methods we will choose the common one as the final results of α and θ . Table 4 collects these final results.

Table 3. The results of angle θ [$^{\circ}$]

	α	θ^1	θ^2	AVE.	ϵ_{n-1}
a(Sn)	25.6	124.08	123.16	123.6	0.6
		55.92	-	-	-
	76.8	47.77	48.62	48.2	0.6
		132.23	-	-	-
b(Sn)	37.62	28.50	-	-	-
		151.50	-	-	-
	132.85	91.35	92.27	91.81	0.6
		88.65	-	-	-
b(Se)	32.94	12.75	-	-	-
		167.25	-	-	-
	123.60	87.09	-	-	-
		92.91	93.96	93.44	0.7
c(Sn)	122.57	56.65	-	-	-
		123.35	-	-	-
	175.84	46.49	-	-	-
		133.51	132.09	132.8	1
c(Te)	120.62	123.19	-	-	-
		56.81	-	-	-
	174.05	48.88	-	-	-
		131.12	131.59	131.36	0.3

α is the angle in R_1 (Eq.36). θ^1 is from the mathematical method (Eq.52). θ^2 is from the symmetry conditions (Eq.53). ϵ_{n-1} is standard deviation of θ^1 and θ^2 .

Table. 4 The Final Results of Angle (α, θ) [$^{\circ}$]

	α	θ
a(Sn)	26 77	124 48
b(Sn)	133	92
b(Se)	133	93
c(Sn)	176	133
c(Te)	174	131

As we can see from Table 4, the same compound will have the same values of angle α and θ . These values are independent of the nuclei we detect. The angle ϕ can not be determined by this method, due to the shortage of symmetry elements in these compounds.

(2) Determination of Angle ϕ

With the help of a two circle goniometer, we carried out goniometric examination of the crystal, which enables the angles which the various crystal faces make with each other to be determined [73-74]. The details of the measurement are presented in Appendix II.

The single crystal of compound **b** is platelike, the most developed face is $(01\bar{1})$ illustrated in Fig. 19

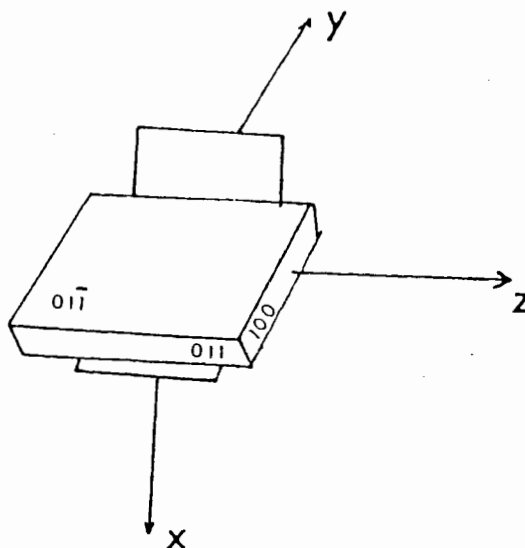


Fig. 19 Miller indices and morphology of a single crystal of $[\text{tBu}_2\text{SnSe}]_2$

The relationship between the crystal coordinate system (a, b, c^*) and the holder system (x, y, z) is illustrated in Fig. 20, using the crystallographic data of reference [50].

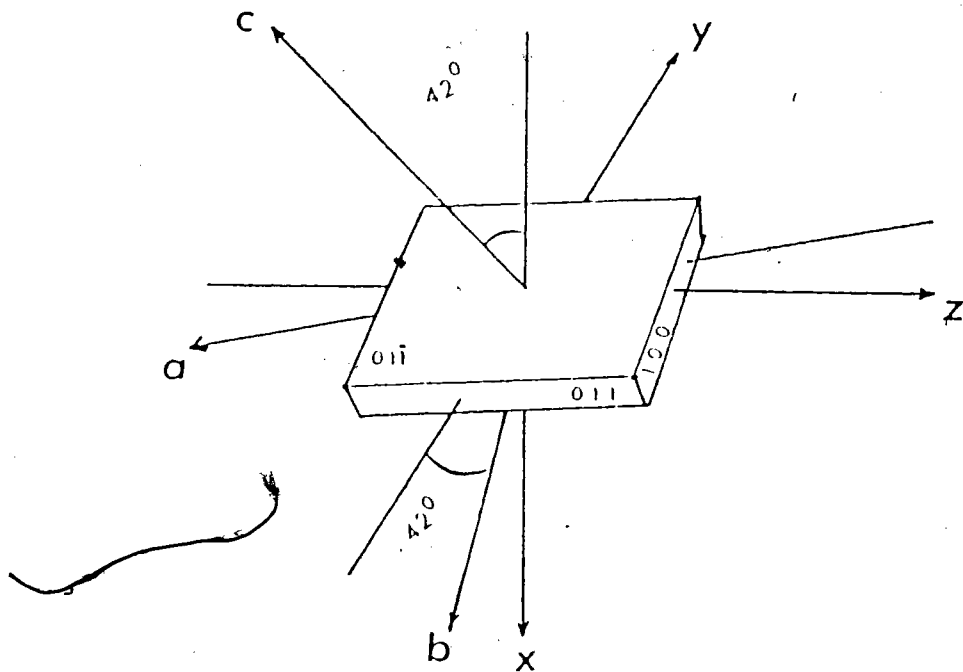


Fig. 20 Relationship between (a, b, c^*) and (x, y, z) of single crystal $[t\text{Bu}_2\text{SnSe}]_2$

Since we attached the crystal to holder in such a way that the normal of the face $(01\bar{1})$ is the $-x$ -axis, and the normal of the face (011) has an angle 6° with the $-y$ -axis, then the b -axis should be in the xy plane and have an angle of 133° with the y -axis. This is in agreement with that we get from NMR by using symmetry argument. In Fig. 15, after a rotation about the z -axis by 133° , the y -axis will be along the c -axis then a rotation about the c -axis by 92° , the z -axis will be along the

b-axis and the x-axis will be automatically brought into the ac(y)-plane. The angle between the a-axis and the c-axis is 115° , [50] therefore the angle between the a-axis and the y-axis is also 115° . A rotation about the b-axis by 115° will bring the y-axis along the a-axis and automatically the x-axis will be along the c^* -axis, so the angle ϕ is determined to be 115° .

The single crystal of compound c is also platelike, but the most developed face is $(\bar{1}20)$ rather than $(01\bar{1})$. The relationship between (a,b,c) and (x,y,z) is illustrated in Fig.21.

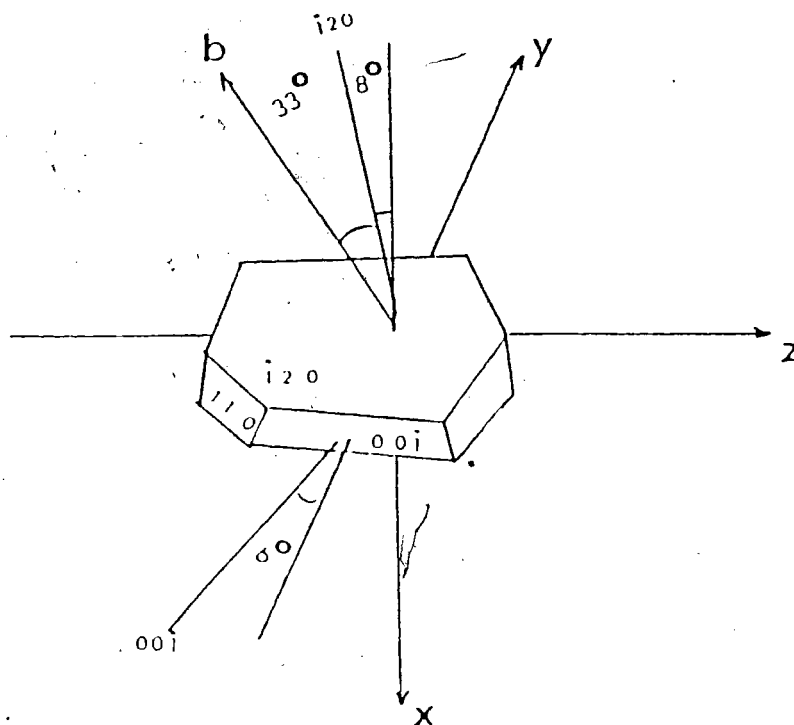


Fig.21 Miller indices and morphology of a single crystal of $[t\text{Bu}_2\text{SnTe}]_2$

Using a digital service height gauge and a digital caliper, we measured that the angle between the normal of the face $(00\bar{1})$ and the $-y$ -axis is $6^\circ \pm 2^\circ$ and the angle between the normal $(\bar{1}20)$ and the $-x$ -axis is $8^\circ \pm 2^\circ$. From the interplanar angle calculation we know that the angle between face $(\bar{1}20)$ and face (010) is 33° , so the angle between face (010) and the $-x$ -axis is approximately 41° . From NMR, we find the angle between the $-x$ -axis and the face (010) is 42° , they are in good agreement. After the first two transformations, the z -axis will be brought along the b -axis, and the xy -plane and the ac -plane will be the same plane. The angles between the y -axis and the $-c$ -axis and the a -axis and the $-c$ -axis are 6° and 66° , respectively. A rotation around the b -axis by an angle of 72° will bring the y -axis to the a -axis and automatically the x -axis to the c^* -axis. So the ϕ angle of compounds c is 72° .

3. Determination of Principal Values of Chemical Shielding in Crystallographic Axes

Knowing the Eulerian angle (α, θ, ϕ) , we can transform chemical shielding tensors in the holder system (x, y, z) to the crystallographic system (a, b, c^*) by using equations 36, 41, and 44. The result is presented in Table 5. Table 6. collects the

principal values and direction cosines of D tensors in crystallographic axis system.

Table. 5 Principal Values and Direction Cosines of the Chemical Shift Tensors Relative to the Crystallographic Axes (ppm)

	principal values	direction cosines with respect to			
		c	a	b	
b (Sn1)	σ_{11}	-314	-.02033	-.8976	-.4404
	σ_{22}	204	-.1371	.4388	-.8881
	σ_{33}	244	-.9904	-.04231	.1320
b (Sn2)	σ_{11}	-314	-.02468	-.8976	.4400
	σ_{22}	204	.2026	-.4355	-.8771
	σ_{33}	246	-.9790	-.06750	-.1926
b (Se1)	σ_{11}	-745	.2038	-.4589	-.8648
	σ_{22}	-595	-.9777	-.05013	-.2038
	σ_{33}	-176	-.05020	-.8871	.4589
b (Se2)	σ_{11}	-727	-.2253	.4435	-.8675
	σ_{22}	-601	-.9724	-.04638	.2288
	σ_{33}	-176	-.06126	-.8951	-.4417
c (Sn1)	σ_{11}	-767	.4017	-.8002	.4454
	σ_{22}	134	.5765	-.1569	-.8019
	σ_{33}	206	-.7115	-.5789	-.3983

Table. 5 Continued

c (Sn2)	σ_{11}	-746	.4152	-.7949	-.4425
	σ_{22}	150	-.5363	-.1791	-.8248
	σ_{33}	195	-.7349	-.5797	.3520
c (Te1)	σ_{11}	-3150	-.8553	-.5181	.01155
	σ_{22}	-251	.2443	-.3835	.8906
	σ_{33}	380	.4570	-.7646	-.4546
c (Te2)	σ_{11}	-3164	-.8553	-.5180	-.01068
	σ_{22}	-255	-.2418	.3808	.8925
	σ_{33}	391	.4582	-.7659	.4510
<hr/>					
a (Sn1)	σ_{11}	-130		(Sn2) σ_{11}	-127
	σ_{22}	227		σ_{22}	242
	σ_{33}	255		σ_{33}	245

¹The standard deviation from the MINUIT are as follow; ± 3 ppm for a(Sn), ± 4 ppm for b(Sn), ± 9 ppm for c(Sn), ± 0.2 ppm for b(Se), and ± 4 ppm for c(Te).

²Shifts were measured from Me_4Sn , Me_2Se , and Me_2Te for ^{119}Sn , ^{77}Se , and ^{125}Te , respectively, with positive values for high frequency shift.

Table. 6 Principal Values and Direction Cosines
of the D Tensors Relative to the
Crystallographic Axes (Hz)

	principal values		direction cosines with respect to		
			c	a	b
b (Sn1)	D11	594	.7690	-.9006	-.4279
	D22	909	-.8091	-.3072	.5010
	D33	1060	-.5826	.3077	-.7522
b (Sn2)	D11	686	.06347	.7705	-.6342
	D22	872	-.9751	-.08747	-.2038
	D33	1025	-.2126	.6314	.7458
c (Sn1)	D11	1808	-.5866	.7267	-.3574
	D22	2071	-.7961	-.4363	.4194
	D33	2263	.1489	.5306	.8345
c (Sn2)	D11	1648	.4609	-.7685	-.4438
	D22	2197	-.8311	-.5492	.08791
	D33	2354	-.3113	.3283	-.8918
c (Te1)	D11	1825	.8965	.3337	.2916
	D22	1952	-.4180	.8551	.3066
	D33	2204	-.1470	-.3968	.9061
c (Te2)	D11	1681	-.5378	.7050	-.4624
	D22	2088	-.7697	-.6343	-.07196
	D33	2301	-.3440	.3172	.8838

The standard deviation from the MINUIT is ± 5 Hz.

Table 7. The Isotropic Values of the Chemical Shift and J-coupling

compound	SC	MAS	Solution NMR
a(Sn)	+118	+120	+126
b(Sn)	+45 (858)	+47.7 (913)	+54.6 (915)
b(Se)	-503	-509 (900)	-494 (922)
c(Sn)	-138 (2057)	-130 (2122)	-121 (2117)
c(Te)	-1008 (2008)	-1020 (2122)	-1099 (2117)

SC: single crystal method. MAS: magic angle spinning method. The value of chemical shift is in ppm. Values in parentheses are J-coupling values in Hz.

The error in these results is mainly from the error in angle measurements. As we see from Eq. 33-35, the error in chemical shielding and the D tensor is dependent of the rotation angle and the parameters of chemical shielding and D-coupling in the holder system. For an error of $\pm 2^\circ$ in angle measurements, it may introduce an error having magnitude of the order of 10^2 ppm (for chemical shieldings) and 3×10^2 Hz (for D-coupling).

The principal values of the tensor for the three compounds, presented in Table 5 show that the anisotropy, defined as $\sigma = \sigma_{33} - 1/2 (\sigma_{11} + \sigma_{22})$, is quite large and

increased from Sn tensors to Te tensors, and from compound **a** to compound **c** in the case of Sn tensors. [197 ppm for Sn in compound **a**, 300 ppm for Sn in compound **b**, 508 ppm for Sn in compound **c**, 491 ppm for Se in compound **b**, and 2090 ppm for Te in compound **c**]. The shielding tensor of Sn in compound **a** is almost axially symmetric ($\sigma_{22} \approx \sigma_{33}$). The Sn and Se in compound **b** also display approximately axially symmetric shielding tensors. The Sn and Te in compound **c** are completely non-axially symmetric with the largest anisotropy.

We are not able to find the direction cosines of the principal values in compound **a**. The reason for this is that the crystal faces of the single crystal are not ideal for the two-circle goniometer investigation, so we cannot find the orientation of the single crystal in the holder system by this means. On the other hand, the crystal itself has not enough non-redundant symmetry elements to enable us to find the direction cosines by the mathematical method we developed.

As shown in Table 5, the principal value of the same nuclei in the same compound is the same, only direction cosines are different. This means that these two nuclei are only different in the orientation. Comparing the Sn chemical shielding in compound **b** and **c**, we found a big difference in σ_{11} , for the other two tensor elements, only small differences

existed. This means that σ_{11} is more sensitive to the substitution of X than σ_{22} and σ_{33} . So σ_{11} is probably the in-plane component close to the Sn—X bond direction or the bisection of the X—Sn—X angle. From Table 7, we can see that the isotropic values of chemical shift and J-coupling are almost the same as those from solution NMR. This means that the crystal packing effects are small, so the orientations of the chemical shift tensors are mainly determined by molecular symmetry. Therefore, the σ_{11} should be near the bisection of the X-Sn-X angle. For compound **b**, the σ_{11} of Sn and the σ_{33} of Se have the same orientation in the crystallographic axis system and they are all approximately perpendicular to c^* . So the direction of the unique axis of compound **b** is the same as the σ_{11} of Sn or the σ_{33} of Se. It is quite likely that the c^* -axis is perpendicular to the ring and the unique axis is parallel to the ring.

The D tensor elements should be the same no matter what spectrum (Sn or Te) we measured. But from Table 6, we can see that the isotropic values of D-tensors for Sn and Te have a small difference. The D-tensor of Sn is a little bigger than that of Te. This is due to the unsolved doublet (^{119}Sn — ^{117}Sn) in Te spectrum, we should multiply by 1.023 to the isotropic values in Te spectrum to get the isotropic values in Sn spectrum.

The dipolar interaction T can be evaluated by using Eq.32, and the given Se—Sn and Te—Sn bond distances. The distances for these two bonds are 2.55 Å and 2.75 Å, respectively.

$$T_{\text{Se-Sn}} = \begin{bmatrix} -515 & 0 & 0 \\ 0 & -515 & 0 \\ 0 & 0 & 1029 \end{bmatrix} \quad (48)$$

$$T_{\text{Te-Sn}} = \begin{bmatrix} 680 & 0 & 0 \\ 0 & 680 & 0 \\ 0 & 0 & -1360 \end{bmatrix} \quad (49)$$

If we know the structure of the crystal, we can get the J-coupling tensor by using Eq. 19 and Eq. 48-49.

As shown in Table 6, the D tensor, under the consideration of the error in measurements, is nearly isotropic. We can also see from Eq. 48-49 that T is not isotropic, therefore, J must not be isotropic and the degree of anisotropy of J must be comparable with that of T to yield the nearly isotropic D tensor. This means that the isotropic Fermi contact term is not the dominant contribution in the J coupling tensor.

As we don't know crystal structures, we cannot transform the data to the molecular system, so we were not able to relate our data with molecular structures. Although we are not able

to get the J-coupling tensor, we still can get the isotropic value of J-coupling because the trace of the dipolar interaction T vanishes.

4. Conclusion

There is always a problem when using the single crystal method to determine the chemical shielding tensor in the crystallographic axis system, that is, when measuring the NMR spectrum, we need a big crystal to get a good signal to noise ratio in a relatively short time, but this will make us unable to figure out the crystal orientation because we cannot easily use X-ray diffraction. Although the Laue back reflection method and the two circle goniometer method in principle can solve this problem, they require a more strict requirement on crystal than NMR, and also those methods need experience.

We developed a mathematical method which enables us to solve this problem by using the NMR data and some lattice data of the crystal. This mathematical method is limited by the symmetry element in the crystal. When the symmetry operation applied to the holder axis z does not change one of the angles θ or ϕ , then this particular angle cannot be determined.

Therefore an additional symmetry element has to be used. If we cannot find this additional symmetry element then we are not able to get all these three Eulerian angles.

The results of our coupling tensor indicate that the Fermi contact terms in ^{119}Sn , ^{77}Se , and ^{125}Te are not the dominant contribution in the J-coupling tensor contrary to previous results[61,77-78]. The isotropic values of chemical shift tensor and J-coupling tensor from our experiment are nearly the same as those from solution NMR, so the crystal packing effects in these compounds are small.

5. Future work

The purpose of our work is to relate the chemical shift tensor and the J-coupling tensor to the molecular structure, which will enable us to relate these tensors with the electronic environment of the nuclei in the molecule. So the next thing to do is to determine the structures of these compounds. On the other hand, it is valuable to determine these tensors in a series compounds with different structures. This will give us important information on the shift tensor/structure relationships. For this investigation, the six-ring compounds $(\text{Me}_2\text{SnX})_3$ or the non-ring compounds $\text{R}_3\text{Sn-X-SnR}_3$ are a good choice.

Theoretical calculation is another worthy work. From these calculations, we can have a further insight of the nature of chemical bonding and its relationship with molecular symmetry.

Figures 8 to 18

Fig 8. ^{119}Sn NMR spectrum of a $[\text{tBu}_2\text{SnS}]_2$ single crystal
when B_0 is in xz-plane

Fig 9a. ^{119}Sn NMR spectrum of a $[\text{tBu}_2\text{SnSe}]_2$ single crystal
when B_0 is in xz-plane

Fig 9b. ^{77}Se NMR spectrum of a $[\text{tBu}_2\text{SnSe}]_2$ single crystal
when B_0 is in yz-plane

Fig 10a. ^{119}Sn NMR spectrum of a $[\text{tBu}_2\text{SnTe}]_2$ single crystal
when B_0 is in xy-plane

Fig 10b. ^{125}Te NMR spectrum of a $[\text{tBu}_2\text{SnTe}]_2$ single crystal
when B_0 is in xz-plane

Fig 11(a-c). Angular dependence of ^{119}Sn NMR lines in (01-03)
for a single crystal of $[\text{tBu}_2\text{SnS}]_2$

Fig 12(a-c). Angular dependence of ^{119}Sn NMR lines in (01-03)
for a single crystal of $[\text{tBu}_2\text{SnSe}]_2$

Fig 13(a-c). Angular dependence of ^{119}Sn NMR lines in (01-03)
for a single crystal of $[\text{tBu}_2\text{SnTe}]_2$

Fig 14(a-c). Angular dependence of ^{77}Se NMR lines in (01-03)
for a single crystal of $[\text{tBu}_2\text{SnSe}]_2$

Fig 15(a-c). Angular dependence of ^{125}Te NMR lines in (01-03)
for a single crystal of $[\text{tBu}_2\text{SnTe}]_2$

Fig 16(a-c). Angular dependence of D(Sn-Se) coupling in (01-03)
for compound **b** (detect ^{119}Sn)

Fig 17(a-c). Angular dependence of D(Sn-Te) coupling in (01-03)
for compound **c** (detect ^{119}Sn)

Fig 18(a-c). Angular dependence of D(Sn-Te) coupling in (01-03)
for compound **c** (detect ^{125}Te)

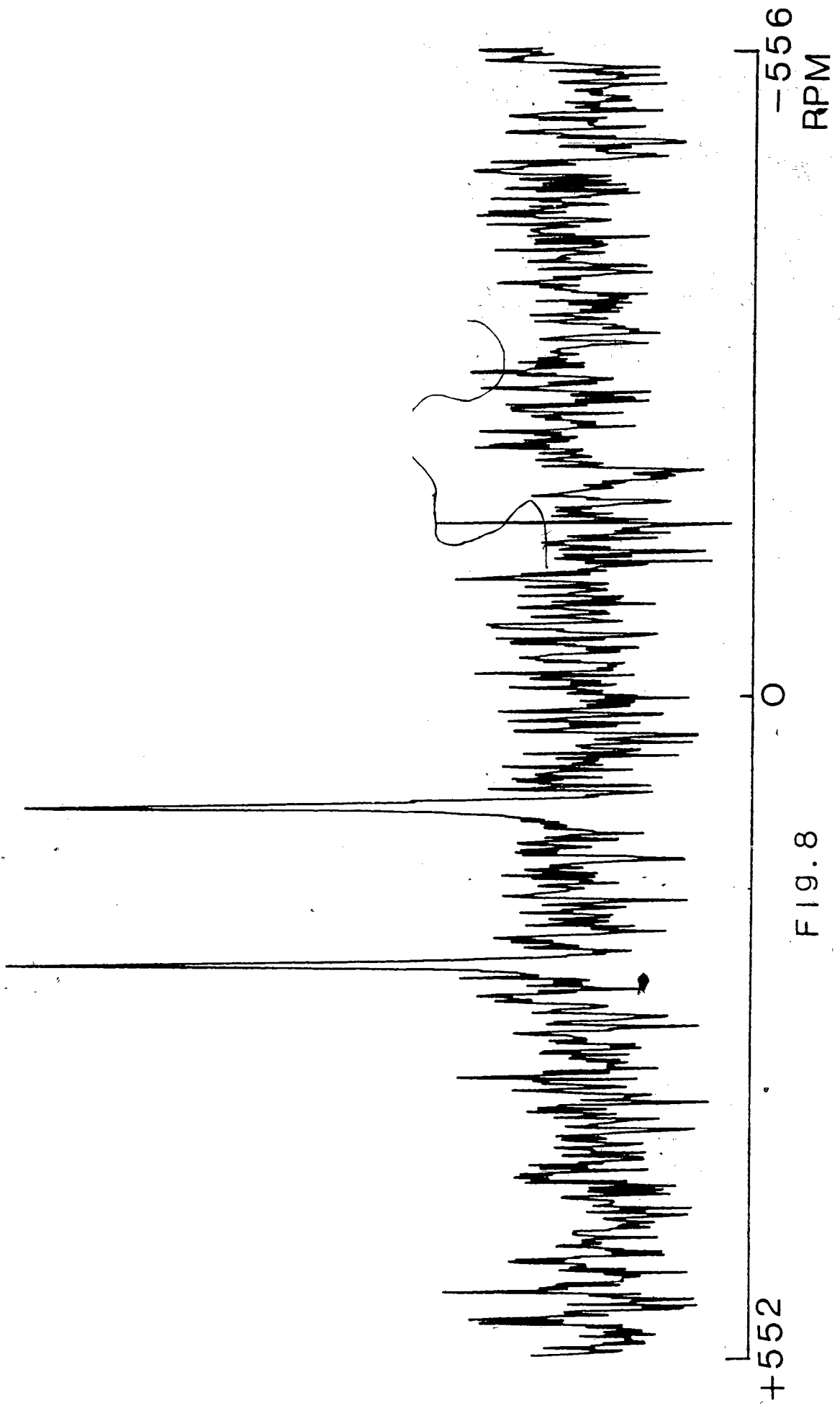


FIG. 8

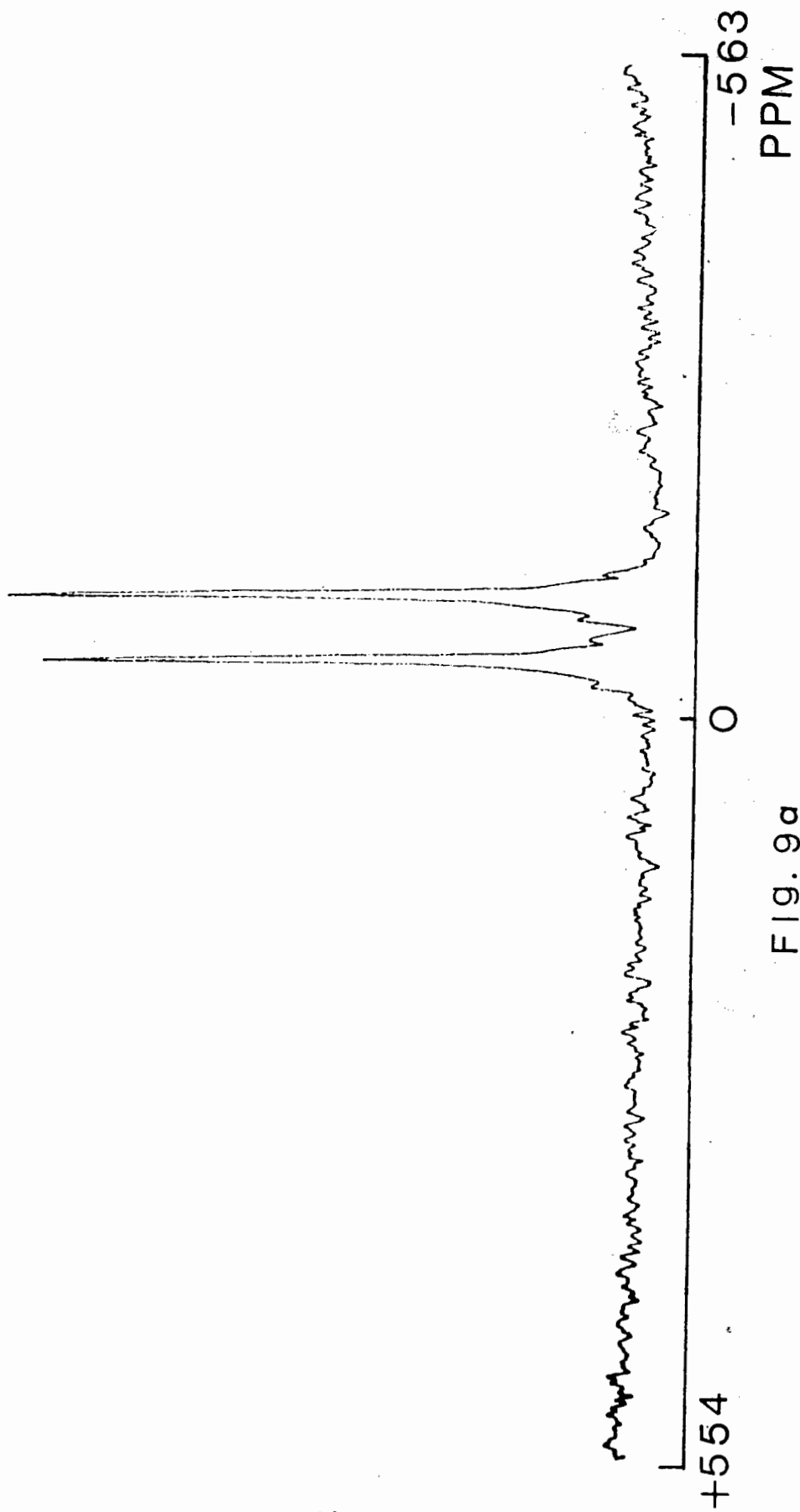


FIG. 9a

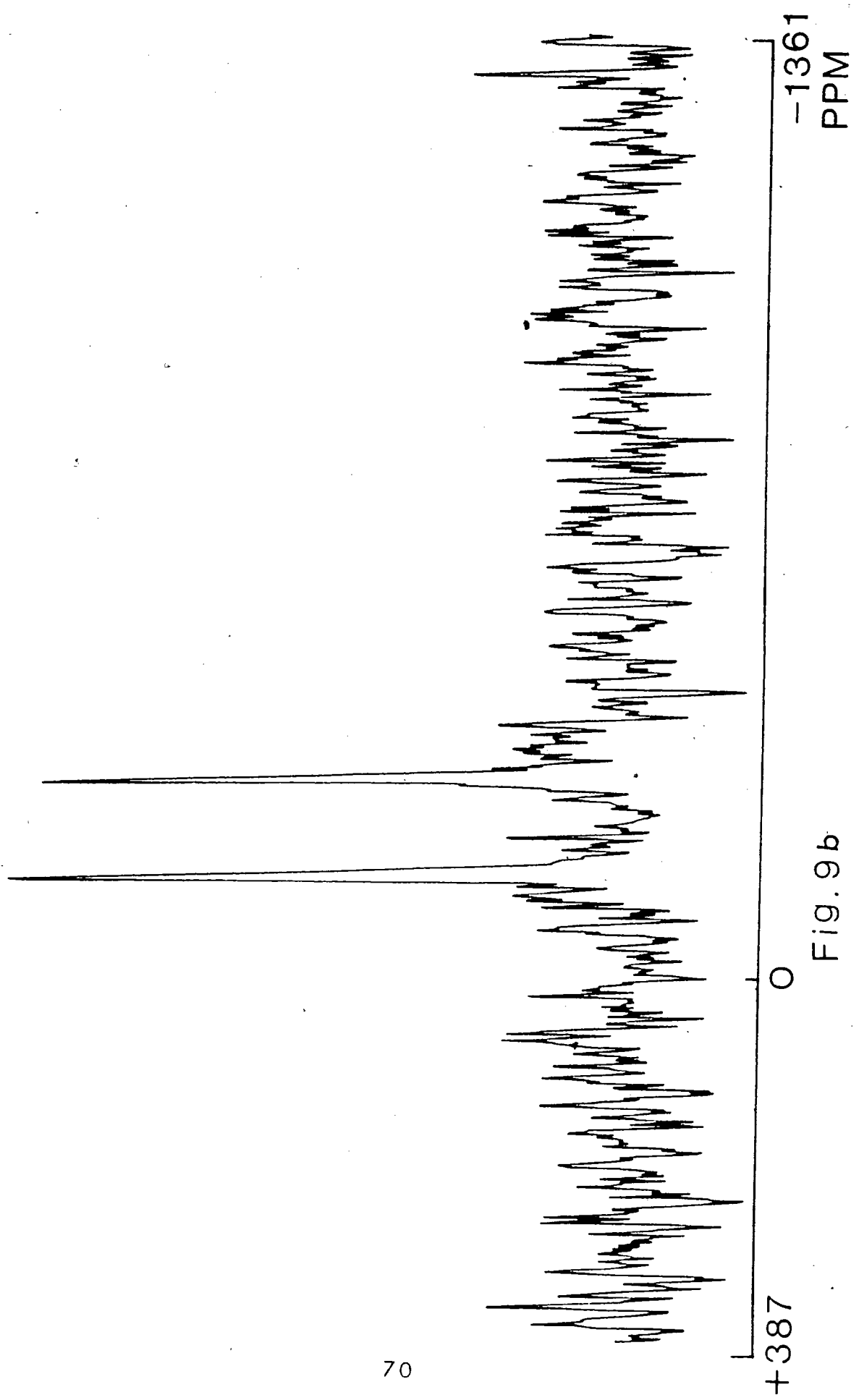


Fig. 9b

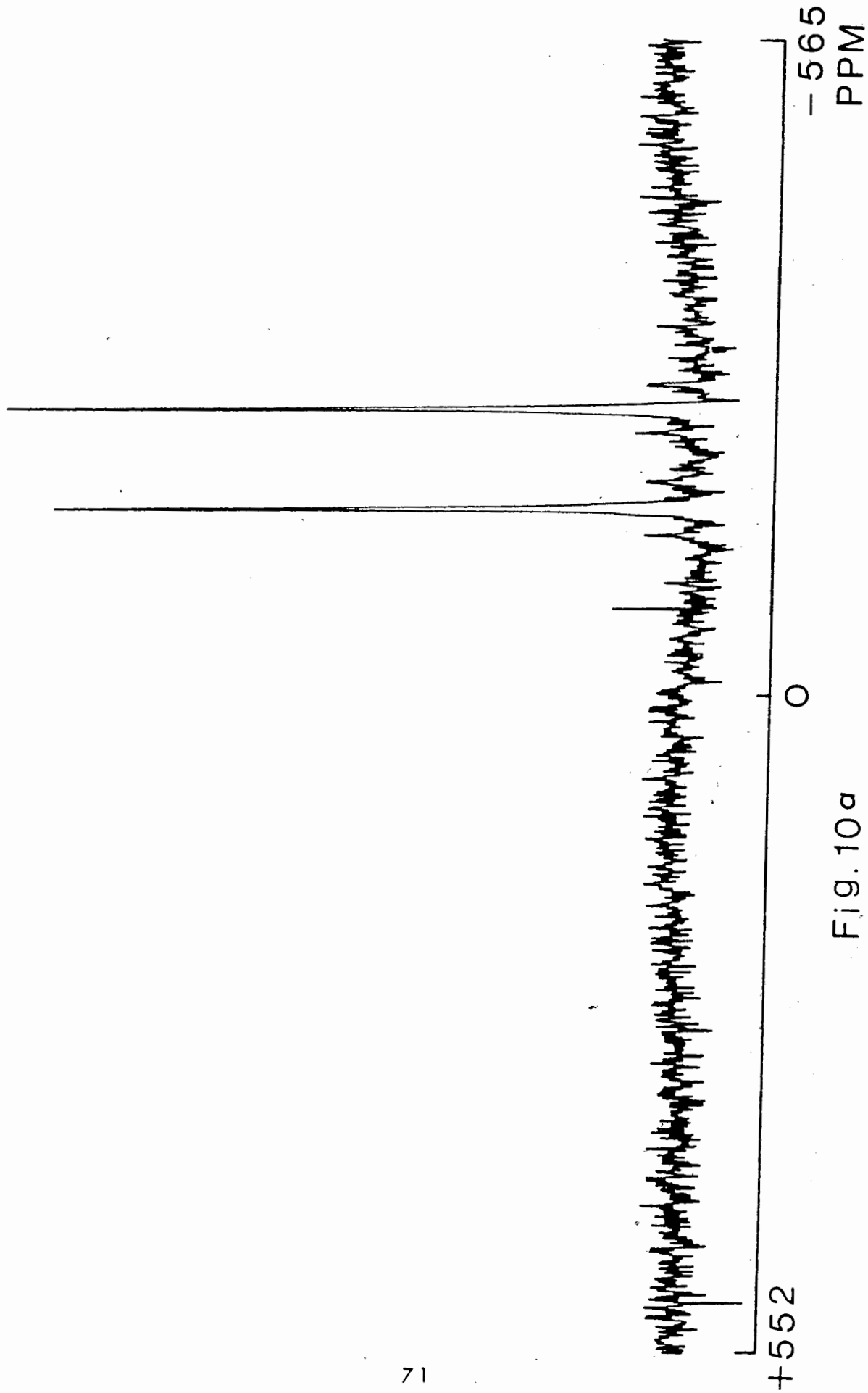
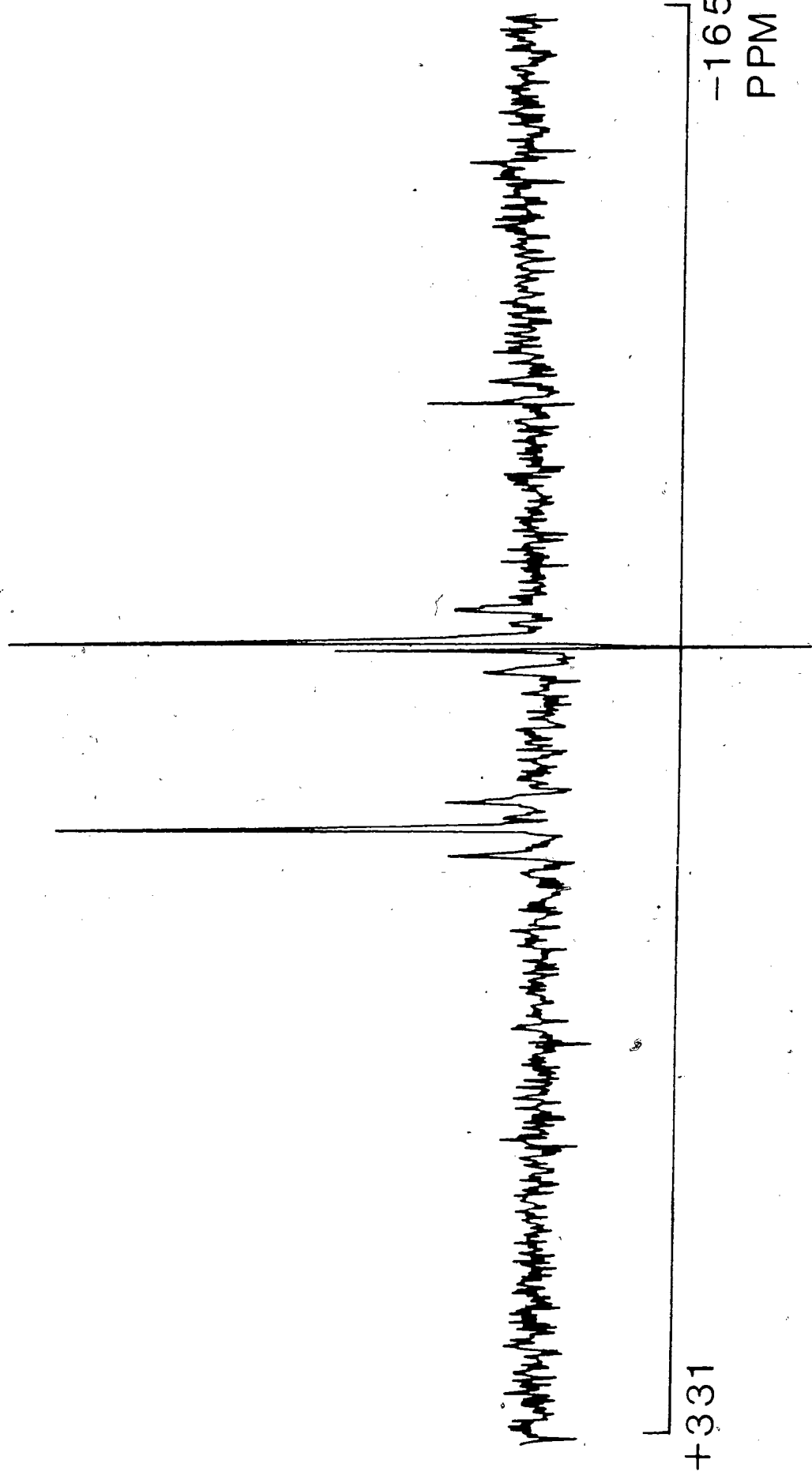


Fig. 10a



+331

-1652
PPM

Fig.10b

Fig. 11a

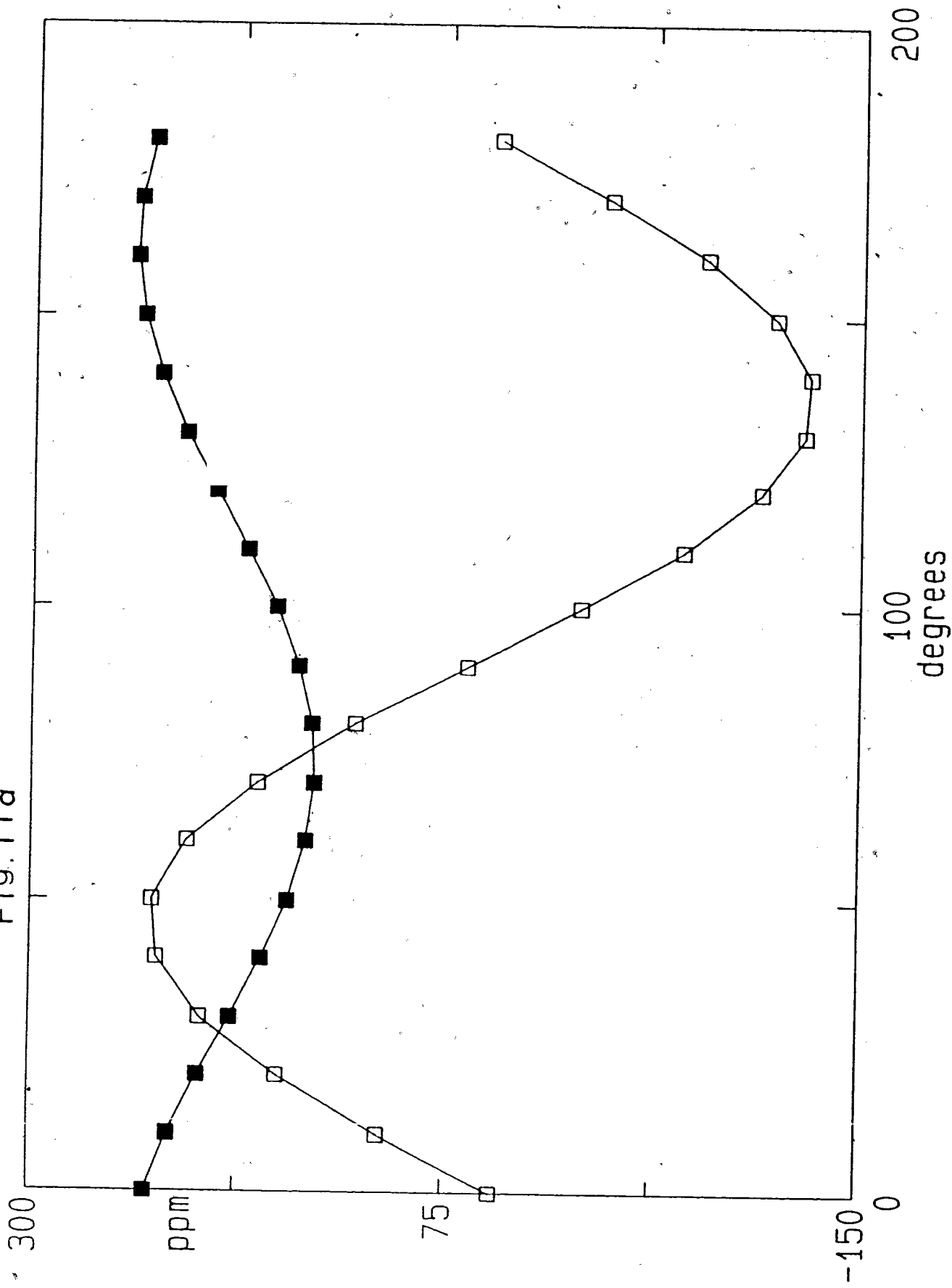


Fig.11b

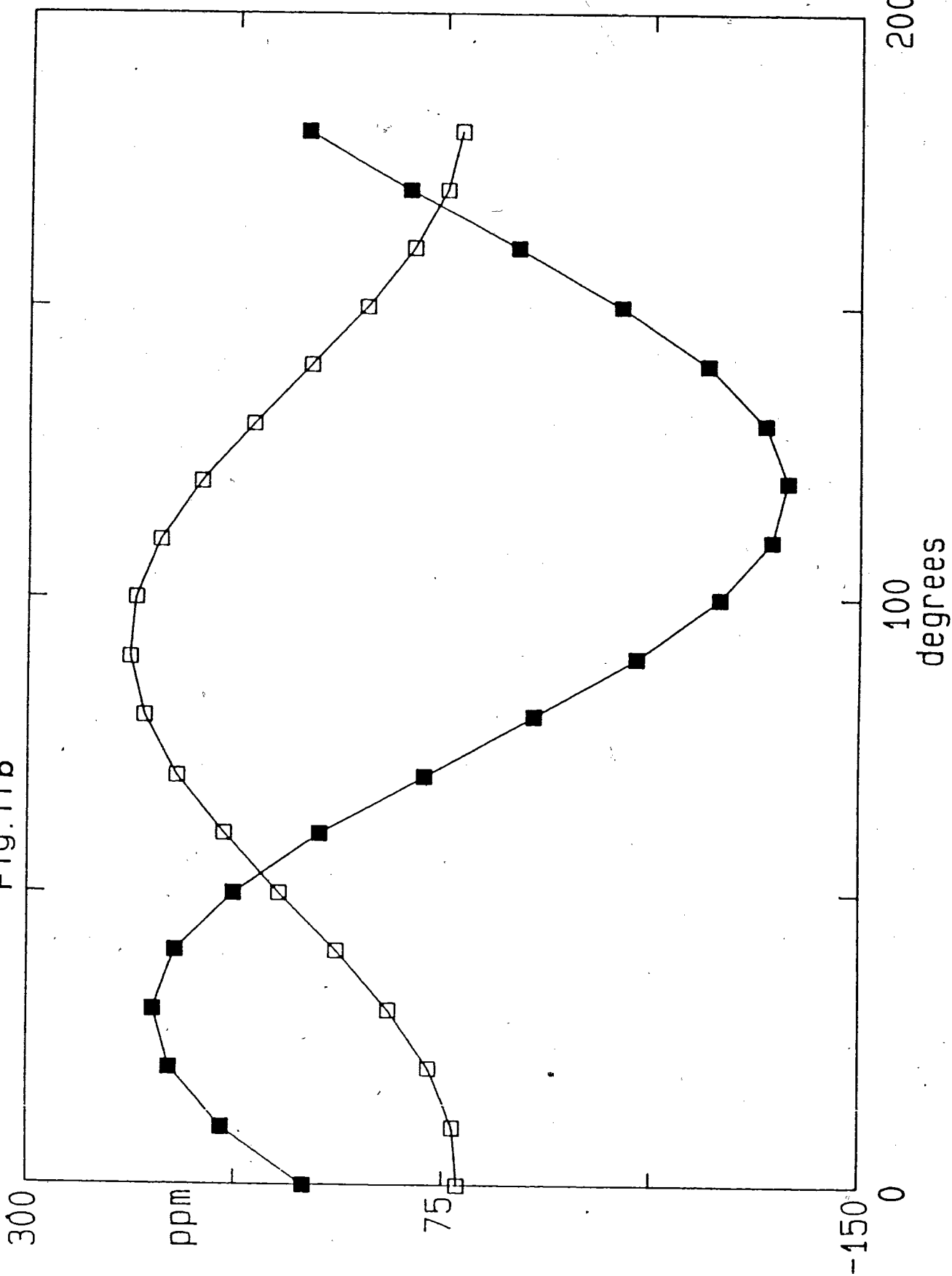


Fig.11 c

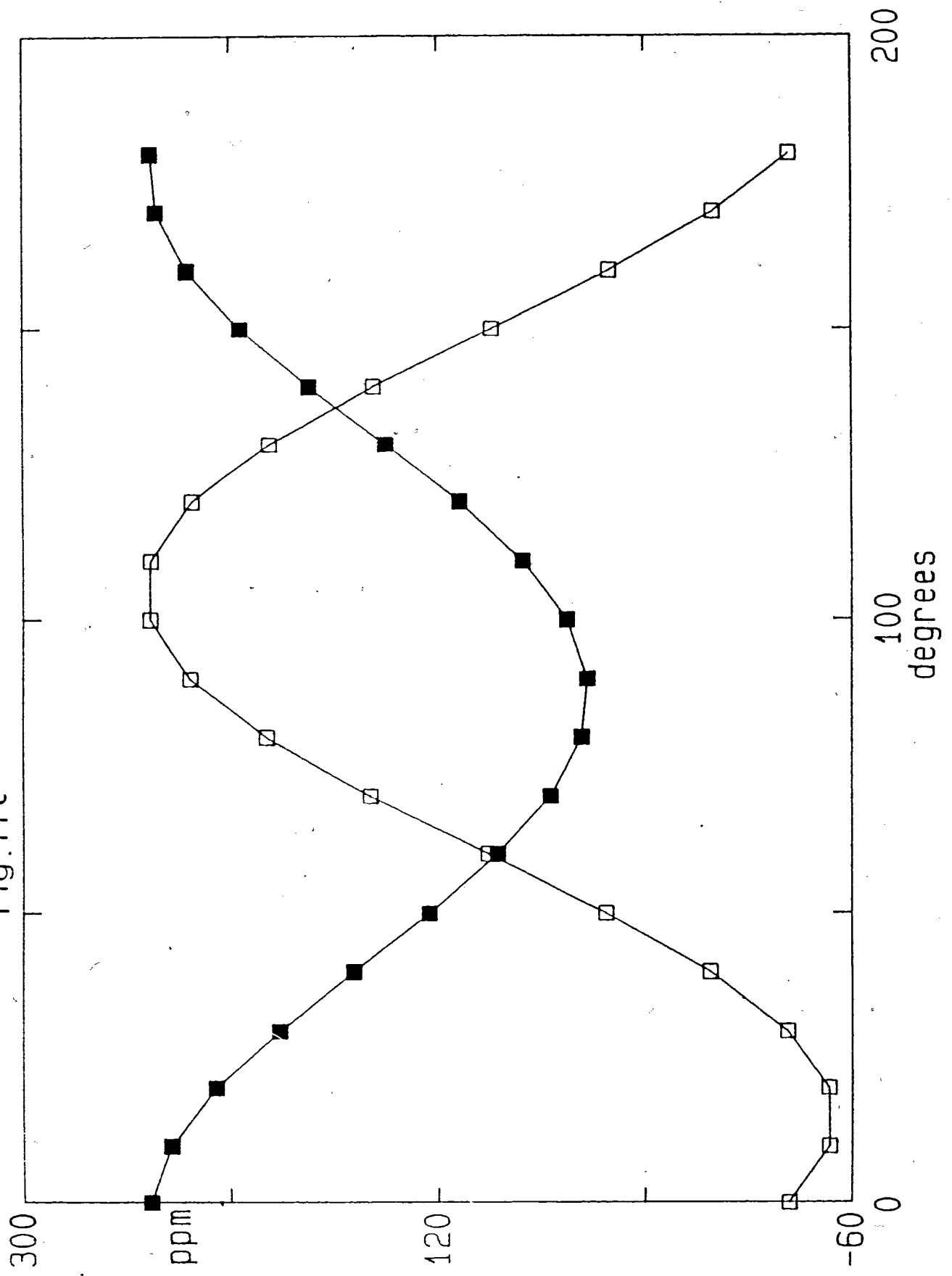


Fig. 12a

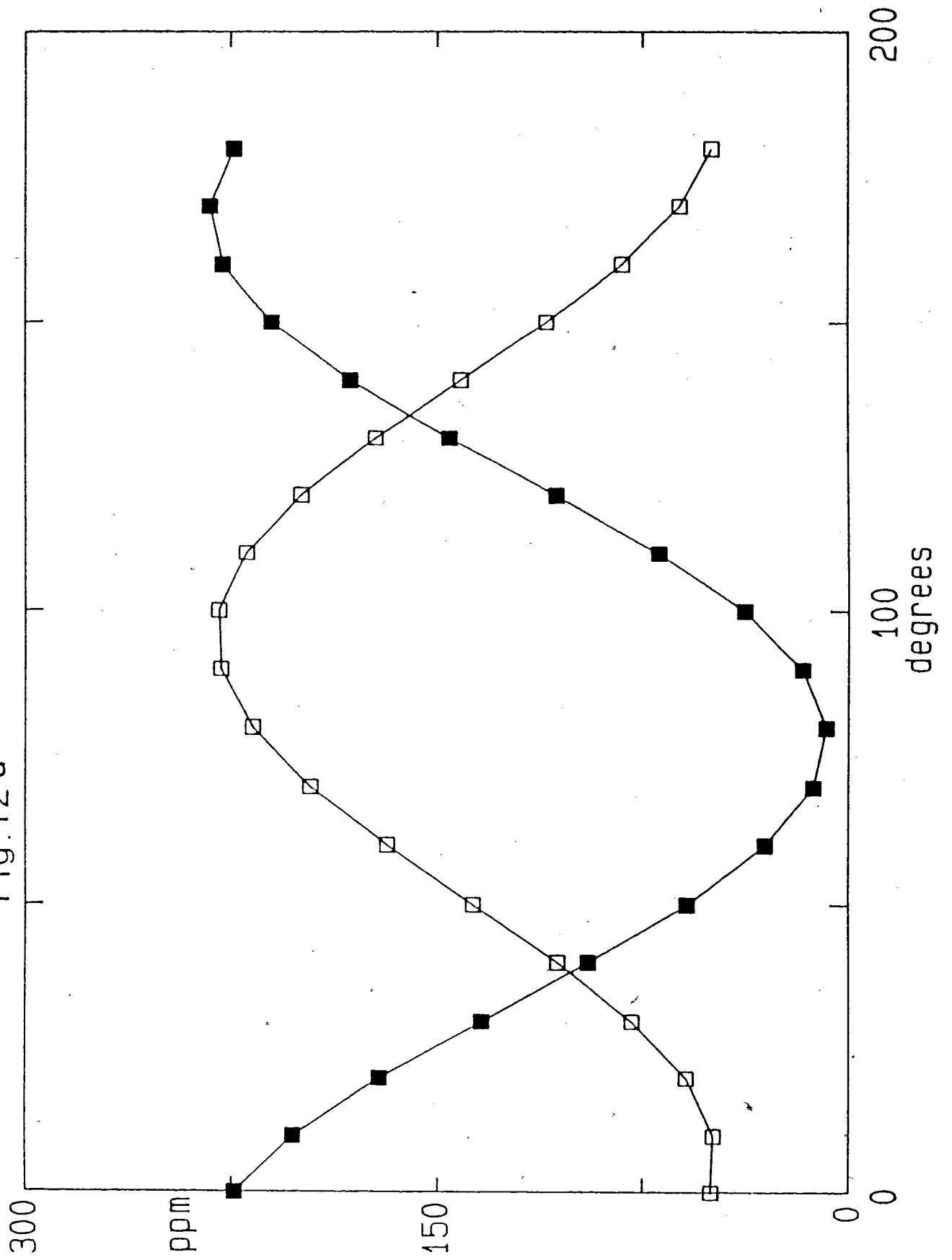


Fig.12 b

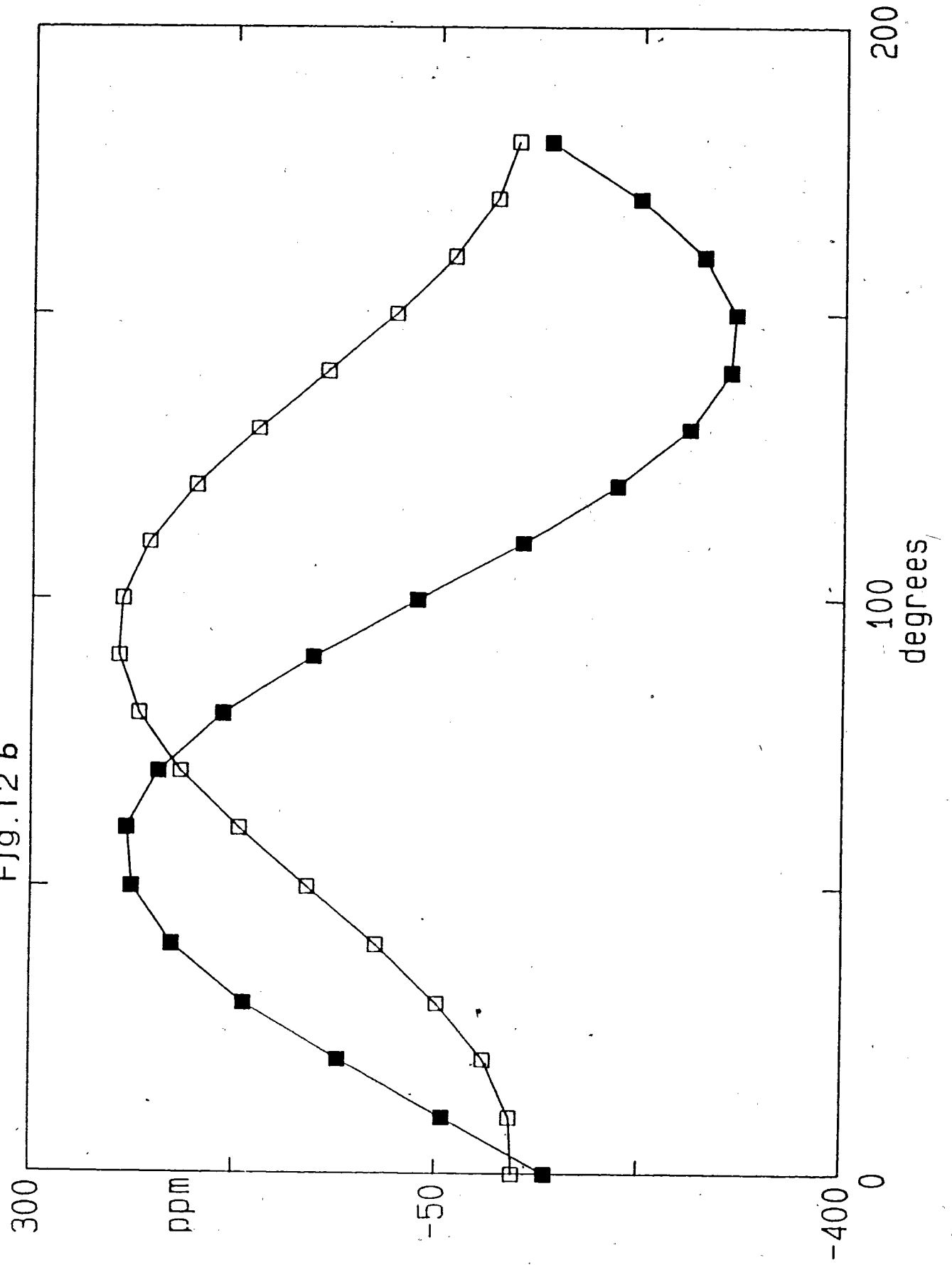


Fig.12 c

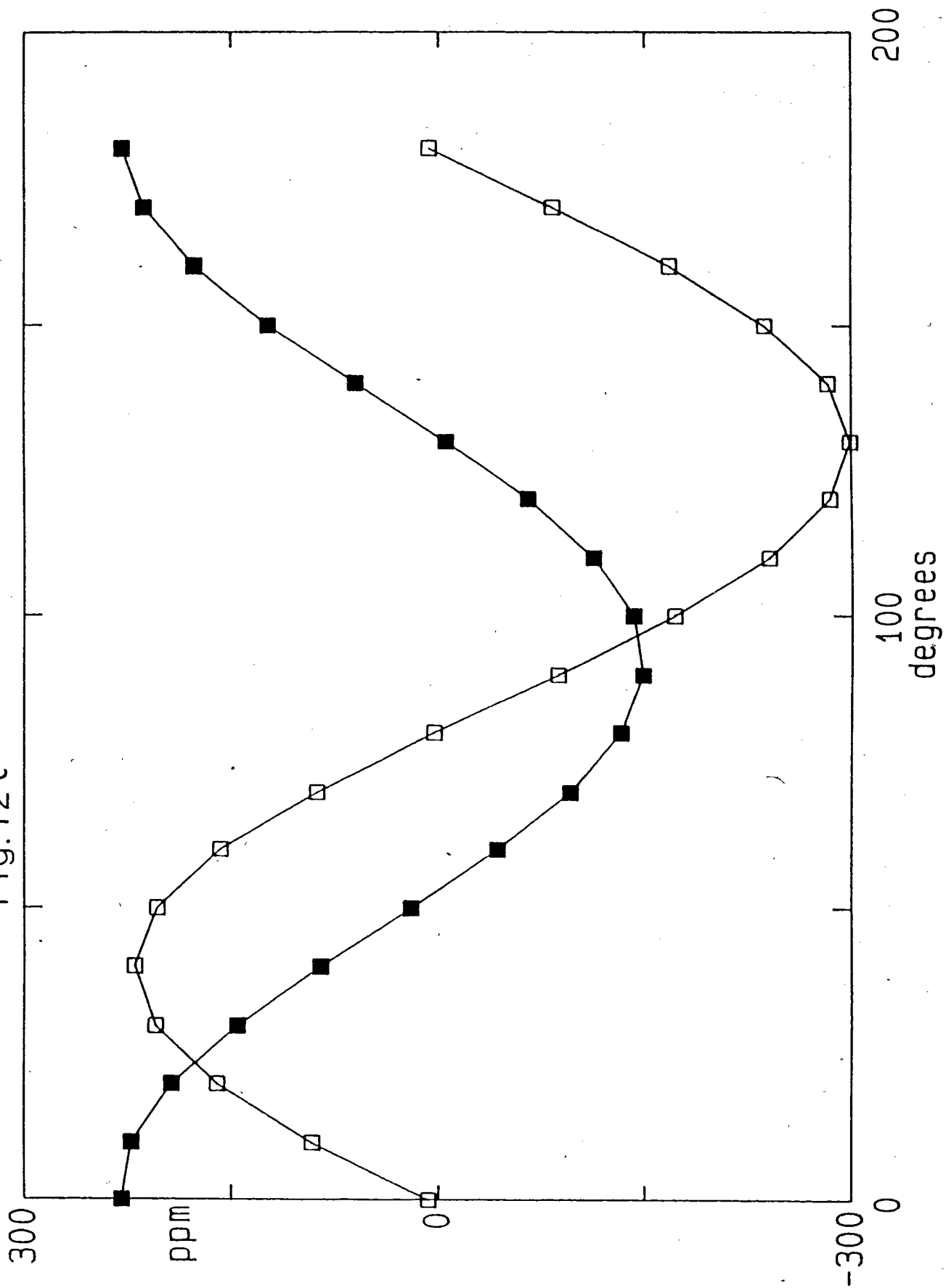


Fig. 13a

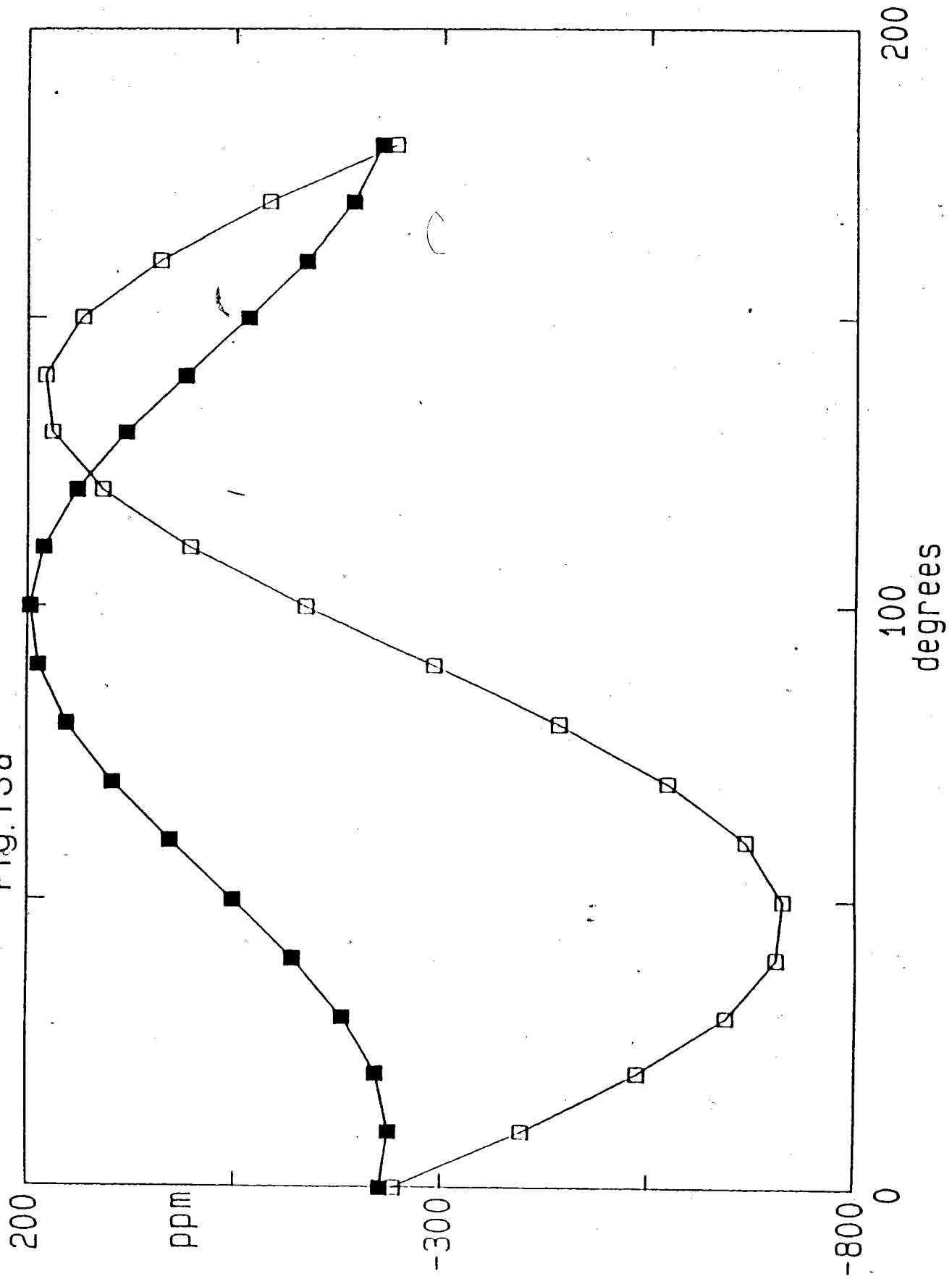


Fig. 13b

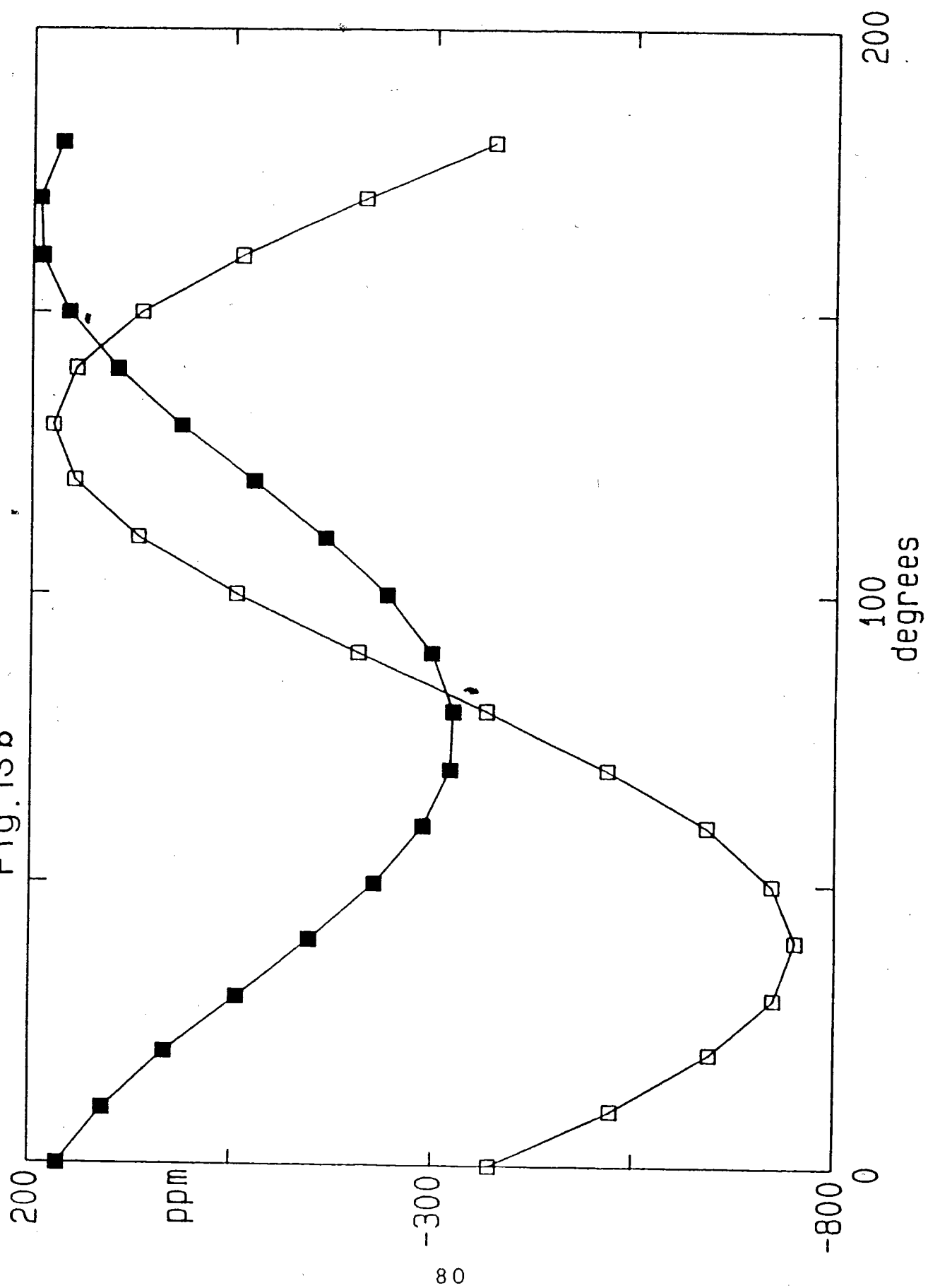


Fig. 13c

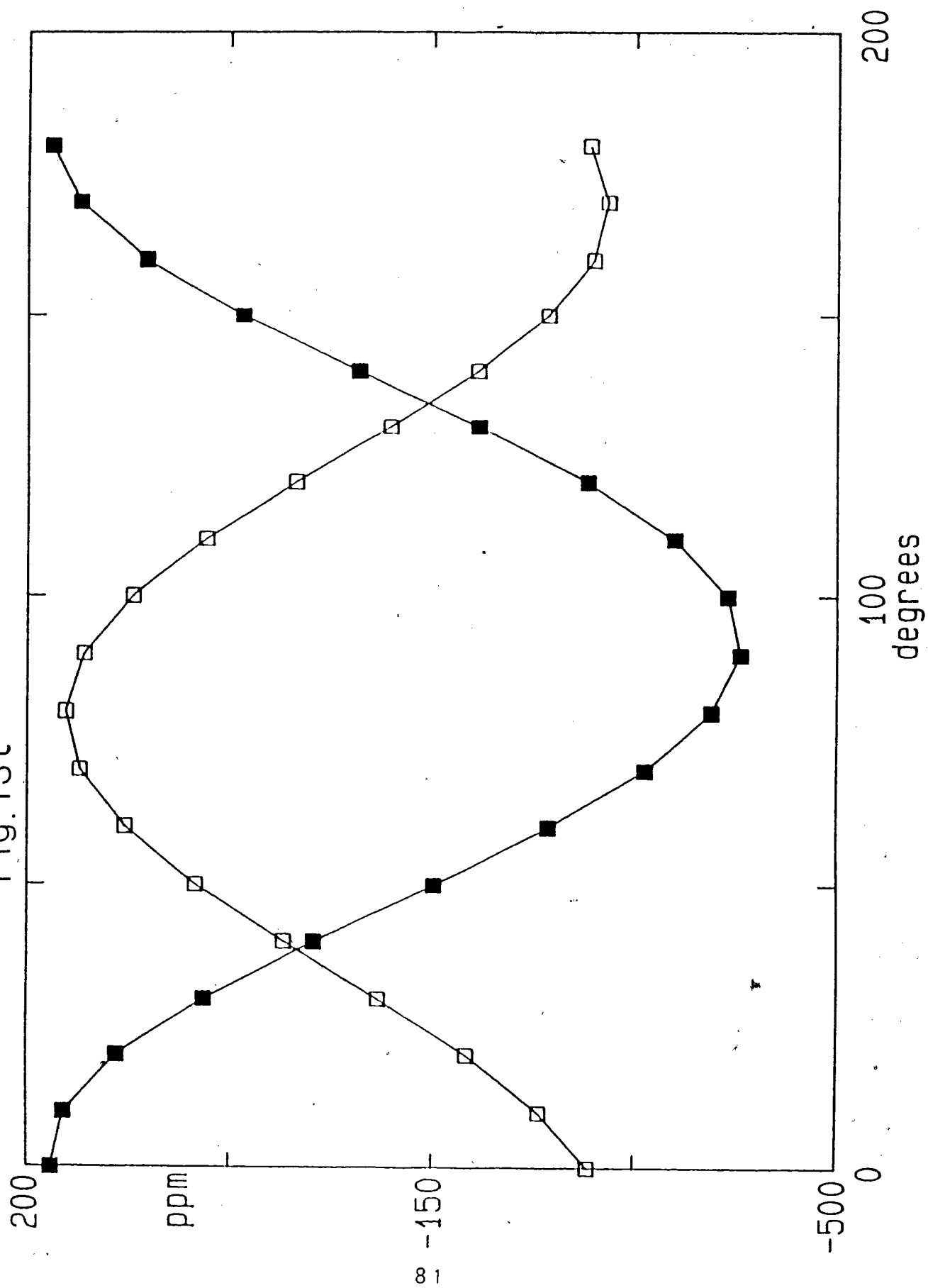


Fig. 14a

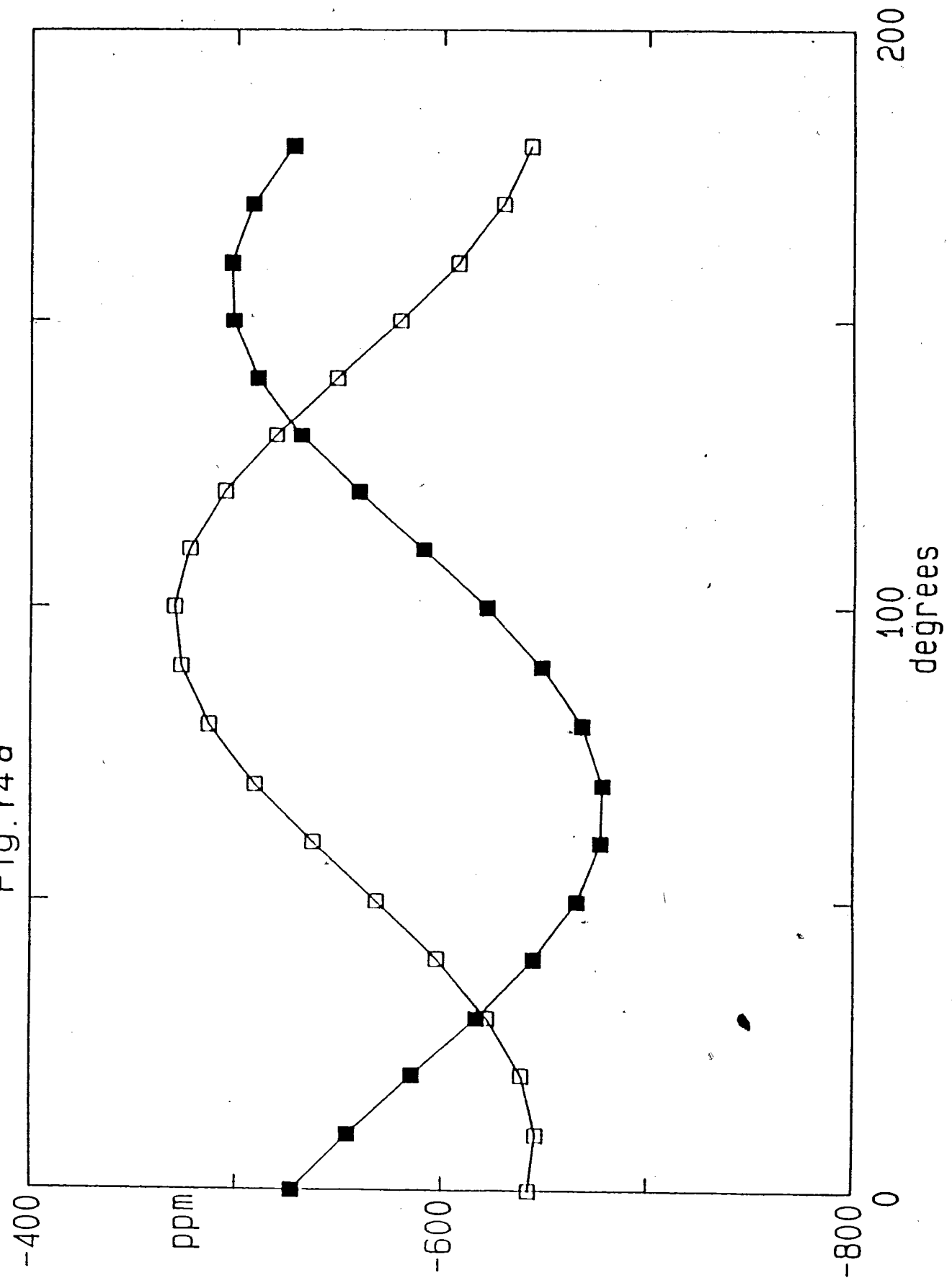


Fig.14 b

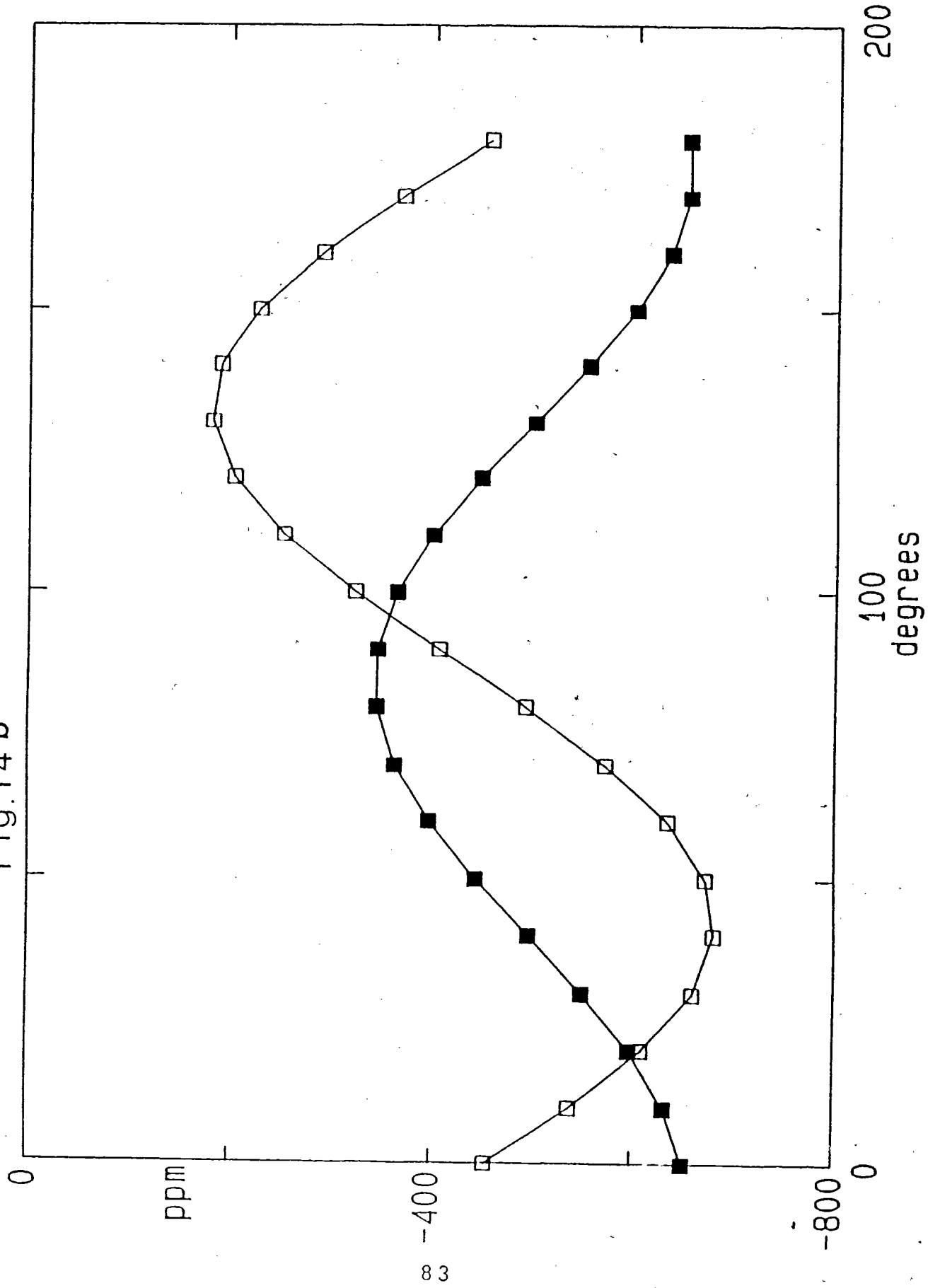


Fig.14C

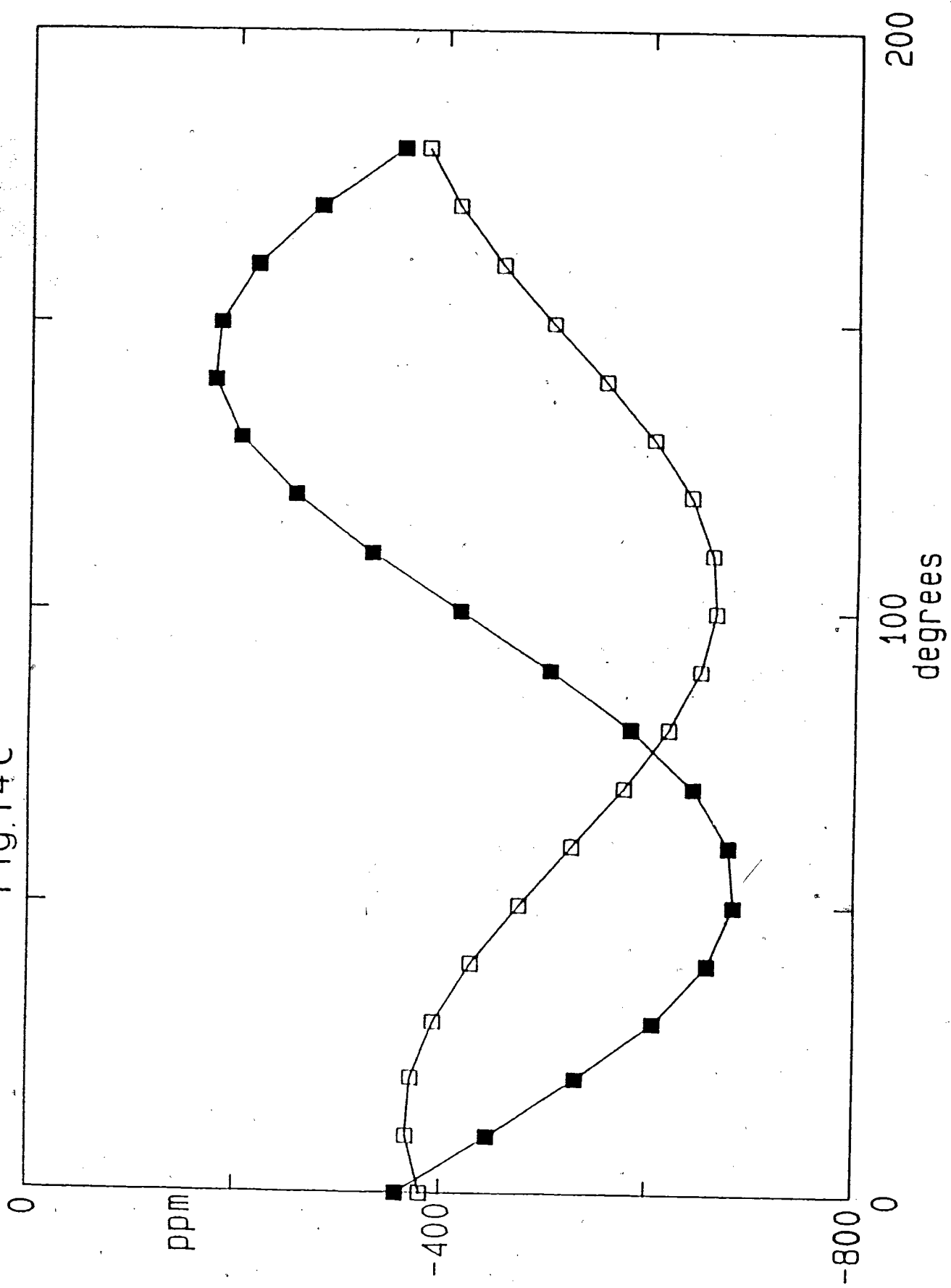


Fig. 15 a

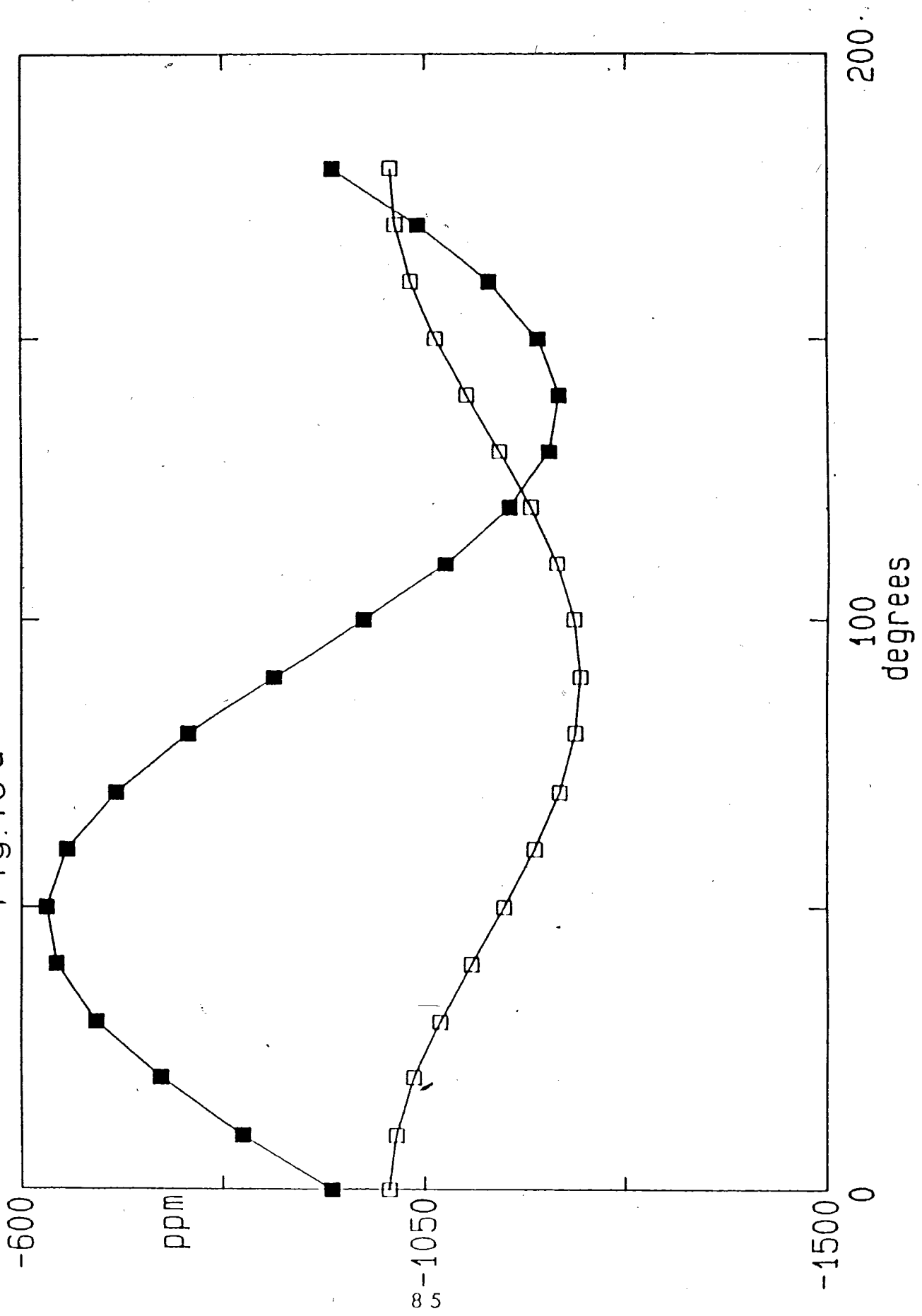


Fig. 15 b

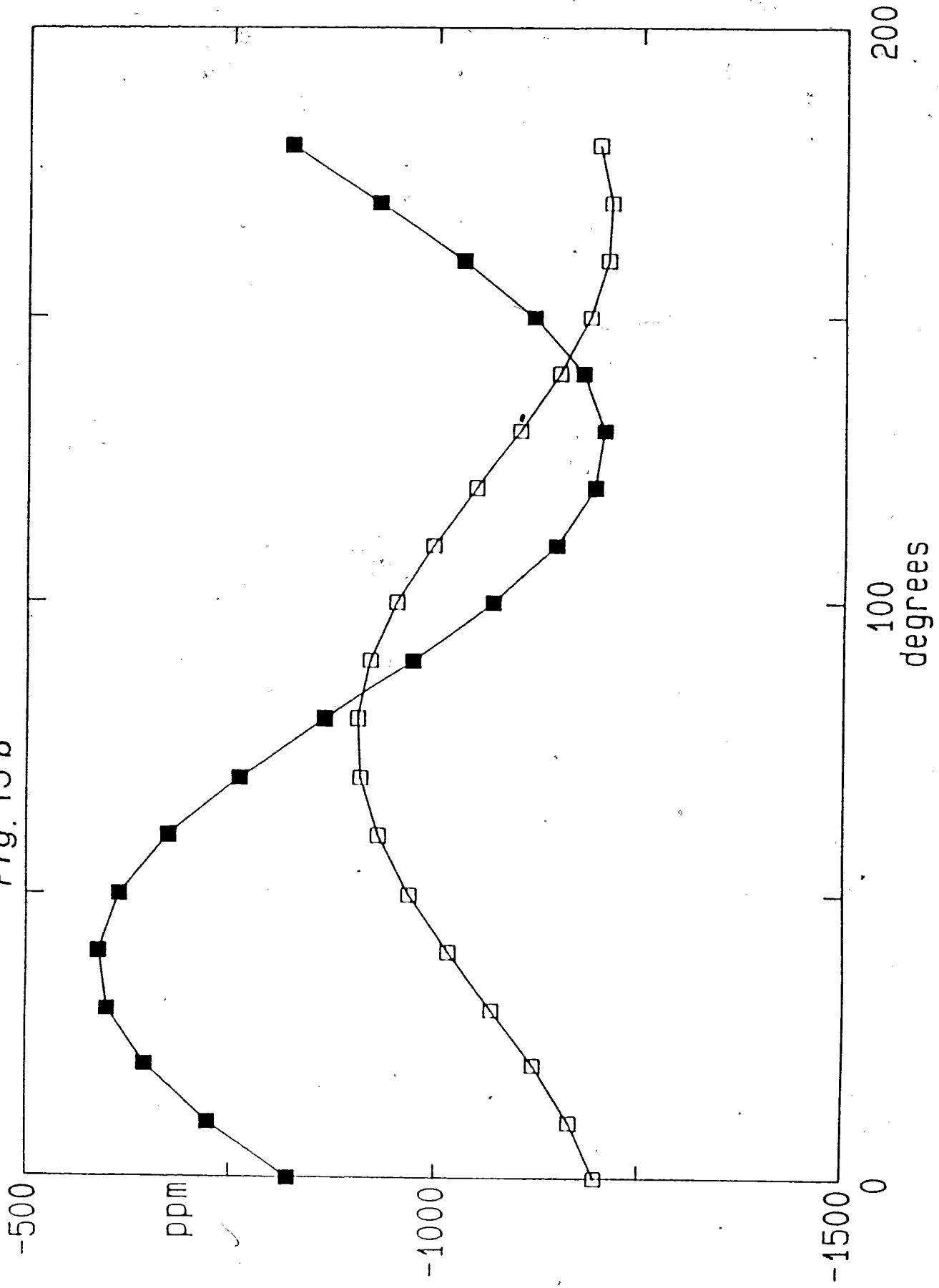


FIG. 15C

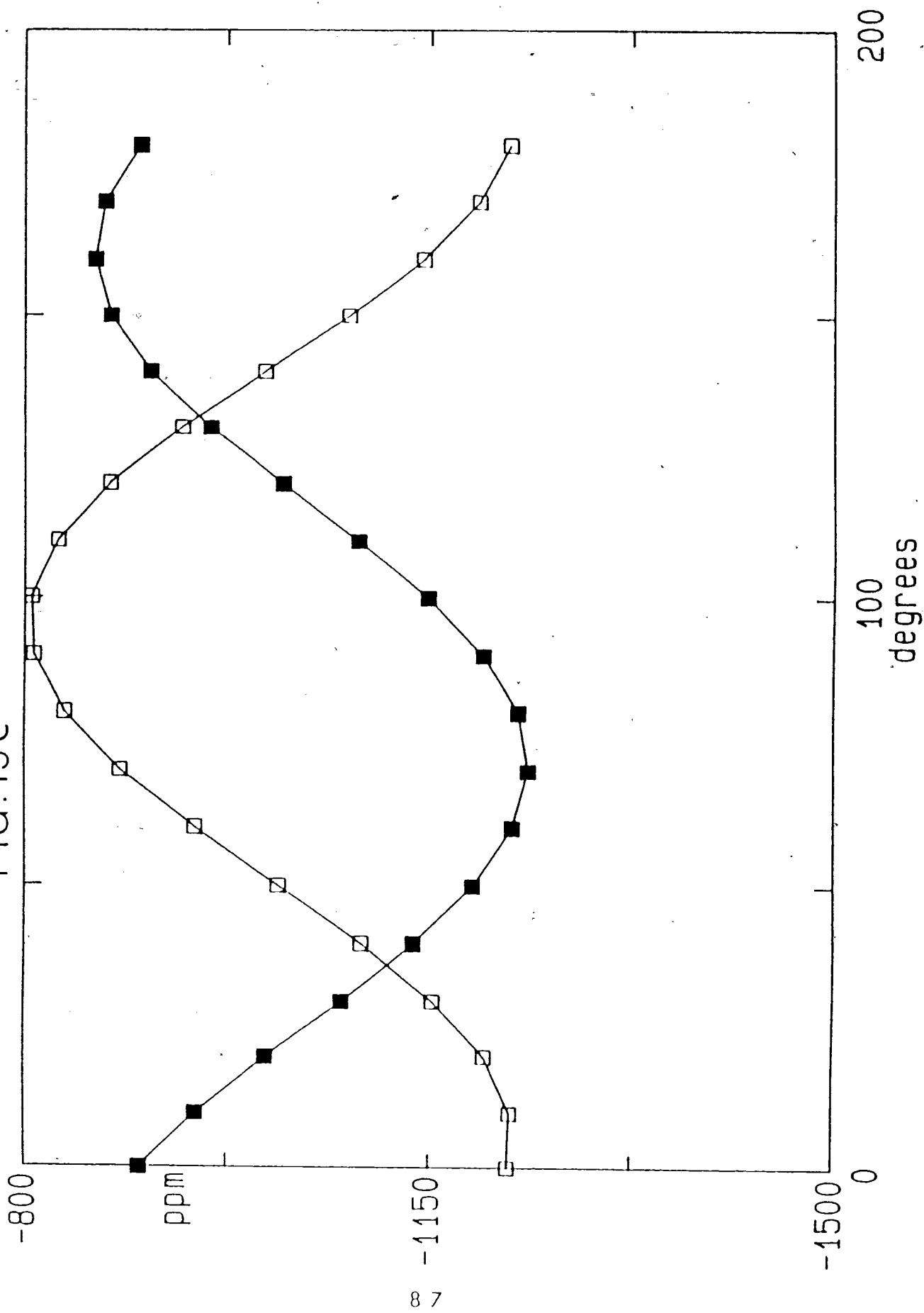


FIG. 16a

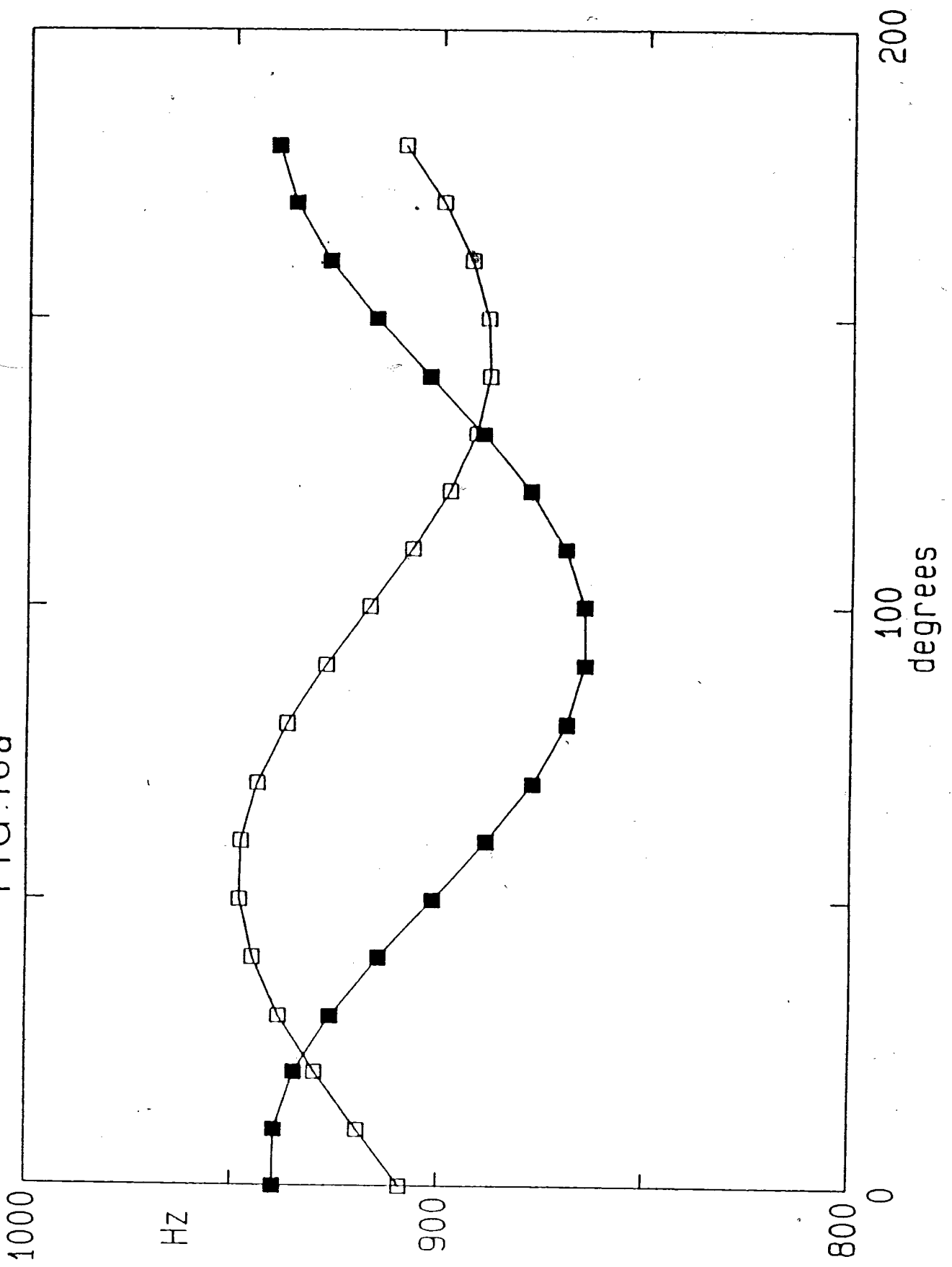


FIG. 16 b

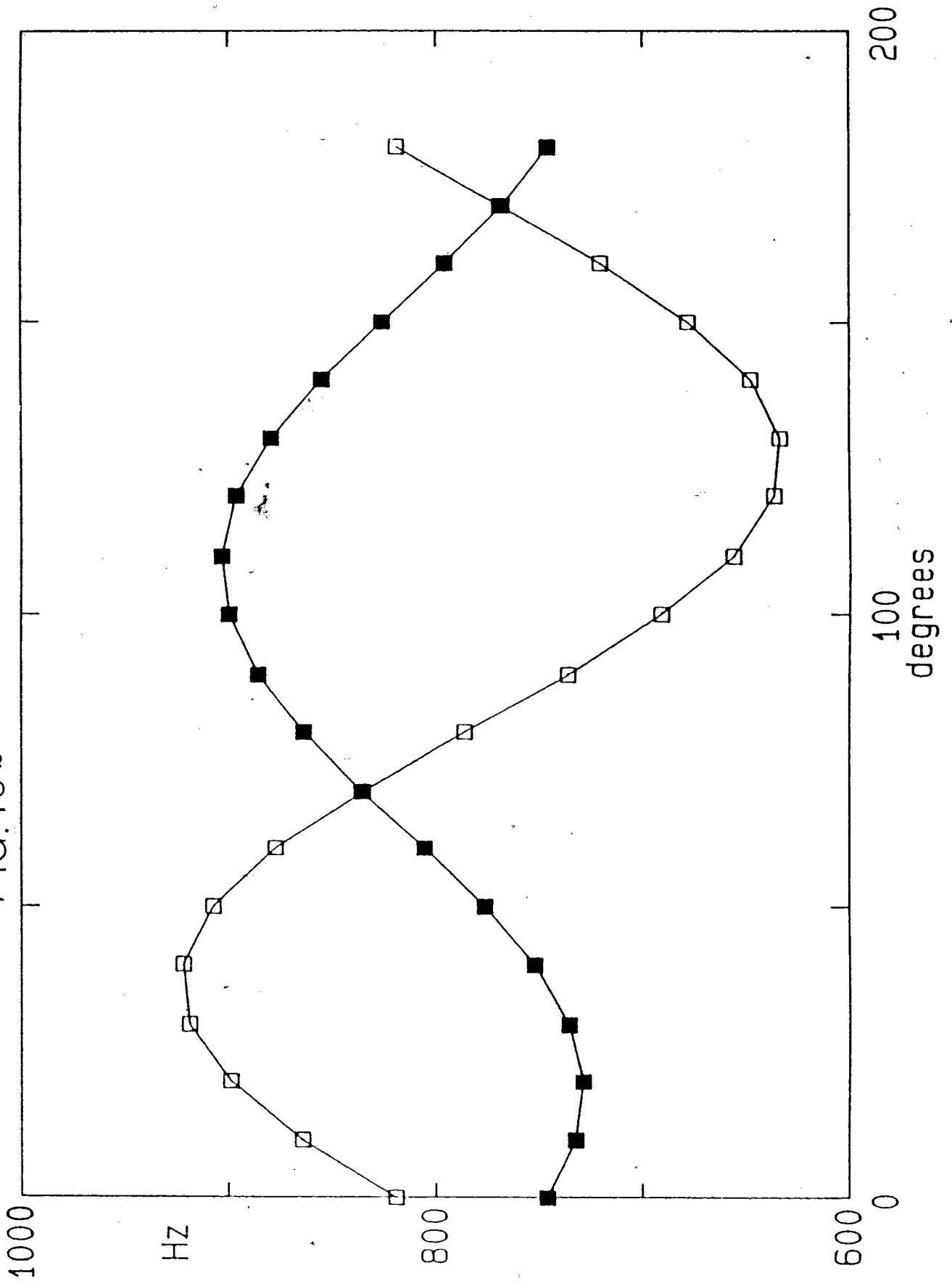


FIG. 16C

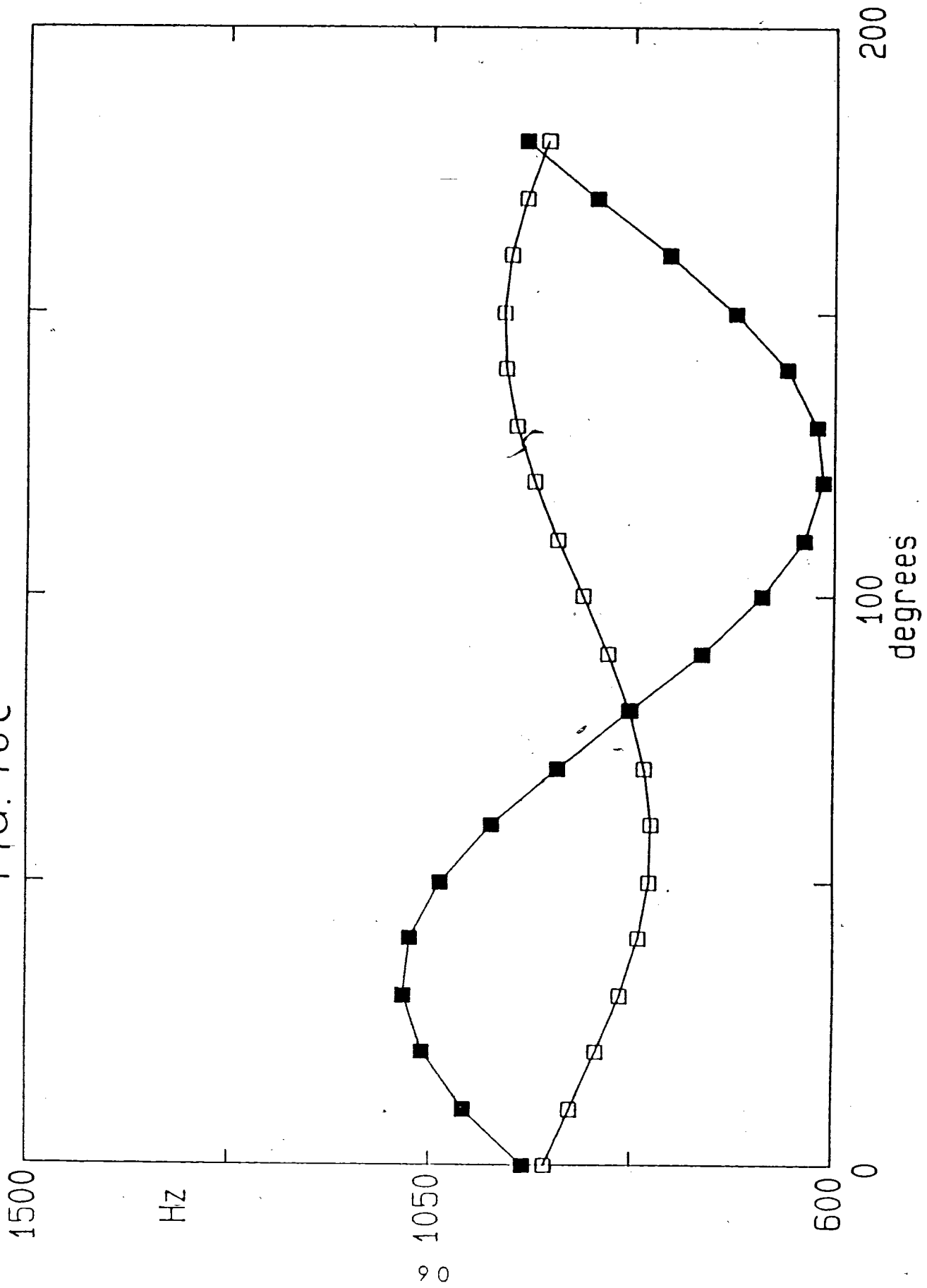


FIG. 17 a

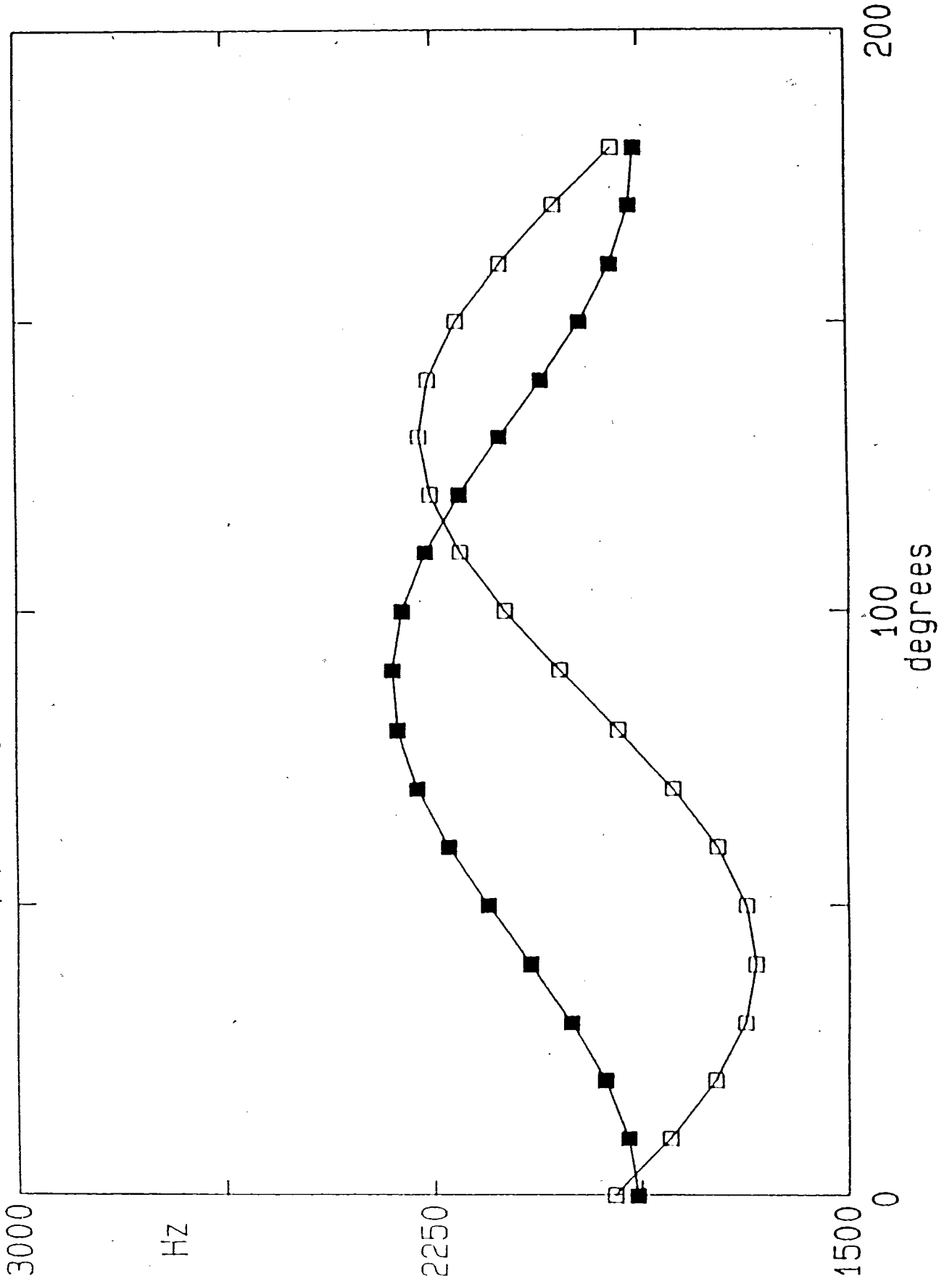


FIG. 17 b

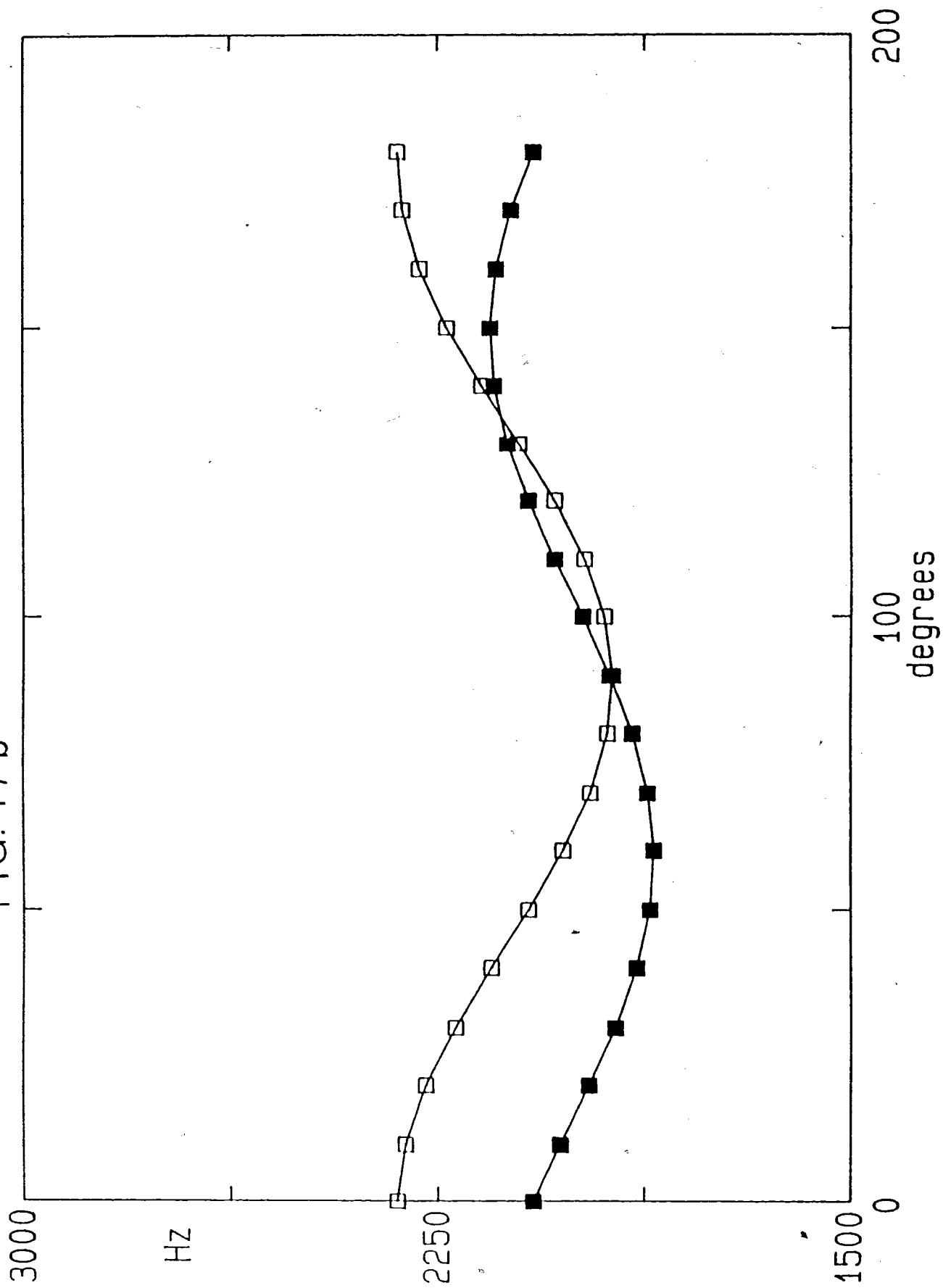


FIG. 17C

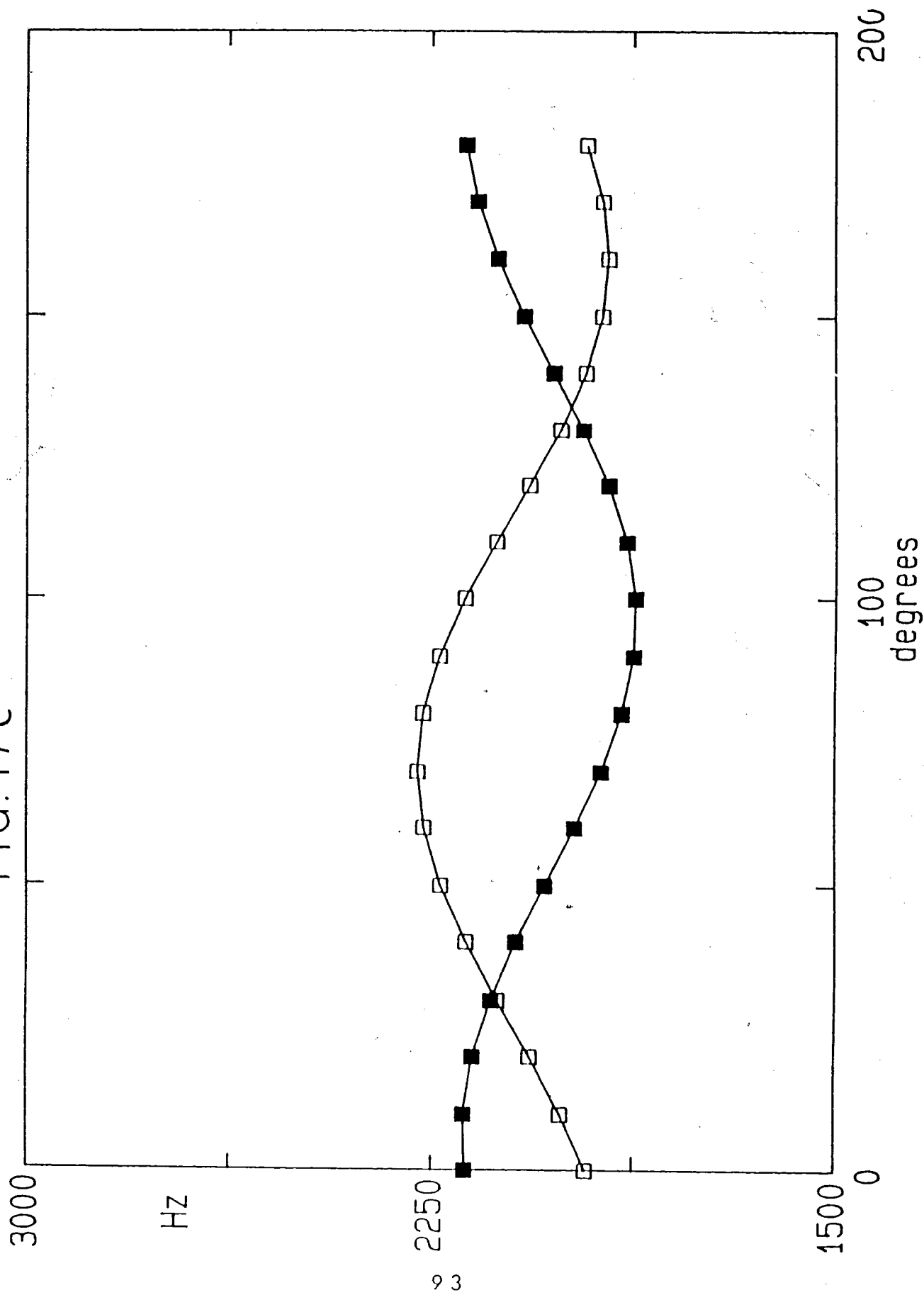


FIG. 18a

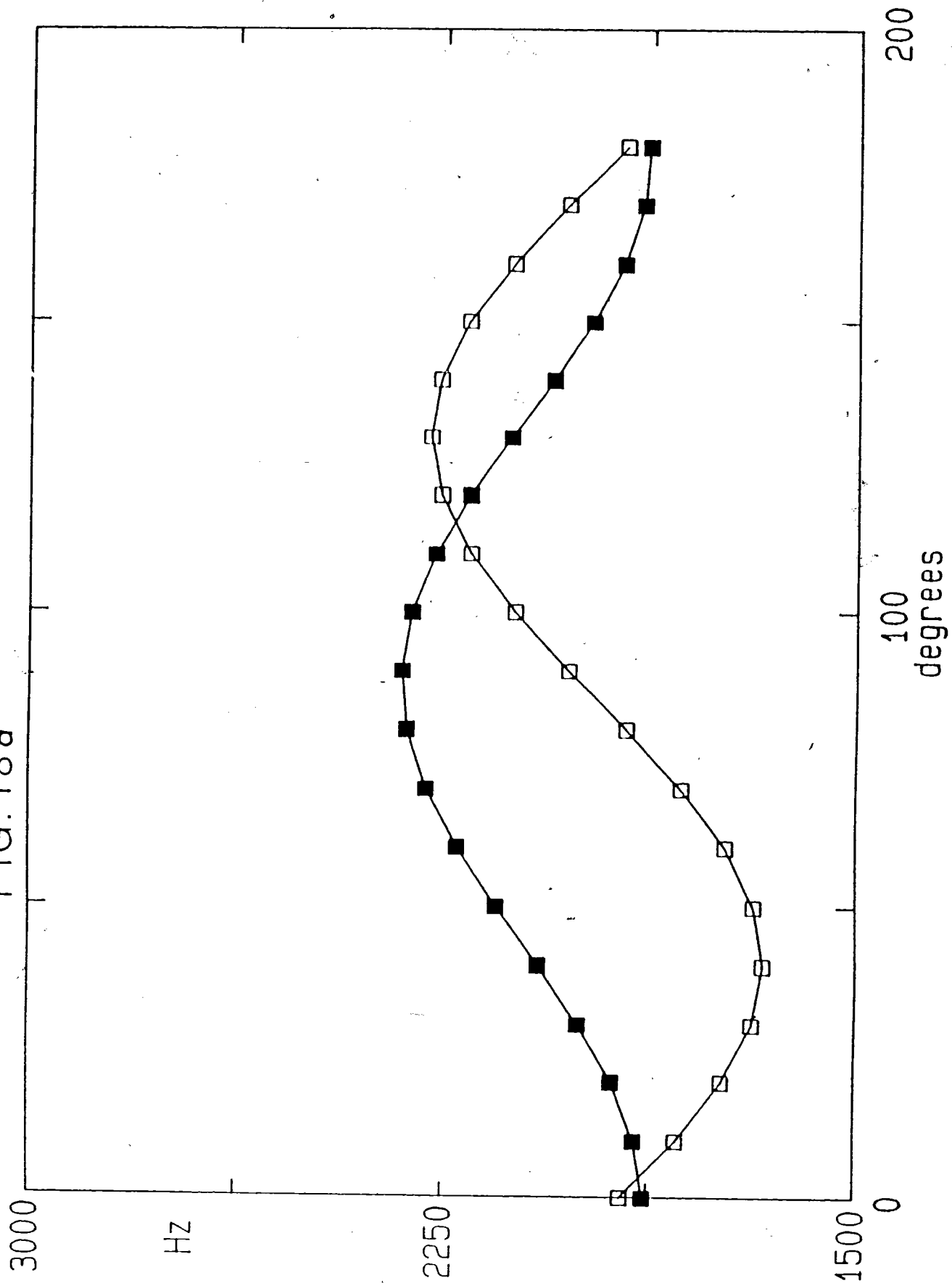


FIG.18 b

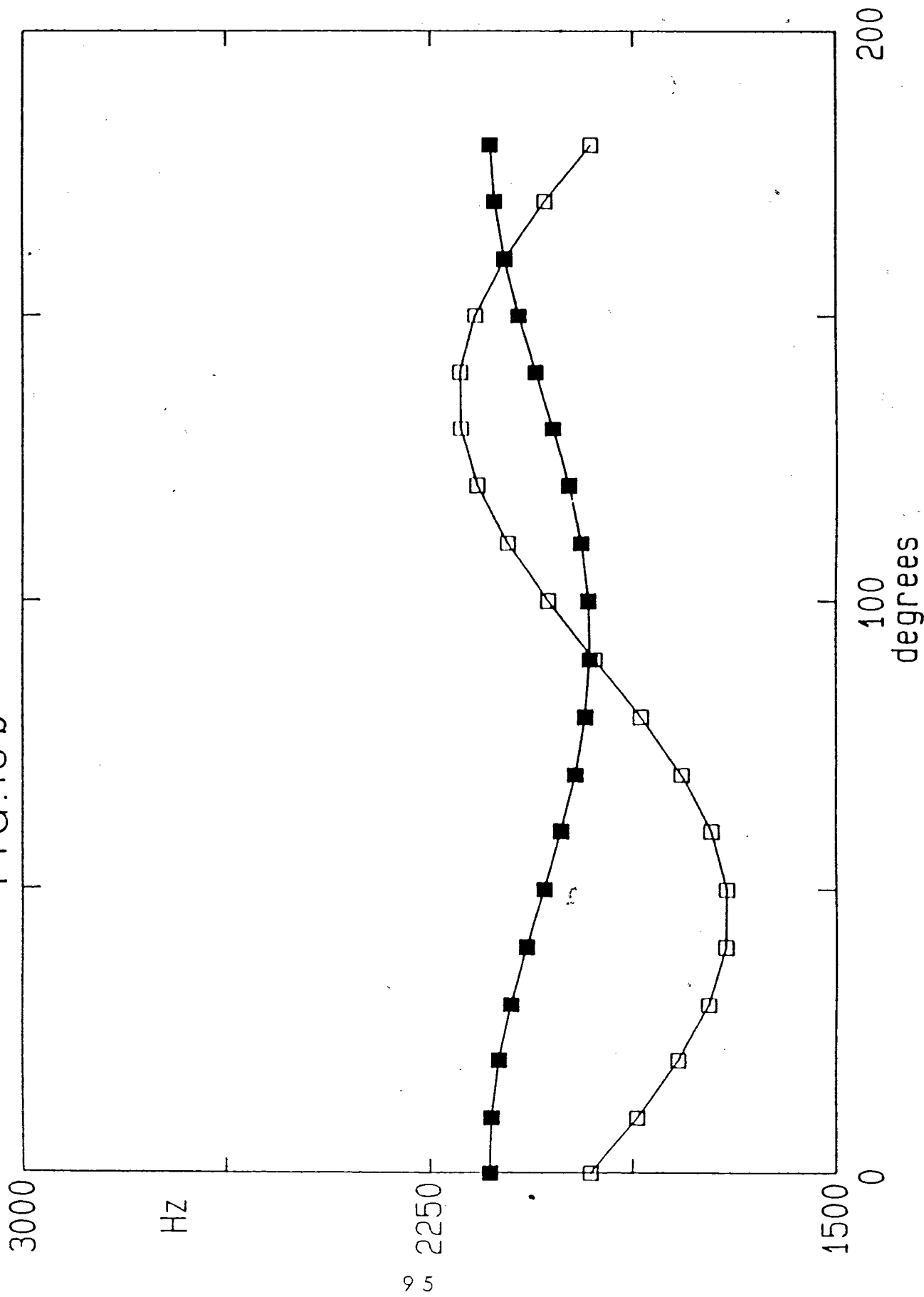
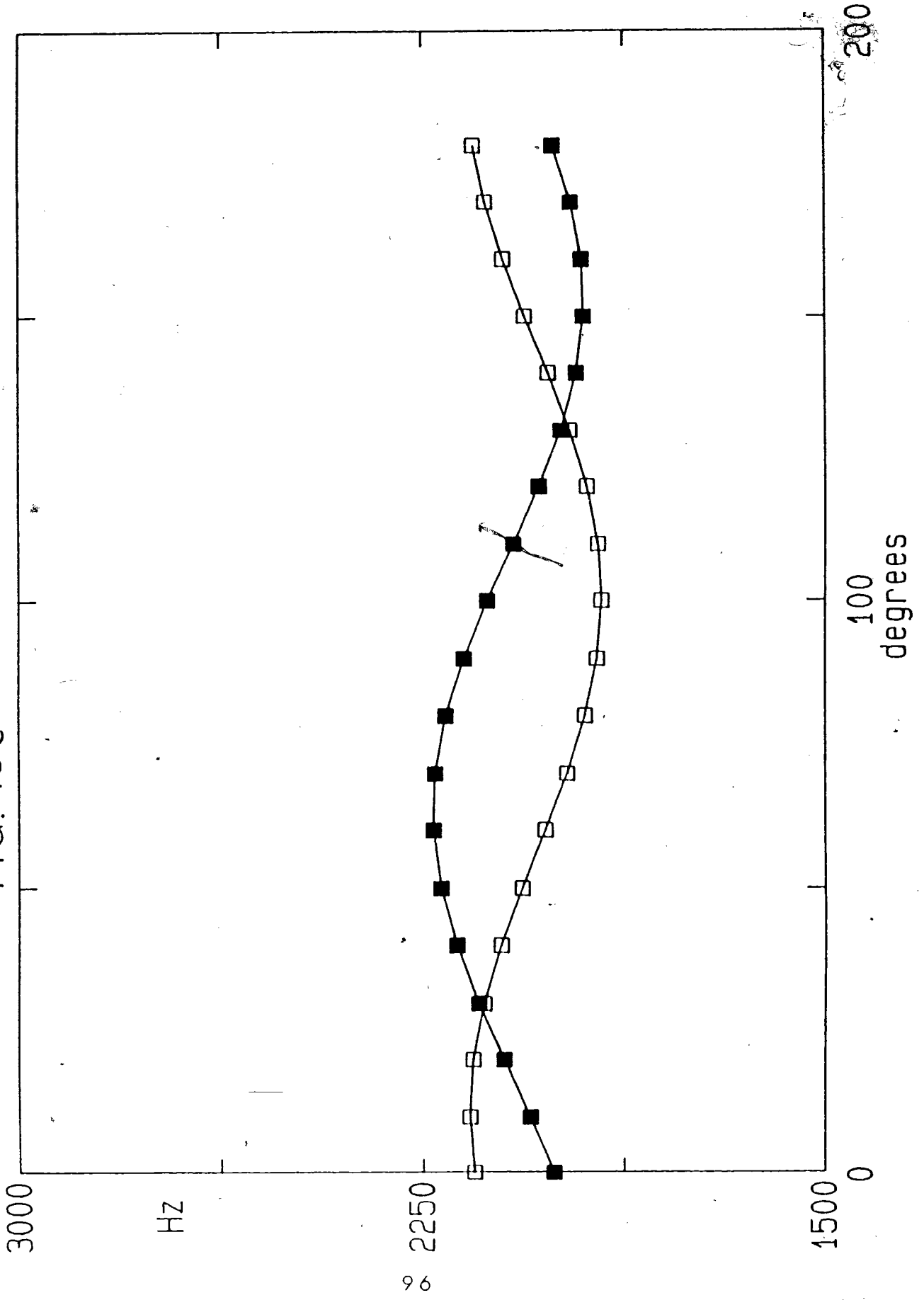


FIG. 18C



APPENDIX I

In this appendix we collected all the data from NMR measurements of single crystals of di-tert-butyltin chalcogenides compounds, and data after MINUIT fitting. The tensor elements of each nuclei are also collected. P1 and P2 in Table 1 to Table 8 of this Appendix stand for peak 1 position and peak 2 position in NMR spectrum, respectively.

Table 1. Sn Chemical Shift in Compound a (ppm)

O1Angle	P1(EXP)	P1(THEOR)	P2(EXP)	P2(THEOR)
0.00	235.60	235.80	47.02	48.30
10.00	223.52	223.47	109.26	109.87
20.00	206.10	207.74	167.83	164.91
30.00	189.79	190.50	207.03	206.79
40.00	173.48	173.85	230.22	230.46
50.00	159.30	159.78	232.31	233.06
60.00	151.49	149.99	214.97	214.28
70.00	145.96	145.67	175.45	176.37
80.00	147.40	147.33	123.75	123.93
90.00	154.94	154.77	64.44	63.26
100.00	166.78	167.11	3.16	1.69
110.00	183.24	182.84	-57.53	-53.35
120.00	199.60	200.07	81.74	-95.23
130.00	215.81	216.73	-117.53	-118.90
140.00	231.13	230.80	-120.17	-121.50
150.00	240.21	240.58	-102.38	-102.72
160.00	244.63	244.91	-65.51	-64.82
170.00	244.29	243.24	-11.98	-12.37
180.00	237.70	235.80	46.76	48.30
O2Angle	P1(EXP)	P1(THEOR)	P2(EXP)	P2(THEOR)
0.00	152.64	149.95	66.47	66.61
10.00	193.00	194.36	72.92	69.47
20.00	222.62	222.61	84.96	82.70
30.00	231.53	231.31	103.87	104.69
40.00	220.40	219.40	133.02	132.80
50.00	190.67	188.32	161.57	163.64
60.00	139.58	141.82	194.01	193.48
70.00	84.13	85.51	220.15	218.72
80.00	28.35	26.17	234.71	236.33
90.00	-30.42	-29.03	243.54	244.18
100.00	-74.12	-73.44	240.86	241.32
110.00	-100.47	-101.69	228.95	228.09
120.00	-110.99	-110.39	207.35	206.10
130.00	-98.28	-98.48	178.85	177.99
140.00	-66.59	-67.40	147.02	147.15
150.00	-20.55	-20.90	116.89	117.31
160.00	33.57	35.41	91.90	92.07
170.00	97.01	94.75	72.13	74.46
180.00	146.16	149.95	64.57	66.61

2

Table 1.

Continued

O3Angle	P1(EXP)	P1(THEOR)	P2(EXP)	P2(THEOR)
0.00	245.54	244.42	-31.67	-32.70
10.00	237.66	235.46	-49.11	-50.16
20.00	215.14	216.16	-49.12	-49.85
30.00	185.62	188.82	-29.51	-31.80
40.00	157.14	156.76	1.97	1.81
50.00	123.24	123.83	46.81	46.93
60.00	95.12	94.02	95.12	98.11
70.00	72.15	70.91	146.47	149.19
80.00	56.92	57.29	195.25	193.99
90.00	54.69	54.81	229.01	227.12
100.00	63.33	63.77	245.29	244.59
110.00	83.02	83.07	245.43	244.28
120.00	110.36	110.41	226.88	226.23
130.00	144.06	142.47	189.81	192.61
140.00	174.73	175.40	147.38	147.50
150.00	203.04	205.21	99.19	96.31
160.00	228.17	228.32	42.60	45.24
170.00	242.05	241.94	-1.10	0.43
180.00	245.50	244.42	-33.54	-32.70

Table 2. Sn Chemical Shift in Compound **b** (ppm)

O1Angle	P1(EXP)	P1(THEOR)	P2(EXP)	P2(THEOR)
0.00	225.09	223.89	53.36	50.08
10.00	202.34	202.60	51.62	49.31
20.00	170.69	171.40	61.25	59.40
30.00	133.77	134.05	78.66	79.13
40.00	90.89	95.06	110.09	106.13
50.00	59.88	59.13	135.38	137.13
60.00	32.19	30.59	166.21	168.39
70.00	13.47	12.89	195.66	196.16
80.00	9.26	8.16	216.12	217.07
90.00	17.44	16.97	228.09	228.61
100.00	38.14	38.26	229.74	229.38
110.00	68.93	69.46	220.30	219.29
120.00	105.09	106.81	201.27	199.56
130.00	145.91	145.80	173.63	172.56
140.00	182.56	181.73	140.71	141.56
150.00	209.05	210.27	110.77	110.30
160.00	227.50	227.97	81.69	82.53
170.00	233.48	232.70	58.35	61.62
180.00	225.97	223.89	45.38	50.08
O2Angle	P1(EXP)	P1(THEOR)	P2(EXP)	P2(THEOR)
0.00	-157.53	-145.21	-119.25	-116.94
10.00	-54.27	-56.02	-111.19	-114.14
20.00	36.11	34.60	-90.38	-91.11
30.00	120.74	115.72	-49.15	-50.61
40.00	178.97	177.57	1.29	2.45
50.00	214.13	212.67	64.42	61.69
60.00	214.48	216.80	121.65	119.96
70.00	195.40	189.46	164.16	170.22
80.00	126.23	133.95	207.54	206.43
90.00	69.53	56.95	222.89	224.20
100.00	-41.23	-32.23	221.68	221.40
110.00	-130.47	-122.85	198.24	198.36
120.00	-204.84	-203.98	159.39	157.87
130.00	-264.21	-265.82	107.30	104.80
140.00	-297.91	-300.93	46.29	45.56
150.00	-299.67	-305.06	-13.84	-12.70
160.00	-271.05	-277.72	-63.40	-62.97
170.00	-213.06	-222.20	-102.15	-99.17
180.00	-160.85	-145.21	-117.13	-116.94

Table 2.

Continued

O3Angle	P1(EXP)	P1(THEOR)	P2(EXP)	P2(THEOR)
0.00	228.11	228.80	2.72	7.13
10.00	220.79	221.83	92.64	91.49
20.00	193.57	192.96	157.21	160.01
30.00	142.33	145.68	205.55	204.43
40.00	83.47	85.70	219.15	219.40
50.00	25.07	20.24	205.13	203.10
60.00	-38.76	-42.80	161.51	157.51
70.00	-96.52	-95.81	87.32	88.12
80.00	-134.29	-132.40	-2.12	3.31
90.00	-148.86	-148.16	-88.22	-86.71
100.00	-141.85	-141.19	-170.13	-171.06
110.00	-114.63	-112.32	-236.58	-239.58
120.00	-65.54	-65.04	-284.11	-284.01
130.00	-3.30	-5.06	-299.38	-298.97
140.00	63.16	60.40	-281.94	-282.68
150.00	122.62	123.44	-238.45	-237.09
160.00	177.33	176.45	-166.28	-167.70
170.00	212.87	213.04	-82.30	-82.88
180.00	228.99	228.80	9.21	7.13

Table 3. Sn Chemical Shift in Compound c (ppm)

O1Angle	P1(EXP)	P1(THEOR)	P2(EXP)	P2(THEOR)
0.00	-260.50	-226.81	-229.33	-243.17
10.00	-244.19	-236.68	-399.52	-397.74
20.00	-221.43	-220.45	-543.63	-536.55
30.00	-169.47	-180.09	-648.99	-642.85
40.00	-112.10	-120.46	-697.69	-703.82
50.00	-44.29	-48.75	-699.38	-712.12
60.00	33.68	26.38	-675.50	-666.72
70.00	98.23	95.88	-579.36	-573.12
80.00	150.48	151.35	-442.96	-442.60
90.00	180.64	186.12	-287.20	-290.91
100.00	187.54	195.99	-133.07	-136.34
110.00	171.48	179.76	1.31	2.47
120.00	135.33	139.40	108.21	108.78
130.00	79.55	79.77	170.42	169.75
140.00	14.88	8.06	177.32	178.04
150.00	-53.85	-67.07	129.96	132.65
160.00	-116.70	-136.57	40.70	39.05
170.00	-171.06	-192.04	-97.89	-91.47
180.00	-251.23	-226.81	-243.23	-243.17
O2Angle	P1(EXP)	P1(THEOR)	P2(EXP)	P2(THEOR)
0.00	165.47	163.02	-364.13	-372.63
10.00	106.98	107.49	-522.23	-523.01
20.00	35.05	30.95	-639.12	-645.18
30.00	-56.39	-57.38	-722.32	-724.41
40.00	-155.04	-146.83	-750.57	-751.12
50.00	-224.68	-226.62	-721.82	-722.11
60.00	-284.68	-287.13	-640.51	-640.87
70.00	-319.33	-321.06	-518.24	-517.19
80.00	-322.86	-324.31	-370.76	-366.01
90.00	-294.67	-296.49	-208.02	-205.55
100.00	-249.48	-240.97	-50.32	-55.16
110.00	-164.72	-164.42	65.30	67.01
120.00	-74.21	-76.10	147.55	146.23
130.00	16.40	13.36	174.66	172.94
140.00	93.95	93.15	146.24	143.93
150.00	155.01	153.66	62.46	62.69
160.00	184.60	187.59	-59.96	-60.98
170.00	188.83	190.84	-216.02	-212.17
180.00	161.52	163.02	-388.39	-372.63

Table 3.

Continued

O3Angle	P1(EXP)	P1(THEOR)	P2(EXP)	P2(THEOR)
0.00	186.49	178.63	-289.82	-285.24
10.00	171.76	167.37	-233.41	-243.08
20.00	118.89	121.60	-168.66	-179.76
30.00	41.48	46.86	-95.39	-102.93
40.00	-51.28	-47.85	-20.37	-21.85
50.00	-153.39	-151.11	51.31	53.70
60.00	-247.07	-250.45	107.57	114.61
70.00	-335.04	-333.90	149.15	153.53
80.00	-389.97	-391.40	162.17	165.77
90.00	-412.18	-416.00	147.98	149.85
100.00	-402.40	-404.73	111.26	107.69
110.00	-357.61	-358.97	46.92	44.37
120.00	-288.29	-284.22	-26.12	-32.46
130.00	-194.44	-189.51	-108.52	-113.54
140.00	-85.03	-86.26	-190.25	-189.10
150.00	12.02	13.09	-252.05	-250.01
160.00	94.98	96.54	-292.49	-288.93
170.00	152.80	154.03	-307.54	-301.16
180.00	180.61	178.63	-295.53	-285.24

Table 4. Se Chemical Shift in Compound b (ppm)

O1Angle	P1(EXP)	P2(EXP)	P1(THEOR)	P2(THEOR)
0.00	-530.56	-643.78	-527.23	-642.72
10.00	-558.01	-647.10	-554.24	-646.06
20.00	-585.52	-637.21	-585.29	-638.79
30.00	-619.40	-619.40	-616.63	-621.79
40.00	-643.81	-596.23	-644.50	-597.10
50.00	-664.33	-568.42	-665.52	-567.71
60.00	-674.95	-538.27	-677.16	-537.16
70.00	-677.52	-510.49	-678.02	-509.13
80.00	-667.48	-487.08	-668.00	-487.00
90.00	-647.60	-473.30	-648.29	-473.45
100.00	-623.26	-469.61	-621.29	-470.11
110.00	-592.40	-476.70	-590.24	-477.38
120.00	-558.64	-493.48	-558.89	-494.38
130.00	-531.34	-520.46	-531.03	-519.06
140.00	-510.61	-547.91	-510.01	-548.46
150.00	-496.77	-578.95	-498.36	-579.01
160.00	-496.51	-606.11	-497.50	-607.04
170.00	-504.17	-629.65	-507.53	-629.16
180.00	-524.09	-644.07	-527.23	-642.72
O1Angle	P1(EXP)	P2(EXP)	P1(THEOR)	P2(THEOR)
0.00	-650.83	-459.67	-651.04	-454.99
10.00	-630.21	-544.55	-631.94	-538.52
20.00	-609.57	-599.33	-596.75	-609.09
30.00	-545.08	-663.44	-549.71	-659.19
40.00	-496.26	-681.89	-496.50	-679.89
50.00	-445.11	-674.54	-443.53	-671.58
60.00	-394.80	-632.83	-397.20	-634.26
70.00	-359.98	-565.65	-363.09	-572.43
80.00	-343.56	-490.72	-345.31	-493.55
90.00	-346.19	-412.29	-346.02	-407.13
100.00	-366.82	-325.49	-365.12	-323.60
110.00	-404.52	-250.93	-400.31	-253.02
120.00	-445.80	-206.68	-447.34	-203.93
130.00	-504.06	-183.01	-500.56	-182.22
140.00	-552.15	-190.37	-553.52	-190.53
150.00	-598.68	-227.04	-599.86	-227.85
160.00	-630.45	-285.44	-633.97	-289.68
170.00	-650.29	-367.95	-651.75	-368.57
180.00	-650.20	-452.20	-651.04	-454.98

Table 4.

Continued

O1Angle	P1(EXP)	P2(EXP)	P1(THEOR)	P2(THEOR)
0.00	-356.56	-384.55	-358.09	-381.56
10.00	-445.53	-371.14	-445.72	-367.50
20.00	-530.91	-370.54	-531.50	-371.24
30.00	-609.97	-391.32	-605.09	-392.32
40.00	-660.24	-429.44	-657.61	-428.20
50.00	-680.98	-473.08	-682.72	-474.54
60.00	-675.11	-524.21	-677.40	-525.77
70.00	-643.88	-572.45	-642.29	-575.70
80.00	-578.90	-619.92	-581.62	-618.31
90.00	-506.95	-649.98	-502.71	-648.46
100.00	-411.43	-663.46	-415.08	-662.51
110.00	-327.07	-661.14	-329.30	-658.77
120.00	-257.97	-639.83	-255.71	-637.70
130.00	-203.28	-599.54	-203.19	-601.82
140.00	-179.52	-551.50	-178.08	-555.47
150.00	-186.65	-503.50	-183.40	-504.24
160.00	-217.58	-455.89	-218.51	-454.32
170.00	-278.50	-408.52	-279.18	-411.71
180.00	-354.30	-381.70	-358.09	-381.56

Table 5. Te Chemical Shift in Compound c (ppm)

O1Angle	P1(EXP)	P1(THEOR)	P2(EXP)	P2(THEOR)
0.00	-944.74	-946.35	-1006.52	-1010.73
10.00	-841.24	-847.21	-1022.69	-1018.25
20.00	-758.52	-756.15	-1040.01	-1037.70
30.00	-681.96	-684.14	-1069.01	-1066.75
40.00	-641.55	-639.86	-1102.36	-1101.90
50.00	-630.15	-628.66	-1138.96	-1138.90
60.00	-654.61	-651.89	-1174.34	-1173.29
70.00	-709.84	-706.75	-1200.46	-1200.92
80.00	-783.82	-786.62	-1216.41	-1218.46
90.00	-875.72	-881.86	-1221.82	-1223.79
100.00	-984.09	-980.99	-1215.93	-1216.28
110.00	-1074.09	-1072.06	-1196.56	-1196.82
120.00	-1143.89	-1144.07	-1169.07	-1167.77
130.00	-1189.84	-1188.35	-1133.12	-1132.63
140.00	-1200.35	-1199.54	-1099.67	-1095.63
150.00	-1174.45	-1176.31	-1060.80	-1061.24
160.00	-1125.57	-1121.46	-1035.10	-1033.61
170.00	-1040.50	-1041.59	-1014.69	-1016.07
180.00	-948.25	-946.35	-1003.95	-1010.73
O2Angle	P1(EXP)	P1(THEOR)	P2(EXP)	P2(THEOR)
0.00	-823.67	-821.63	-1197.98	-1197.25
10.00	-723.45	-723.79	-1166.49	-1165.62
20.00	-645.76	-646.81	-1120.47	-1121.10
30.00	-601.79	-599.98	-1071.13	-1069.04
40.00	-588.78	-588.95	-1017.25	-1015.74
50.00	-614.13	-615.04	-968.24	-967.61
60.00	-673.79	-675.12	-929.58	-930.47
70.00	-761.46	-761.94	-907.67	-908.80
80.00	-862.06	-865.01	-903.55	-905.20
90.00	-980.03	-971.92	-919.56	-920.11
100.00	-1068.43	-1069.77	-952.11	-951.74
110.00	-1145.94	-1146.75	-996.48	-996.27
120.00	-1192.84	-1193.58	-1050.47	-1048.32
130.00	-1203.27	-1204.61	-1102.19	-1101.63
140.00	-1177.55	-1178.51	-1149.63	-1149.75
150.00	-1117.97	-1118.43	-1187.11	-1186.89
160.00	-1034.94	-1031.62	-1207.85	-1208.57
170.00	-926.75	-928.54	-1210.57	-1212.16
180.00	-821.01	-821.63	-1195.21	-1197.25

Table 5.

Continued

O3Angle	P1(EXP)	P1(THEOR)	P2(EXP)	P2(THEOR)
0.00	-897.36	-900.32	-1218.63	-1218.74
10.00	-947.47	-948.55	-1221.00	-1220.81
20.00	-1004.57	-1008.80	-1199.02	-1197.88
30.00	-1071.30	-1073.80	-1153.66	-1152.73
40.00	-1138.45	-1135.72	-1088.94	-1090.79
50.00	-1187.44	-1187.09	-1019.96	-1019.55
60.00	-1221.38	-1221.71	-950.11	-947.58
70.00	-1236.68	-1235.40	-885.45	-883.58
80.00	-1228.74	-1226.51	-834.14	-835.27
90.00	-1195.24	-1196.12	-802.89	-808.46
100.00	-1151.13	-1147.89	-805.33	-806.39
110.00	-1084.34	-1087.64	-830.91	-829.32
120.00	-1017.78	-1022.63	-877.88	-874.47
130.00	-960.51	-960.71	-937.18	-936.41
140.00	-910.93	-909.35	-1007.33	-1007.65
150.00	-875.65	-874.73	-1081.27	-1079.62
160.00	-862.88	-861.04	-1140.68	-1143.61
170.00	-872.72	-869.93	-1190.77	-1191.93
180.00	-903.66	-900.32	-1218.40	-1218.74

Table 6. Sn D-Coupling in Compound **b** (Hz)

O1Angle	D1(EXP)	D1(THEOR)	D2(EXP)	D2(THEOR)
0.00	926.97	939.67	915.73	909.03
10.00	1053.66	939.43	905.62	919.42
20.00	968.21	934.70	923.32	929.67
30.00	865.38	926.04	905.49	938.54
40.00	915.82	914.50	930.36	944.96
50.00	999.54	901.46	1058.37	948.15
60.00	969.80	888.51	1016.92	947.73
70.00	811.84	877.20	1038.00	943.76
80.00	820.38	868.89	919.88	936.71
90.00	909.17	864.60	704.24	927.41
100.00	824.84	864.83	806.39	917.02
110.00	796.72	869.56	933.49	906.78
120.00	744.07	878.22	876.05	897.90
130.00	1048.93	889.76	1175.60	891.48
140.00	1022.12	902.80	964.42	888.29
150.00	929.44	915.75	726.57	888.70
160.00	998.50	927.06	857.96	892.68
170.00	825.22	935.37	955.50	899.74
180.00	746.83	939.66	823.65	909.03
O2Angle	D1(EXP)	D1(THEOR)	D2(EXP)	D2(THEOR)
0.00	889.17	745.84	738.92	819.14
10.00	808.81	732.19	378.15	864.12
20.00	886.53	728.64	779.27	898.66
30.00	986.48	735.59	804.14	918.61
40.00	1019.02	752.22	794.73	921.55
50.00	928.29	776.53	796.53	907.15
60.00	1014.20	805.59	806.49	877.12
70.00	842.90	835.88	845.42	835.10
80.00	818.20	863.75	750.30	786.15
90.00	957.78	885.84	955.80	736.17
100.00	655.46	899.49	816.38	691.21
110.00	774.99	903.05	977.70	656.66
120.00	633.71	896.09	975.72	636.71
130.00	649.81	879.45	855.47	633.76
140.00	634.23	855.15	697.00	648.17
150.00	628.28	826.09	908.66	678.20
160.00	640.46	795.81	842.66	720.22
170.00	675.76	767.93	747.48	769.17
180.00	913.61	745.84	963.37	819.15

Table 6.

Continued

O3Angle	P1(EXP)	P1(THEOR)	P2(EXP)	P2(THEOR)
0.00	737.86	944.67	772.81	920.49
10.00	924.36	1011.38	901.59	892.56
20.00	1220.67	1058.15	1429.29	863.84
30.00	792.44	1079.36	1002.66	837.79
40.00	800.95	1072.43	1000.08	817.56
50.00	857.55	1038.20	911.29	805.60
60.00	760.13	980.82	994.15	803.34
70.00	737.91	907.18	966.39	811.05
80.00	1208.33	826.18	844.98	827.79
90.00	498.91	747.59	793.97	851.57
100.00	804.07	680.88	596.24	879.50
110.00	843.03	634.10	673.91	908.22
120.00	894.40	612.90	657.78	934.26
130.00	1082.42	619.82	643.81	954.49
140.00	1131.01	654.05	499.18	966.45
150.00	1210.70	711.44	779.96	968.72
160.00	871.19	785.07	817.42	961.01
170.00	779.83	866.08	890.22	944.26
180.00	716.54	944.68	1001.57	920.49

Table 7. Sn D-Coupling in Compound c (Hz)

O1Angle	D1(EXP)	D1(THEOR)	D2(EXP)	D2(THEOR)
0.00	2242.35	1882.22	2398.77	1923.03
10.00	1942.98	1899.63	1904.97	1823.63
20.00	2021.58	1941.64	1793.70	1742.19
30.00	2042.05	2003.18	1780.93	1688.51
40.00	2111.98	2076.85	1681.55	1669.07
50.00	2121.42	2153.73	1251.52	1686.23
60.00	2215.22	2224.57	1902.56	1737.92
70.00	2256.99	2280.81	1876.95	1817.89
80.00	2303.56	2315.69	1962.54	1916.50
90.00	2301.56	2324.98	2091.66	2021.86
100.00	2307.03	2307.57	2162.90	2121.26
110.00	2270.88	2265.56	2196.49	2202.71
120.00	2253.43	2204.02	2075.97	2256.39
130.00	2042.08	2130.35	2234.56	2275.81
140.00	2100.53	2053.47	2346.19	2258.65
150.00	2117.25	1982.63	2267.81	2206.97
160.00	2068.27	1926.39	2232.65	2126.99
170.00	1489.39	1891.51	1742.01	2028.38
180.00	1540.45	1882.22	1527.58	1923.02
O2Angle	D1(EXP)	D1(THEOR)	D2(EXP)	D2(THEOR)
0.00	2123.01	2076.15	2045.02	2323.21
10.00	2265.79	2027.20	1923.60	2308.43
20.00	2222.62	1975.78	1833.50	2271.85
30.00	2211.81	1928.11	2928.30	2217.90
40.00	2142.63	1889.92	1225.00	2153.07
50.00	2140.79	1865.82	1781.90	2085.19
60.00	2072.39	1858.73	1844.40	2022.45
70.00	2020.50	1869.48	1906.80	1972.41
80.00	2070.76	1896.80	1929.71	1941.10
90.00	1783.87	1937.39	2073.54	1932.31
100.00	1882.43	1986.34	2217.16	1947.11
110.00	1984.82	2037.76	1613.90	1983.68
120.00	2121.10	2085.43	1802.60	2037.64
130.00	2124.99	2123.63	2438.55	2102.46
140.00	1347.14	2147.72	2410.92	2170.35
150.00	3262.66	2154.81	2024.39	2233.08
160.00	2204.38	2144.05	2194.70	2283.13
170.00	2338.42	2116.74	2043.58	2314.43
180.00	2302.87	2076.15	1958.86	2323.22

Table 7.

Continued

O3Angle	D1(EXP)	D1(THEOR)	D2(EXP)	D2(THEOR)
0.00	2267.61	2187.47	2078.35	1962.02
10.00	2227.94	2190.10	1929.19	2008.88
20.00	2109.35	2173.64	1597.00	2066.60
30.00	2144.35	2140.05	2171.82	2128.25
40.00	1957.60	2093.39	2318.32	2186.38
50.00	2164.94	2039.29	2315.66	2233.77
60.00	2114.33	1984.28	2324.09	2265.28
70.00	1559.19	1934.97	2270.56	2276.55
80.00	2008.99	1897.36	2291.23	2266.41
90.00	1931.78	1875.93	2168.34	2236.08
100.00	1964.07	1873.29	2151.25	2189.23
110.00	1948.68	1889.76	2153.93	2131.50
120.00	2029.00	1923.35	2146.00	2069.85
130.00	1741.68	1970.00	1871.62	2011.74
140.00	1944.56	2024.10	1910.20	1964.14
150.00	2113.10	2079.12	1940.80	1932.82
160.00	2092.56	2128.40	2003.92	1921.55
170.00	2195.12	2166.04	2039.13	1931.70
180.00	2243.58	2187.47	2065.70	1962.03

Table 8. Te D-Coupling in Compound c (Hz)

O1Angle	D1(EXP)	D1(THEOR)	D2(EXP)	D2(THEOR)
0.00	2003.23	1834.15	1918.68	1912.78
10.00	1890.89	1857.27	2091.26	1959.38
20.00	1876.45	1878.91	2005.70	2020.59
30.00	1784.57	1896.44	2113.22	2089.04
40.00	1793.35	1907.77	2230.11	2156.49
50.00	1853.80	1911.51	2210.84	2214.78
60.00	1960.87	1907.23	2188.11	2256.89
70.00	2069.40	1895.43	2237.89	2277.73
80.00	1923.47	1877.54	2197.15	2274.81
90.00	1957.45	1855.73	2208.79	2248.47
100.00	1918.04	1832.60	2212.14	2201.88
110.00	2163.35	1810.97	2281.37	2140.65
120.00	834.26	1793.43	2393.67	2072.20
130.00	1606.68	1782.11	1646.34	2004.76
140.00	1951.42	1778.36	1917.67	1946.47
150.00	2266.51	1782.64	2059.75	1904.37
160.00	1769.25	1794.44	1603.50	1883.52
170.00	2080.21	1812.33	2078.21	1886.44
180.00	1244.98	1834.15	1769.58	1912.78
O2Angle	D1(EXP)	D1(THEOR)	D2(EXP)	D2(THEOR)
0.00	1963.38	2139.51	2200.72	1952.42
10.00	1833.55	2136.76	1727.25	1867.11
20.00	1911.77	2123.21	2240.41	1791.70
30.00	1693.70	2100.50	2100.92	1735.30
40.00	1752.92	2071.37	2183.63	1704.72
50.00	1598.57	2039.33	2071.44	1703.65
60.00	1830.19	2008.25	2044.42	1732.19
70.00	1744.44	1981.86	1986.28	1786.93
80.00	1760.33	1963.36	1802.23	1861.26
90.00	1889.45	1954.99	1949.37	1946.20
100.00	2250.88	1957.74	2002.28	2031.52
110.00	2177.77	1971.28	2015.99	2106.92
120.00	2153.84	1993.99	2043.80	2163.31
130.00	1924.27	2023.13	1857.04	2193.89
140.00	2229.18	2055.17	2106.41	2194.98
150.00	2326.74	2086.26	2133.91	2166.42
160.00	2052.46	2112.63	2191.27	2111.69
170.00	2085.85	2131.13	2104.43	2037.37
180.00	1863.76	2139.51	2230.54	1952.43

Table 8.

Continued

O3Angle	D1(EXP)	D1(THEOR)	D2(EXP)	D2(THEOR)
0.00	1914.17	2006.07	2157.75	2154.50
10.00	1862.61	2049.81	2275.61	2162.68
20.00	2614.89	2098.29	2010.00	2156.00
30.00	2027.76	2145.68	2273.73	2135.28
40.00	2230.18	2186.27	2043.82	2103.01
50.00	2055.50	2215.14	2054.28	2063.08
60.00	2291.42	2228.82	2045.36	2020.31
70.00	2228.21	2225.68	1955.01	1979.85
80.00	2151.83	2206.07	1959.61	1946.60
90.00	2191.65	2172.36	1929.43	1924.55
100.00	2154.44	2128.62	1897.48	1916.37
110.00	2026.65	2080.14	1910.15	1923.05
120.00	2053.12	2032.74	1963.03	1943.77
130.00	2009.87	1992.17	1993.74	1976.04
140.00	1990.48	1963.29	2007.10	2015.98
150.00	2039.05	1949.60	2086.72	2058.75
160.00	1903.80	1952.76	2067.11	2099.20
170.00	1991.97	1972.37	2118.15	2132.46
180.00	1870.78	2006.08	2117.86	2154.50

Table 9. Sn Chemical Shift Tensor of Compounds **a**
in Cube System (x,y,z) (ppm)

XX1	152 ± 3	XX2	65 ± 2
YY1	231 ± 6	YY2	52 ± 5
ZZ1	-31 ± 3	ZZ2	244 ± 1
XY1	22 ± 1	XY2	-185 ± 3
XZ1	-152 ± 3	XZ2	0.76 ± 3
YZ1	67 ± 3	YZ2	3 ± 2

Table 10. Sn Chemical Shift Tensor of Compound **b**
in Cube System (x,y,z) (ppm)

XX1	12 ± 7	XX2	229 ± 1
YY1	224 ± 1	YY2	54 ± 5
ZZ1	-102 ± 6	ZZ2	-147 ± 2
XY1	39 ± 2	XY2	13 ± 4
XZ1	-260 ± 4	XZ2	-18 ± 4
YZ1	17 ± 4	YZ2	-248 ± 9

Table 11. Se Chemical Shift Tensor of Compound **b**
in Cube System (x,y,z) (ppm)

XX1	-650 ± 2	XX2	-464 ± 13
YY1	-515 ± 17	YY2	-646 ± 4
ZZ1	-352 ± 8	ZZ2	-394 ± 18
XY1	68 ± 1	XY2	25 ± 3
XZ1	-29 ± 2	XZ2	248 ± 3
YZ1	243 ± 1	YZ2	-65 ± 1

Table 12. Sn Chemical Shift Tensor of Compound **c**
in Cube System (x,y,z) (ppm)

XX1	182 ± 5	XX2	-288 ± 4
YY1	-216 ± 15	YY2	-270 ± 38
ZZ1	-394 ± 31	ZZ2	156 ± 9
XY1	61 ± 9	XY2	443 ± 12
XZ1	-24 ± 7	XZ2	89 ± 12
YZ1	450 ± 10	YZ2	118 ± 7

Table 13. Te Chemical Shift Tensor of Compound **c**
in Cube System (x,y,z) (ppm)

XX1	-891 ± 13	XX2	-1221 ± 3
YY1	-933 ± 18	YY2	-991 ± 27
ZZ1	-1197 ± 1	ZZ2	-815 ± 9
XY1	-1276 ± 5	XY2	-988 ± 5
XZ1	-876 ± 5	XZ2	-949 ± 4
YZ1	-1059 ± 2	YZ2	-1291 ± 4

Table 14. Sn D-Coupling Tensor of Compound **b**
in Cube System (x,y,z) (Hz)

XX1	905 ± 56	XX2	924 ± 5
YY1	913 ± 38	YY2	823 ± 122
ZZ1	747 ± 1	ZZ2	835 ± 23
XY1	-6	XY2	-29
XZ1	-212	XZ2	75
YZ1	52	YZ2	-139

Table 15. Sn D-Coupling Tensor of Compound **c**
in Cube System (x,y,z) (Hz)

XX1	2256 ± 97	XX2	1992 ± 42
YY1	1910 ± 39	YY2	1928 ± 6
ZZ1	1976 ± 142	ZZ2	2279 ± 62
XY1	-12	XY2	299
XZ1	-35	XZ2	-112
YZ1	131	YZ2	9

Table 16. Te D-Coupling Tensor of Compound **c**
in Cube System (x,y,z) (Hz)

XX1	1931 ± 106	XX2	2201 ± 67
YY1	1894 ± 85	YY2	1930 ± 24
ZZ1	2156 ± 23	ZZ2	1938 ± 20
XY1	-66	XY2	-107
XZ1	-113	XZ1	-44
YZ1	-8	YZ2	-249

APPENDIX II

The Goniometer Measurement of Single Crystals
of $[t\text{-Bu}_2\text{SnSe}]_2$ and $[t\text{-Bu}_2\text{SnTe}]_2$

The arrangement sketched in Fig.1 will serve to illustrate the principle of two circle goniometer.

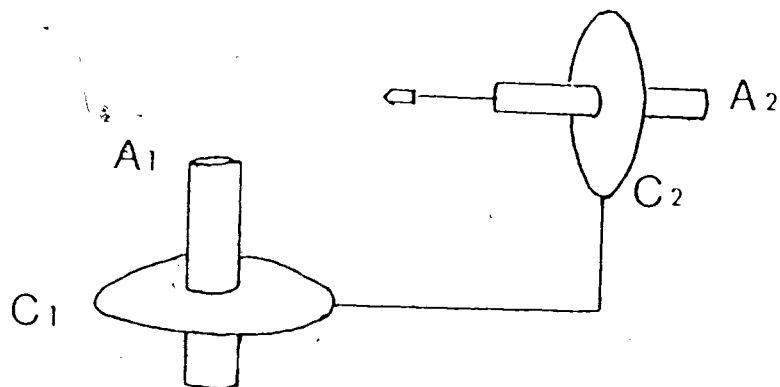


Fig.1 The Principle of Two Circle Goniometer

The disc C_1 which can be rotated about the fixed vertical axis A_1 carries a second disc C_2 parallel to the axis of A_1 . The rotational axis A_2 which is perpendicular to the disc C_2 carries the crystal. By turning the crystal through the required angles about the two axes, each of the crystal faces could be brought in turn into the reflecting position. The pole of a face will be determined relatively to the system by the co-ordinates ϕ and β . The numerical values of these two angles are equal to the readings of the circles C_2 and C_1 respectively at the moment which the face is correctly 'set'.

With the help of values ϕ and β determined in this way, a stereogram can be constructed. Transferring data from the goniometer to the projection is direct and simple, for readings on the horizontal circle, *i.e.* C_1 , of the goniometer correspond to radial distances from the center of the projection and readings on the vertical circle, *i.e.* C_2 , correspond to azimuthal positions around the center. Using the crystal data published in reference [50], we can construct the interplanar angle table. With the aid of the table of interplanar angles, one can find the orientation of the crystal, by determining which calculated interplanar angles match the experimental ones. The detailed theories of the goniometer and stereogram can be found in references [73.74]

The results are listed in the following tables.

Table 1. Data from Goniometer Measurement

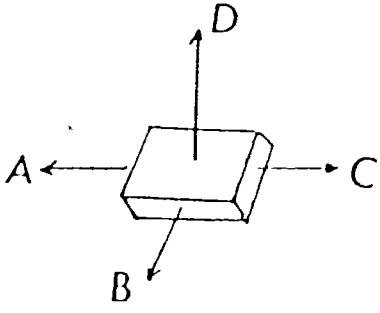
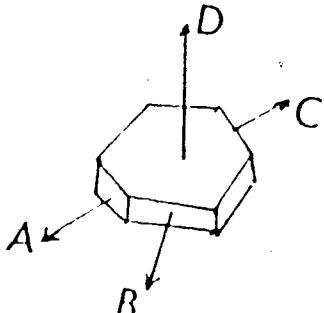
Compound b			Compound c		
					
Face	$\beta [^\circ]$	$\phi [^\circ]$	Face	$\beta [^\circ]$	$\phi [^\circ]$
A	284.7	25.5	A	268.4	347.0
B	194.9	137.2	B	289.9	281.9
C	256.8	204.8	C	273.8	169.5
D	278.5	133.7	D	192.5	277.5

Table 2. The Interplanar Angles [°]

1. Compound b

Face	A	B	C	D	Face	100	011	01 $\bar{1}$
A		72	2	105	100		73	72
B			71	96	011			96
C				107	010	90	43	43

D is (01 $\bar{1}$), A and C are the same plane (100), B is (011)

2. Compound c

Face	A	B	C	D	Face	110	00 $\bar{1}$	$\bar{1}20$
A		110	3	82	110		109	85
B			109	79	00 $\bar{1}$			77
C				83	010	52	90	33

D is ($\bar{1}20$), A and C are the same plane (110), B is (00 $\bar{1}$).

REFERENCES

1. M.Barfield and D.M.Grant: Advances in Magn. Reson., ed. J.S.Waugh, Vol. 1, p149, Academic Press, New York and London (1965)
2. N.F.Ramsey: Phys. Rev. 91, 303 (1953)
3. C.J.Jameson: Nuclear Magnetic Resonance, ed. G.A.Webb, vol.16, p1, (1987)
4. C.J.Jameson: Nuclear Magnetic Resonance, ed. G.A.Webb, vol.15, p1, (1986)
5. U.Haeberlen: Adv. Magn. Reson. Suppl.1, ed. J.S.Waugh, Academic Press, New York, 1976
6. U.Haeberlen, U.Kohlschutter, J.Kempf, H.W.Spiese and H.Zimmermann: Chem. Phys. 3, 248 (1974)
7. A.M.Achlama, U.Kohlschutter, U.Haeberlen: Chem. Phys. 7, 287 (1975)

8. J.J.Chang, R.G.Griffin, A.Pines: J. Chem. Phys. 60, 5130 (1975)
9. A.Pines, J.J.Chang, R.G.Griffin: J. Chem. Phys. 61, 1021 (1974)
10. M.Mehring: High Resolution NMR in solids, Berlin-Heidelberg-New York. Springer 1983
11. H.W.Spiess: NMR: Basic Principles and Progress, Vol.15. Berlin-Heidelberg-New York, Springer 1978
12. W.S.Veeman: Progress in Nuclear Magnetic Resonance Spectroscopy 16, 193 (1984)
13. H.Looser and D.Brinkmann: J. Magn. Reson., 64, 76 (1985)
14. R.T.C.Brownlee, M.J.O'Connor, B.P.Shehan and A.G.Wedd: J. Magn. Reson., 64, 142 (1985)
15. Marie-Rose Van Calsteren, G.I.Birnbaum and I.C.P.Smith: J. Chem. Phys., 86, 5405 (1987)
16. J.Tritt-Goc, N.Pislewski and U.Haeberlen: Ser. Fiz. Ramis.(Poznan) 53, 111 (1985)

17. J.Tritt-Goc, N.Pislewski and U.Haeberlen: Chem. Phys. 102, 133 (1986)
18. N.Schuff and U.Haeberlen: J. Magn. Reson. 62, 406 (1985)
19. K.Takegoshi, A.Naito and C.A.McDowell: J. Magn. Reson., 65, 34 (1985)
20. K.Takegoshi and C.A.McDowell: Chem. Phys. Lett., 123, 159 (1986)
21. K.Takegoshi and C.A.McDowell: J. Am. Chem. Soc., 108, 6852 (1986)
22. C.E.Pflugger and P.D.Boyle: J. Chem. Soc., Perkin Trans. 2, 1547 (1985)
23. C.Connor, A.Naito, K.Takegoshi and C.A.McDowell: Chem. Phys. Lett., 113, 123 (1985)
24. M.Durand-Le Floch, J.Pannetier, C.Doremieux-Morin and H.Arribart: J.Chem. Phys., 84, 4760 (1986)

25. J.F.Hinton, K.R.Metz, G.L.Turner, D.L.Bennett and F.S.Millett: J. Magn. Reson., 64, 120 (1985)
26. J.C.Facelli, D.M.Grant, and J.Michl: Acc. Chem. Res., 20, 152 (1987)
27. M.S.Solum, J.C.Facelli, J.Michl, D.M.Grant: J. Am. Chem. Soc., 108, 6464 (1986)
28. J.C.Facelli, A.M.Orendt, M.S.Solum, G.Depke, D.M.Grant and J.Michl: J. Am. Chem. Soc., 108, 4268 (1986)
29. J.C.Facelli A.M.Orendt, A.J.Beeler, M.S.Solum, G.Depke, K.D.Malsch, J.W.Downing, P.S.Murthy, D.M.Grant and J.Michl: J.Am. Chem. Soc., 107, 6749 (1985)
30. A.M.Orendt, J.C.Facelli, A.J.Beeler, K.Reuter, W.J.Horton, P.Cutts, D.M.Grant and J.Michl: J. Am. Chem. Soc., 110, 3386 (1988)
31. A.J.Beeler, A.M.Orendt, D.M.Grant, P.W.Cutts, J.Michl, K.W.Zilm, J.W.Downing, J.C.Facelli, M.Schindler and W.Kutzelnigg: J. Am. Chem. Soc. 106, 7672 (1984)

32. A.M.Orendt, J.C.Facelli, D.M.Grant, J.Michl, F.H.Walker, W.P.Dailey, S.T.Waddell, K.B.Wiberg, M.Schindler and W.Kutzelnigg: *Theor. Chim. Acta* 68, 421 (1985)
33. C.M.Carter, D.W.Alderman, J.C.Facelli and D.M.Grant: *J. Am. Chem. Soc.*, 109, 2639 (1987)
34. D.T.Amm and B.K.Hunter: *J. Chem. Phys.*, 82, 2529 (1985)
35. R.E.Wasylishen, J.O.Friedrich, S.Mooibroek and J.B.Macdonald: *J. Chem. Phys.*, 83, 548 (1985)
36. P.N.Tutunjian and J.S.Waugh: *J. Chem. Phys.*, 76, 1223 (1982)
37. J.Jokisaari, Y.Hiltunen and J.Lounila: *J. Chem. Phys.*, 85, 3198 (1986)
38. J.Lounila and J.Jokisaari: *Progr. NMR Spectr.*, vol. 15, p249 (1982)
39. J.W.Emsley, L.Phillips and V.Wray: *Progr. NMR Spectr.* vol. 10, p83 (1976)

40. P.E.Hansen: Progr. NMR Spectr., vol. 14, p175 (1981)
41. J.Kowalewski: Progr. NMR Spectr., vol. 11, p1 (1977)
42. E.M.Bastiaan, C.Maclean, P.C.M.Van Zijl and A.A.Bothner-By: Ann. Reports on NMR Spectr., vol.19 p35 (1987)
43. J.W.Emsley and J.C.Lindon: NMR spectroscopy using liquid crystal solvents, Pergamon Press, Oxford (1975)
44. B.R.Appleman, and B.P.Dailey: Advan. Magn. Res., 7, 231 (1974)
45. A.Pines, M.G.Gibby and J.S.Waugh: J. Chem. Phys., 59, 569 (1973)
46. S.R.Hartmann and E.L.Hahn: Phys. Rev., 128, 2042 (1962)
47. M.M.Maricq and J.S.Waugh: J. Chem. Phys., 70, 3300 (1979)
48. J.Herzfeld and A.E.Berger: J. Chem. Phys., 73, 6021 (1980)

49. D.L.Klayman and T.S.Griffin: J. Am. Chem. Phys., 95, 197 (1973)
50. H.Puff, R.Gattermayer, R.Hundt and R.Zimmer: Angew. Chem. Ind. Ed. Engl., 16, 547 (1977)
51. R.Gattermayer: Dissertation, University Bonn 1974.
52. B.Zshoche: Staatsexamensarbeit, Bonn 1977
53. W.Schun: Staatsexamensarbeit, Bonn 1977
54. 'NMR and the periodic table' ed. R.K.Harris and B.E.Mann; Academic Press, London, New York, 1978.
55. N.F.Ramsey: Phys. Rev., 78, 699 (1950)
56. N.F.Ramsey: Phys. Rev., 86, 243 (1952)
57. A.D.Buckingham and S.M.Malm: Mol. Phys., 22, 1127 (1971)
58. T.W.Marshall and J.A.Pople: Mol. Phys., 1, 199 (1958)

59. A.D.Buckingham and K.P.Lawley: Mol. Phys., 3, 219 (1960)
60. R.H.Schneider: J. Chem. Phys., 48, 4905 (1968)
61. A.D.Buckingham and I.Love: J. Magn. Reson., 2, 338
(1970)
62. H.S.Gutowsky and D.W.McCall: Phys. Rev., 82, 748(1951)
63. H.S.Gutowsky, D.W.McCall and C.P.Slichter: Phys. Rev.,
84, 589 (1951)
64. E.L.Hahn and D.E.Maxwell: Phys. Rev., 84, 1246 (1951)
65. E.L.Hahn and D.E.Maxwell: Phys. Rev., 88, 1070 (1952)
66. N.F.Ramsey and E.M.Purcell: Phys. Rev., 85, 143 (1952)
67. E.Fermi: Z. Physik 60, 320 (1930)
68. A.D.Buckingham and J.A.Pople: Trans. Faraday Soc., 59,
2421 (1963)
69. R.Ditchfield and P.D.Ellis: "Topics in Carbon-13 NMR
Spectroscopy", vol.2, John Wiley & Sons, 1976

70. J. Van Dongen Torman, W.S. Veeman and E. De Boer: J. Magn. Reson., 32, 49 (1978)
71. D.M. Brink, G.R. Satchler: Angular Momentum, Oxford Univ. Press, London (1968)
72. J.F. Nye: Physical Properties of Crystals, Oxford Univ. Press, London (1964)
73. P. Terpstra and L.W. Codd: Crystallometry Academic Press, New York 1961
74. C.S. Barrett and T.B. Massalski: Structure of Metals. McGraw-Hill Inc., 1966
75. F. James: "Function Minimization in Proc. of the 1972 CERN Computing and Data Processing School", CERN 72-21 (1972)
76. W.T. Eadie, D. Drijard, F.E. James, M. Roos, and B. Sadoulet: "Statistical Methods in Experimental Physics", North-Holland Publ. Co., Amsterdam (1971)
77. P. Lazzeretti and R. Zanasi: J. Chem. Phys., 77, 2448 (1982)

78. J.A.Pople, W.G.Schneider and H.J.Bernstein:"high-resolution nuclear magnetic resonance", Mcgraw-Hill book company, Inc., (1959)